Crystal Engineering of Porosity

Gareth Owen Lloyd

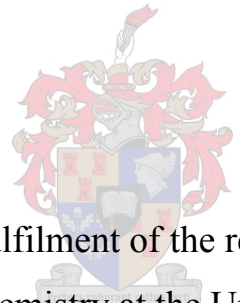

Thesis presented in partial fulfilment of the requirements for the degree of
Master of Science in Chemistry at the University of Stellenbosch

December 2006

Supervisor: Prof. L. J. Barbour

Declaration

I, the undersigned, hereby declare that the work contained in this thesis is my own original work and has not previously, in its entirety or in part, been submitted at any university for a degree.

Signature:…….…….Date:……30 November 2006……

Abstract

Inclusion and porosity properties of the following supramolecular solid-state hosts were investigated:

- 2,7-dimethylocta-3,5-diyne-2,7-diol
- 2-methyl-6-phenylhexa-3,5-diyn-2-ol
- Dianin's compound
- *p-tert*-butyl-calix[4]arene
- 5,11,17,23-tetra-*tert*-butyl-25,26,27,28-tetramethoxy-2,8,14,20-tetrathiacalix[4]arene
- Two discrete coordination metallocycles, $[Ag_2IMID_2](BF_4)_2$ and $[Cu_2(BITMB)_2(Cl)_4]$

All of these compounds form well-defined crystalline host structures. Inclusion phenomena involving encapsulation of liquids were studied using single-crystal x-ray diffraction methods. Several guest-free host structures (α phases) were structurally elucidated and their gas sorption properties were investigated.

Studies of the sorption properties of seemingly nonporous materials were carried out to provide insight into this rare phenomenon. Water and iodine sorption by a polymorph of 5,11,17,23-tetra-*tert*-butyl-25,26,27,28-tetramethoxy-2,8,14,20-tetrathiacalix[4]arene shows that the conventional perception of sorption through the solid-state requires reassessment.

Gas sorption studies were carried out using apparatus devised and presented here. These include sorption apparatus and a device to determine single-crystal structures under controlled gas atmospheres.

Abstrak

Insluitings- en porositeits-eienskappe van die volgende supramolekulêre, vaste-toestand gasheerverbindings is ondersoek:

- 2,7-dimetielokta-3,5-diyn-2,7-diol
- 2-methyl-6-fenielheksa-3,5-diyn-2-ol
- Dianin se verbinding
- *p-ters*-butielkaliks[4]areen
- 5,11,17,23-tetra-*ters*-butiel-25,26,27,28-tetrametoksi-2,8,14,20-tetratiakaliks[4]areen
- Twee diskrete ko-ordinasie komplekse, $[Ag_2IMID_2](BF_4)_2$ en $[Cu_2(BITMB)_2(Cl)_4]$

Al hierdie verbindings form goed-gedefiniëerde kristallyne gasheer-strukture. Insluitings fenomene wat enkapsulering van vloeistowwe behels is bestudeur met die gebruik van enkelkristal-X-straal diffraksie metodes. Verskeie leë gasheer-strukture (α fases) is struktureel opgeklaar en hulle gassorpsie-eienskappe is ondersoek.

'n Ondersoek na die sorpsie eienskappe van oënskynlike nie-poreuse materiale is uitgevoer om insig in hierdie rare fenomeen te bekom. Water en jodium absorpsie deur 'n polimorf van 5,11,17,23-tetra-*ters*-butiel-25,26,27,28-tetrametoksi-2,8,14,20-tetratiakaliks[4]areen dui daarop dat die konvensionele persepsie van sorpsie deur die vaste toestand herevalueer moet word.

Gassorpsie-studie is uitgevoer met die apparaatuur wat ontwikkel is en hier beskryf word. Dit sluit in 'n sorpsieapparaat en 'n toestel vir die bepaling van enkel-kristalstrukture onder verskeie gas atmosfere.

Acknowledgements

This thesis was completed thanks to the following:

My supervisor: Prof. Len Barbour, who has taught me more than I could ever have dreamt of. Thank you for introducing me into the realm of Supramolecular Chemistry.

The Supramolecular Materials Chemistry Group: Thanks to Dr Martin Bredenkamp for his help with synthetic work, Dr Catharine Esterhuysen for her knowledge of crystallography and dynamics, Dr Liliana Dobrzańska for being the best laboratory partner one could ask for, Jo Alen for his work in synthesising the diacetylenes and the rest of the group (Tia Jacobs, Dr Elijane de Vries, Dr Clive Oliver) for all the help that they provided.

My Family: To all of you thanks for the support. Especially to my mother, Shân, you are my number one fan, and I yours, as always, this one is for you.

Abbreviations

1D, 2D and 3D	One, two and three dimensional
ATR	Attenuated Total Reflection
BITMB	1,3-bis(imidazol-1-ylmethyl)-2,4,6-trimethylbenzene
CSD	Cambridge Structural Database
DNA	Deoxyribonucleic acid
DSC	Differential Scanning Calorimetry
FT-IR	Fourier-Transform Infrared
G	Guest
H	Host
IMID	1,4-bis(2-methylimidazol-1-ylmethyl)benzene
IR	Infrared
K	Equilibrium constant
kJ	kilojoule
MeOTBCS	5,11,17,23-tetra-*tert*-butyl-25,26,27,28-tetramethoxy-2,8,14,20-tetrathiacalix[4]arene
MOF	Metal-Organic Framework
mol	mole
NMR	Nuclear Magnetic Resonance
P	Pressure
R	Universal gas constant
RNA	Ribonucleic Acid
SBU	Secondary Building Unit
SCD	Single-Crystal Diffraction
SHG	Second Harmonic Generation
STP	Standard Temperature and Pressure
T	Temperature
TBC4	*p*-*tert*-butylcalix[4]arene
TGA	Thermogravimetric Analysis
UV	Ultraviolet
ΔG	Gibbs free energy
ΔH	Enthalpy change
ΔH_{iso}	Isosteric heat of sorption
ΔS	Entropy change

Publications, Posters and Seminars

All publications, posters and PowerPoint presentations for all talks are available on the enclosed CD.

Publications of work presented here

1. Diffusion of water in a nonporous hydrophobic crystal. P. K. Thallapally, G. O. Lloyd, J. L. Atwood & L. J. Barbour, *Angew. Chem. Int. Ed.*, **2005**, *44*, 3848. (N.B. Editor's Choice Letter in Science as Highlight in the Recent Literature titled 'Chemistry: No Need For Pores?', *Science*, **2005**, *308*, 1521.)

2. Polymorphism of pure *p-tert*-butylcalix[4]arene: subtle thermally-induced modifications. J. L. Atwood, L. J. Barbour & G. O. Lloyd, *Chem. Commun.,* **2004**, 922.

3. A discrete metallocyclic complex that retains its solvent-templated channel structure on guest removal to yield a porous, gas sorbing material. L. Dobrzańska, G. O. Lloyd, H. G. Raubenheimer & L. J. Barbour, *J. Am. Chem. Soc.*, **2005**, *127*, 13134.

4. Enclathration of morpholinium cations by Dianin's compound: salt formation by partial host-to-guest proton transfer. G. O. Lloyd, M. W. Bredenkamp & L. J. Barbour, *Chem. Commun.*, **2005**, 4053.

5. Permeability of a seemingly nonporous crystal formed by a discrete metallocyclic complex. L. Dobrzańska, G. O. Lloyd, H. G. Raubenheimer & L. J. Barbour, *J. Am. Chem. Soc.*, **2006**, *128*, 698.

6. Organic crystals absorb hydrogen gas under mild conditions. P. K. Thallapally, G. O. Lloyd, T.B. Wirsig, M.W. Bredenkamp, J. L. Atwood & L. J. Barbour, *Chem. Commun.,* **2005**, 5272.

7. (*S*)-4-(4-Hydroxyphenyl)-2,2,4-trimethylchroman. M. W. Bredenkamp & G.O. Lloyd, *Acta Crystallogr.. Section E*, **2005**, *E61*, o1512.

8. Solid-State Self-Inclusion: The Missing Link. G. O. Lloyd, J. Alen, M. W. Bredenkamp, E. J. C. de Vries, C. E. Esterhuysen & L. J. Barbour, *Angew. Chem. Int. Ed.*, **2006**, *45*, 5354.

Oral Presentations of work described here

1. Gas sorption and separation using supramolecular materials chemistry.
   SACI Young Chemist Mini Symposium **2005**, Stellenbosch, South Africa.
2. Solid-state dynamics.
   SACI Young Chemist Mini Symposium **2006**, Cape Town, South Africa.

Poster Presentations of work described here

1. Jo Alen, Gareth O. Lloyd, Leonard J. Barbour, Martin W. Bredenkamp, Erik van der Eycken, Wim Dehaen, Wim De Borggraeve & Frans Compernolle, „Dianin's Compound - Prototype of an inclusion compound". 8th SIGMA-ALDRICH Organic Synthesis Meeting, **2004**, Sol Cress-Spa-Belgium.

2. Gareth O. Lloyd, Leonard J. Barbour & Jo Allen. "New helical host system showing true self-inclusion". XX Congress of the IUCR, **2005**, Florence, Italy.

3. Tia Jacobs, Gareth O. Lloyd, Martin W. Bredenkamp & Leonard J. Barbour. "Supramolecular cocrystallisation: a new paradigm for the organic solid state". Frank Warren Conference, **2006,** Cape Town, South Africa.

4. Tia Jacobs, Gareth O. Lloyd, Martin W. Bredenkamp & Leonard J. Barbour. "Supramolecular cocrystallisation: a new paradigm for the organic solid state". European Crystallographic Meeting **2006**, Leuven, Belgium.

5. Gareth O. Lloyd, Liliana Dobrzańska & Leonard J. Barbour. "Permeability of a seemingly nonporous crystalline material composed of a discrete metallocyclic complex". International Coordination Chemistry Conference, **2006**, Cape Town, South Africa

Publications of work not presented in this thesis.

1. Water-assisted self-assembly of harmonic single and triple helices in a polymeric coordination complex. G. O. Lloyd, L. J. Barbour & J. L. Atwood, *Chem. Commun.*, **2005**, 1845.

2. (2E)-N,N'-Bis(pyridin-4-ylmethyl)but-2-enediamide dehydrate. G.O. Lloyd, *Acta Crystallogr. Section E*, **2005**, *E61*, o1218.

3. catena-Poly[[[tetraaquazinc(II)]-μ-[(2E)-N,N'-bis(pyridin-4-ylmethyl)but-2-enediamide]] dinitrate]. G. O. Lloyd, *Acta Crystallogr. Section E*, **2005**, *E61*, m1204.

4. N,N'-Bis(pyridin-4-ylmethyl)succinamide-terephthalic acid (1/1). C. L. Oliver, G. O. Lloyd & E. J. C. de Vries, *Acta Crystallogr. Section E*, **2005**, *E61***,** o2605.

5. Resolution of (S,S)-4-(2,2,4-trimethylchroman-4-yl)phenyl camphanate and its 4-chromanyl epimer by crystallization. C. Esterhuysen, M.W. Bredenkamp & G.O. Lloyd, *Acta Crystallogr. Section C*, **2005**, *C61*, o32.

6. 1,4,7,10-Tetrakis(carbamoylmethyl)-1,4,7,10-tetraazacyclododecane. R. C. Luckay & G. O. Lloyd, *Acta Crystallogr. Section E*, **2005**, *E61*, o3405.

7. (4-Pyridylmethyl)aminium chloride. E. J. C. de Vries, C. L. Oliver & G.O. Lloyd, *Acta Crystallogr. Section E*, **2005**, *E61*, o1577.

8. 3,3'-(Quinoxaline-2,3-diyldimethylene)bis(pentane-2,4-dione). L. Dobrzańska & G. O. Lloyd, *Acta Crystallogr. Section E*, **2005**, *E61*, o2114.

9. O-[4-(2,2,4-Trimethylchroman-4-yl)phenyl] N,N-dimethylthiocarbamate. E. J. C. de Vries, G. O. Lloyd, M. W. Bredenkamp & T. Jacobs, *Acta Crystallogr. Section E*, **2005**, *E61*, o2871.

10. 2,2’-(Butane-1,4-diyl)dibenzimidazolium dichloride dehydrate. L. Dobrzańska & G. O. Lloyd, *Acta Crystallogr. Section E*, **2006**, *E62*, o1205.

11. S-[4-(2,2,4-Trimethylchroman-4-yl)phenyl] N,N-dimethylthiocarbamate. G. O. Lloyd, J. Alen, T. Jacobs, M. W. Bredenkamp & E. J. C. de Vries, *Acta Crystallogr. Section E*, **2006**, *E62*, o691.

12. Guest-Induced Conformational Switching in a Single Crystal. L. Dobrzańska, G. O. Lloyd, C. E. Esterhuysen & L. J. Barbour, *Angew. Chem. Int. Ed.*, **2006**, *45*, 5856.

13. Catena-Poly[[silver(I)- μ-1,4-bis(2-methyl-1H-imidazol-1-ylmethyl)benzene-$\kappa^2N^3:N^{3l}$] nitrate]. L. Dobrzańska & G. O. Lloyd, *Acta Crystallogr. Section E*, **2006**, *E62*, m1638.

14. Construction of one- and two-dimensional coordination polymers using ditopic imidazole ligands. L. Dobrzańska, G. O. Lloyd, T. Jacobs, I. Rootman, C. L. Oliver, M. W. Bredenkamp & L. J. Barbour, *J. Mol. Struct.*, **2006**, 796, 107.

Posters of work not presented in this thesis.

1. Gareth O. Lloyd and Leonard J. Barbour. "Water-assisted self-assembly of harmonic single and triple helices in a polymeric coordination complex". Inorganic Chemistry Conference **2005**, Petiermaritzburg, South Africa.

2. Liliana Dobrzańska, Gareth O. Lloyd, Leonard J. Barbour. "Chromatic transition associated with single-crystal-to-single-crystal guest exchange". Inorganic Chemistry Conference **2005**, Petiermaritzburg, South Africa.

3. Tia Jacobs, Gareth O. Lloyd, Liliana Dobrzańska and Leonard J. Barbour. "Molecular assembly of isostructural discrete hexagons". International Coordination Chemistry Conference, **2006**, Cape Town, South Africa.

4. Liliana Dobrzańska, Gareth O. Lloyd, and Leonard J. Barbour. "The Phenomenon of Dynamic Cooperativity in the Solid State". European Crystallographic Meeting **2006**, Leuven, Belgium

5. Gareth O. Lloyd, Liliana Dobrzańska and Leonard J. Barbour. “Synthesis and design of new polymeric coordination networks”. Cape Organometallic Symposium **2004**, Cape Town, South Africa

Contents

1. Introduction

Over the past century, research in chemistry has focused intensively on controlling the formation and cleavage of covalent bonds – i.e. interactions between atoms. However, it has long been apparent that molecules, in turn, are capable of interacting with one another, as abundantly evidenced by their aggregation into condensed phases and comparatively far more complex entities such as living organisms. This observation has inspired the notion that gaining control over intermolecular interactions may well represent the next major frontier in the molecular sciences.

In the early 20th century, biochemists observed that substrates interacting with enzymes were undergoing catalytic reactions much faster and more selectively than in analogous laboratory processes, leading Emil Fischer to propose the now well-known lock-and-key concept.[1] Around the same time, the field of inorganic chemistry was significantly enhanced by the development of Alfred Werner's coordination theories.[2] Based on these ideas, Paul Ehrlich introduced the concept of receptor molecules which, in modern parlance, implies "host-guest chemistry".[3] The term *Übermoleküle* (supermolecule) was coined for the description of organised entities arising from the association of coordinatively saturated species such as the acetic acid dimer.[4] The accumulation of such ideas, together with early studies of the molecular recognition of alkali metal ions using natural antibiotics and synthetic macro(poly)cyclic polyethers,[5] Schiff's base macrocycles[6] and cyclophanes[7] led to the development of the new field of Supramolecular Chemistry in the late 1970's.[8] Jean-Marie Lehn succinctly defined supramolecular chemistry as "chemistry beyond the molecule" and stated that "supermolecules are to molecules and the intermolecular bond what molecules are to atoms and the covalent bond".[9] A subjective and non-comprehensive timeline of several milestones in supramolecular chemistry is outlined in Table 1.[10]

Since intermolecular interactions are the "glue" that holds supermolecules together, gaining an understanding of these relatively feeble forces is one of the primary goals of supramolecular chemistry.[11] Owing mostly to size considerations, the interactions between two molecules associated by means of non-covalent forces are difficult to study and, consequently, it is preferable to instead investigate larger aggregates. Aggregates of molecules in solution have successfully been studied using powerful spectrophotometric techniques such as UV-visible, infrared and fluorescence

Table 1 Chronology of the development of Supramolecular Chemistry.[i]

1810	-	Sir Humphrey Davy: discovery of chlorine hydrate
1823	-	Michael Faraday: formula of chlorine hydrate
1841	-	C. Schafhäutl: study of graphite intercalates
1849	-	F. Wöhler: β-quinol H_2S clathrate
1891	-	Villiers and Hebd: cyclodextrin inclusion compounds
1893	-	Alfred Werner: coordination chemistry
1894	-	Emil Fischer: *lock and key* concept
1906	-	Paul Ehrlich: introduction of the concept of a *receptor*
1937	-	K. L. Wolf: the term *Übermoleküle* is coined to describe organised entities arising from the association of coordinatively saturated species (e.g. the acetic acid dimer)
1939	-	Linus Pauling: hydrogen bonds are included in the groundbreaking book *The Nature of the Chemical Bond*
1940	-	M. F. Bengen: urea channel inclusion compounds
1948	-	H. M. Powell: x-ray crystal structures of β-quinol inclusion compounds; the term 'clathrate' is introduced to describe compounds where one component is enclosed within the framework of another
1949	-	Brown and Farthing: synthesis of [2.2]paracyclophane
1953	-	Watson and Crick: structure of DNA
1956	-	Dorothy Crowfoot Hodgkin: x-ray crystal structure of vitamin B_{12}
1959	-	Donald Cram: attempted synthesis of cyclophane charge transfer complexes with $(NC)_2C=C(CN)_2$
1961	-	N. F. Curtis: first Schiff's base macrocycle from acetone and ethylene diamine
1964	-	Busch and Jäger: Schiff's base macrocycles
1967	-	Charles Pedersen: crown ethers
1968	-	Park and Simmonds: *Katapinand* anion hosts
1969	-	Jean-Marie Lehn: synthesis of the first cryptands
1969	-	Jerry Atwood: liquid clathrates from alkyl aluminium salts
1973	-	Donald Cram: spherand hosts produced to test the importance of reorganisation
1978	-	Jean-Marie Lehn: introduction of the term 'supramolecular chemistry', defined as the 'chemistry of molecular assemblies and of the intermolecular bond'
1979	-	Gokel and Okahara: development of the lariat ethers as a subclass of host
1981	-	Vögtle and Weber: podand hosts and development of nomenclature
1987	-	Nobel Prize for Chemistry awarded to Donald J. Cram, Jean-Marie Lehn and Charles J. Pedersen for their work in supramolecular chemistry
1990	-	D. A. Tomalia, G. R. Newkome and F. Diederich; dendrimers
1991	-	J. F. Stoddart and F. Vögtle: Knots, catenanes and rotaxanes
1995	-	M. Fujita and P. J. Stang: coordination cages
1996	-	Atwood, Davies, MacNicol & Vögtle; publication of *Comprehensive Supramolecular Chemistry* containing contributions from almost all the key groups and summarising the development and state of the art of Supramolecular Chemistry
1996	-	Nobel Prize for Chemistry award to Kroto, Smalley, Curl for their work on the chemistry of the fullerenes
1996	-	J. Rebek, J. L. Atwood, L. R. MacGillivray and L. J. Barbour: hydrogen bonded nanocapsules
1998	-	D. Braga and G. R. Desiraju: modern crystal engineering comes into its own
1998	-	O. M. Yaghi, M. Eddaoudi, M. J. Zaworotko, G. Férey and S. Kitagawa and others: Crystal engineering of metal-organic coordination polymers
2002	-	*Supramolecular Chemistry & Self-Assembly*, Special Edition in *Science* magazine.

[i] Most of the chronology from 1810 to 1996 has been adapted from *Supramolecular Chemistry* by J. L. Atwood and J. W. Steed.[10]

spectrometry, as well as nuclear magnetic resonance spectroscopy. However, none of these techniques provide highly accurate positional information for all atoms in a given system. Such data can only be obtained using single-crystal x-ray diffraction methods (provided that crystals can be obtained, of course). Fortunately, the supramolecular interactions that facilitate the packing motifs in crystals are often the same interactions that govern the formation of small aggregates. For this reason, crystals have been described as "one of the finest examples of a supermolecule, a supermolecule *par excellence*."[12]

Crystal Engineering

A molecular crystal can be described as an "infinitely" large supermolecule. Synthetic chemists use a variety of methods to synthesise molecules from atoms. Analogously, supramolecular chemists have recognised the need to develop a rational methodology to combine molecules into supermolecules with their own structural, chemical and physical properties. Such a strategy must take account of the geometric and energetic properties of myriad different types of intermolecular interactions. This methodology, when applied to constructing the "finest examples of supermolecules", is known as Crystal Engineering.[13] The concept of crystal engineering was first proposed by von Hippel in 1962 under the term 'molecular engineering' and Pepinsky in 1955.[14] *Topochemistry*,[15] i.e. the understanding of regioselectivity and product distribution in the solid-state, was also applied to crystal engineering early on. Braga, Grepioni and Desiraju have summarised the two main components of crystal engineering, analysis and synthesis as follows:

> Reason and imagination come into play simultaneously in the quest for new functionalised solids, while experiment and computation are of equal significance in the prediction and design of crystal structures.[16]

In other words, the knowledge (or at least consideration of) the steric, topological and intermolecular bonding properties of the building blocks used in the design and preparation of a crystalline solid is the essence of crystal engineering.

So, how is crystal engineering achieved? Desiraju and coworkers proposed the strategy of using synthons, a direct analogy to the approach used by synthetic organic chemists. This methodology for designing crystals uses the concept of a synthon to represent the identification of molecular precursors after retrosynthetic analysis of a

target crystal network.[17] The accepted definition of supramolecular synthons is thus "units formed by synthetic operations involving intermolecular interactions." Modern crystal engineering is often thought of as a parallel to conventional macroscopic engineering which is based upon known archetypes. However, this idea has been rejected by Moulton and Zaworotko:

> In effect, the principles of design are based upon a blueprint, in many cases a blueprint that is first recognised *via* a serendipitous discovery, and allow the designer to select components in a judicious manner.[18]

No doubt, crystal engineering is still in its infancy – the recognition of the blueprint *via* serendipitous discovery is still a significant component of this science. However, several blueprints *have* been recognised and design strategies are rapidly beginning to play a key role in crystal engineering. Probably the most important example of this is the blueprint concept of reticular synthesis (or chemistry), proposed by Yaghi, Eddaoudi and coworkers. Reticular synthesis, acknowledged by its originators as a subclass of crystal engineering, is the process of assembling judiciously designed rigid molecular building blocks into predetermined ordered structures (networks), which are held together by strong bonding.[19]

This approach has been applied with great success to the design of porous metal-organic frameworks (MOFs) (also commonly referred to as porous coordination polymers). Owing to the long-standing association of porosity with zeolites, Yaghi and coworkers have borrowed the concept of secondary building units (SBUs) from zeolite analysis for "understanding and predicting topologies of structures, and as synthetic modules for the construction of robust frameworks with *permanent* porosity.' Indeed, SBUs for the reticular synthesis of coordination metal-organic frameworks are analogous to the supramolecular synthon used for retrosynthesis of molecular crystals.

One of the ultimate aims of studies in crystal engineering is to gain a comprehensive understanding of intermolecular interactions, and to then exploit this knowledge to routinely construct designer materials. Although this goal is currently far from realisation, much is already known: intermolecular interactions can be divided into two types, *viz*. nondirectional (isotropic) and directional forces. The general term to describe both the dispersion and repulsion components of

nondirectional interactions is “van der Waals forces.” These forces occur in all systems, but are difficult to characterise unless they are the only forces contributing to crystal packing energetics. Dispersive forces are attractive in nature and result from the interactions between fluctuating multipoles of adjacent molecules. They have an approximate inverse sixth power dependence on the interatomic separation and their strength is proportional to the size of the molecule in question, as each polarizable bond or atom contributes. As all of the molecules contribute to the dispersion forces in a crystal, these forces constitute the major share of the overall lattice energy.

There are also repulsive forces, sometimes known as exchange-repulsion forces, which balance out the dispersion forces. The repulsive forces have an approximate inverse twelfth power (or exponentially decreasing) dependence on interatomic distance. These forces are also crucial to crystal packing, particularly in host-guest chemistry, as they define molecular shape and conformation.

Although all atoms within a crystal can participate in van der Waals interactions, it is usual to associate these forces with C···C, C···H and H···H contacts between the separate organic constituents (owing to the predominance of carbon and hydrogen in the stoichiometries of most organic compounds). Higher C:H ratios in aromatic compounds as opposed to aliphatic compounds cause C···C interactions to be more prevalent in the aromatic compounds. Therefore, in the absence of other stronger forces, aromatic compounds have a much greater tendency to stack as a result of the increased number of C···C interactions,[20] especially when the rings are more electron-deficient.[21] C···H type interactions are also prevalent in a wide variety of aromatic compounds and, to a lesser extent, in aliphatic compounds. Optimisation of these interactions is accomplished when neighbouring molecules dovetail, or close-pack in three-dimensions. For planar aromatic compounds, this results in a ‘T-shaped’ configuration of molecules, commonly referred to as the herringbone structure (Figure 1). With their lower C:H ratio, aliphatic molecules and residues experience more H···H interactions. It has been found that these ‘hydrophobic’ forces are generally significant when the alkyl chain lengths are longer than ca. five carbon atoms.

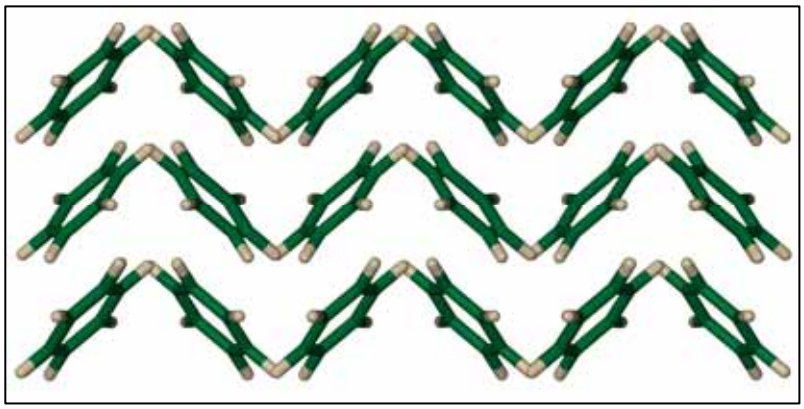

Figure 1. Herringbone structure of benzene. Molecules are shown in capped-stick representation.

Directional forces are generally far more recognisable and definitive in character. Examples of weak directional interactions that have been categorised include halogen···halogen and chalcogen···chalcogen interactions. Indeed, it has long been known that the halogens form short, nonbonding contacts in crystals, although there is some controversy over the exact nature of these interactions: some appear to be merely the result of the elliptical shapes of the atoms, which are therefore only in van der Waals contact with one another.[22] However other interactions are specifically attractive in nature and the atomic polarisation of the halogen atoms causes the efficacy of the interaction to be in the order I > Br > Cl.[23] Since F is not easily polarised, F···F interactions play a far less significant role in crystal packing energetics than the more strongly dipolar F ···H interactions.[24]

In addition to same-halogen and mixed-halogen atom···atom interactions, directional interactions can also exist between halogens and heteroatoms such as nitrogen and oxygen.[25] These types of bonds have many characteristics that are similar to hydrogen bonds and have now been termed ‘halogen bonds’.[26] The least-known and least-understood of the weak directional forces are the chalcogen atom···atom interactions. Of these types of interactions, the best-understood are the S···N, S···S and S···Cl interactions. As with the halogen interactions, these are also brought about by polarisation.[13]

Undoubtedly, the hydrogen bond is the most important and well-understood of all the directional forces. The geometry of a hydrogen bond of the type D-H···A-X (where D is the donor atom, H is the hydrogen atom, A is the acceptor atom and X is

the atom directly bonded to the acceptor atom A) can been defined by specifying the lengths D-A and H-A, the hydrogen bond angle D-H···A (referred to as θ), the H···A-X angle (referred as Φ) and the planarity of the DHAX system (Figure 2). Hydrogen bonds have been classified into three categories of strength; strong, medium and weak. Strong hydrogen bonds are most commonly associated with strong acids, hydrated protons or organic 'proton sponges'. In the case of these types of hydrogen bonds, the θ angle is close to 180^{o} with a short D···A distance normally accompanied by lengthening of the covalent D-H distance such that it appears that the proton is shared nearly equally by the two electronegative atoms. Unlike very strong hydrogen bonds which are not commonplace, medium-strength hydrogen bonds are extensively associated with crystal engineering and, even more importantly, with biological systems. The donor and acceptor atoms are usually oxygen and/or nitrogen. The D···A hydrogen bonding distances for the medium-strength hydrogen bonds vary over a wide range (by ca 0.5Å), and the D-H···A angles (θ) range between 178^{o} and 140^{o}. The most common and well-understood hydrogen bonds encountered in nature occur between the base pairs in DNA and RNA, and the amide groups of β-sheets and α-helices in protein structures.

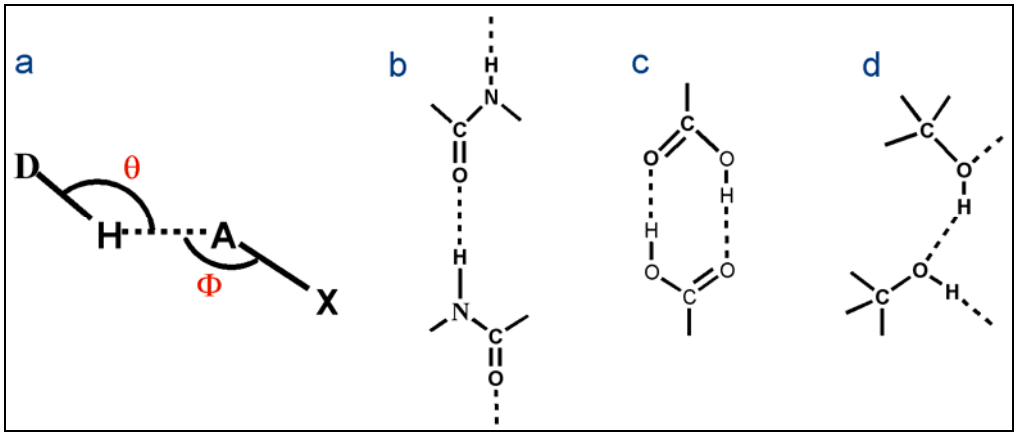

Figure 2. Schematic representation showing **(a)** the hydrogen bonding geometric parameters used to describe the directionality and strength of a hydrogen bond. Included are some examples of common and well-known hydrogen bonds and their donor and acceptor groups. **(b)** Amide-amide hydrogen bonds common to protein structures. **(c)** Dimeric carboxylic acid hydrogen bond. **(d)** Hydroxyl-hydroxyl hydrogen bond.

In crystal engineering and, more specifically host/guest chemistry, the hydrogen bonding between hydroxyl groups is utilised extensively in such exquisite examples as β-hydroquinone clathrates,[27] Dianin's compound,[28] calixarenes[29] and cyclodextrins.[30] Water has also been studied in the context of hydrogen bonding: it also has a rich history of clathrate chemistry and several polymorphs of ice are known.[31] Indeed, the study of water clusters within crystal structures has escalated in recent years.[32] The carboxylic acid group is also a very well-studied hydrogen bonding moiety and has been used in a variety of ways to direct the self-assembly of compounds. The third type of hydrogen bonding, the weak hydrogen bond, has only recently gained recognition. In the case of C-H···(N,O) interactions, the stronger of these types of hydrogen bonds, there is some van der Waals overlap between D and A, but in most cases there is none. In spite of this, the interactions can still be considered significant when there is no van der Waals overlap as the forces are largely electrostatic in nature and therefore have long-range character. Owing to the electrostatic nature of these bonds and the high occurrence of C-H bonds in most organic molecules, these hydrogen bonds are considered more important than dispersion forces in that they have orienting effects on molecules prior to nucleation and crystallisation. As carbon is not as electronegative as nitrogen and oxygen, and because carbon atoms are not often in sterically unhindered positions, (O,N)-H···C,π type hydrogen bonds are very rare. Indeed, only 60-75 of these interactions were found in the 1993 Cambridge Structure Database (CSD).[33]

The study of the coordination bond is a very broad and complicated research field to which due justice cannot reasonably be given here. A coordination bond forms between an acceptor atom (normally a transition metal) and a ligand that donates free electrons (normally in the form of lone pair of electrons) to the acceptor atom. Its main advantages over the other intermolecular bonds are twofold. The first advantage is that the bonds tend to be highly directional. This means that one can use them to direct structure more easily than one can use hydrogen bonds. This design feature has been used extensively to prepare myriad coordination polymers as evidenced by the thousands of recent publications on new topologies and crystal structures covering all possible dimensions of coordination polymeric frameworks. Some of the better-known advocates of the coordination bond in supramolecular crystal research include Michael J. Zaworotko (see his review on supramolecular isomerism and

polymorphism in network solids[18]), Omar. M. Yaghi for his work with reticular synthesis[19] and S. Kitagawa for studies on dynamic coordination polymers.[34] The second advantage of the coordination bond is that it is much stronger in relation to other intermolecular bonds. Although coordination bonds can vary in strength from being comparable to a strong hydrogen bond to being stronger than a covalent bond, the general consensus is that coordination crystals are relatively thermally stable and can therefore be used in the design of materials where stability is a prerequisite of the material.

Host:Guest Chemistry

Whilst the primary stabilising features of a crystal structure may, in some cases, be described in terms of a single type of interaction such as van der Waals or hydrogen bonding, the control of its secondary and tertiary features requires the simultaneous manipulation of both strong and weak intermolecular interactions. This is an immensely difficult task as our understanding of the often subtle role of the weak interaction is far from complete. Therefore, it might be said that comprehending the interplay of these interactions is more of an art than a science.[13] In essence, a crystal structure is the result of compromises between interactions of different strengths, directionalities and distance dependence. These subtleties cause flexibility within structure formation as evidenced by the common occurrence of polymorphism. Indeed, in many cases crystal frameworks are stable enough to allow variation of enclathrated guests while the interactions between the host and the guest allows selectivity. This can often serve as a basis for the study of weak interactions. The complexity of crystallisation, and the prediction of structure, is beautifully revealed by the study of enclathration.

Solid-state host:guest chemistry refers to the crystal forms as lattice-type inclusion compounds, or clathrates. The word “clathrate”, derived from the Latin word *clathratus*, meaning ‘enclosed by the bars of a grating’, was coined to describe inclusion compounds possessing a three-dimensional host lattice with voids for the accommodation of guests in the solid-state.[35] The first examples of these interesting systems, discovered in the 19th century, include the clathrate hydrates,[36] graphite intercalates,[37] β-hydroquinone clathrates[27] and cyclodextrin inclusion compounds.[38] At the time of their initial discovery, these compounds where not fully understood, as the pioneering work on x-ray crystallography had not yet taken place. During the 20th

century, the host:guest chemistry of these complex systems was finally revealed. Some new host compounds added to the list of classical host systems include tri-*o*-thymotide,[39] Dianin's compound,[28] phenol[40] and urea.[41] Most of these systems have now been almost fully characterised using a cornucopia of advanced and simple analytical techniques. The classical systems have one feature in common: the guests entrapped as a result of close-packing effects and van der Waals contact interactions within voids formed by the host, or interstitial spaces in the crystal lattice. With improved understanding of molecular recognition, mostly in solution,[7,11] more directional and stronger interactions have been investigated to form mixed crystals by exploiting complementary functionalities. Although these are nominally host:guest systems, the differentiation between host and guest is blurred.[42] Most of the classical host:guest systems enclathrate solvents as guests. Compounds that include water are known as "hydrates" while those that include other solvents are referred to as "solvates". However, when the guest is not a solvent or even a liquid under atmospheric conditions, the definitions become obscure. When two solids (i.e. solid under atmospheric conditions) are crystallised together, the complexes formed can generally be referred to as "cocrystals". However, not all cocrystals can be defined as host:guest systems as neither species can unequivocally be characterised as divergent or convergent. The term "host:guest" is often still used for such systems when the "host" is known to form a variety of adducts with other "guests".

Why are studies of inclusion chemistry important if the different species involved often interact *via* weak forces of attraction, and therefore have low association constants? One answer to this question is that the many important applications of host:guest chemistry include the separation of mixtures of closely related compounds and enantiomers, storage of gases and toxic substances, stabilisation of reactive compounds, slow release of drugs under physiological conditions, and control of reaction pathways by inclusion within reaction vessels or channels (topochemistry). Many of these applications impact on industrially and scientifically topical fields such as nanotechnology. Given the difficulties associated with definitions that are not as yet universally accepted, and conflicting information about definitions, the following rules will be applied here:

Host:guest system[7] :- complexes or host:guest systems are composed of two or more molecules or ions held together in unique structural relationships by electrostatic forces other than those constituting covalent bonds.

Host[7] :- the host component of a complex structure is defined as a compound(s) whose "binding sites" converge in the complex.

Guest[7] :- the guest component of a complex structure as any molecule(s) whose "binding sites" diverge in the complex.

Isostructural :- when two or more crystal structures are essentially identical, except for chemical composition, e.g. replacement of a transition metal results in the same crystal structure where only slight differences occur in coordination geometry.

Isoskeletal[18,43] **:-** a series of inclusion compounds can be described as isoskeletal when the host packing motifs are essentially isostructural (identical in structure) even though variation in the guest is possible. Good examples include Dianin's compound,[28] cholic acid,[44] calix[4]arene,[45] hydroquinone,[27] Werner clathrates,[46] cyclodextrins[30] and Bishop's alicyclic diol molecules.[47]

Cocrystal :- owing to the controversies surrounding the use of this term[48] the following definition will be used. Cocrystals are multi-component crystals in which two or more of the individual components are solids at standard temperature and pressure (STP), and the components amalgamate *via* non-covalent interactions other than ion-pairing.[49]

Framework (network) :- an infinite n-dimensional (1D, 2D and 3D) connection of molecules *via* intermolecular forces such as hydrogen bonds, coordination bonds and $\pi - \pi$ interactions. Interpenetration[50] or inclusion of guest molecules[51] normally arises.

Metal-organic framework *or* coordination polymer :- formed when the coordination of a multivalent ligand results in the propagation of metal centers in one or more dimensions.[18,19,34]

After the host:guest chemistry has been established for a particular system, the possibility usually exists of removing the guests and thereby producing a new crystal form of the host.[52] Removal of the guest often results in total degradation of the single crystallinity of the material although, in rare cases, the host can retain its single crystallinity after guest-removal. It is presumed that mechanical stress associated with the structural changes that accompany guest removal causes powdering (i.e. extensive fracturing) of the crystals. These powders are generally still crystalline, having a well-defined structure, and can be characterised using spectroscopic methods as well as x-ray powder diffraction. However, these methods generally fall far short of single-crystal x-ray diffraction as a characterisation tool and thus retention of single crystallinity is a much-desired result. These single-crystal to single-crystal transformations, first described for topochemical reactions involving the light-induced dimerisation of double bonds,[15] are immensely useful for understanding dynamics in the crystalline state. Why do some crystals remain intact when large transformations occur, and yet in other cases small transformations cause the crystals to fracture? This question is currently unanswered. Single-crystal transformations also provide insight into what is feasible in the crystal state. Is the crystal really the "chemical cemetery" as Dunitz *et al.* stated it to be regarded as by many chemists?[53] The simple answer to this is a resounding NO! The decomposition of many host:guest systems can even result in three or more different phases. An apohost phase can result, which is defined as the host with no guest, or partial decomposition can occur to yield a new phase with a lower guest:host stoichiometry. In some cases the guest can be completely removed with retention of the host lattice. This phase is referred to as being porous and therefore zeolite-like as it has the potential to absorb and desorb chemical species. This phenomenon is the primary focus of this thesis.

Porosity

Porosity is a term that needs to be defined. A simple dictionary definition of *porosity* is 'the quality or state of being *porous* or the ratio of the volume of interstices of a material to the volume of its mass'. *Porous* is defined as possessing or being full of *pores* or being *permeable* to fluids (both air and liquid), or capable of being penetrated. The latter concept of being *permeated* is easy to understand but what is a pore? Once again, according to the dictionary a pore is 'a minute opening especially in an animal or plant by which matter passes through a membrane', or a pore is 'a

small interstice admitting absorption or passage of liquid or gas'. From these definitions it can be understood that a crystalline solid can be said to possess porosity in terms of interstitial volume in relation to the mass of the material. In addition to this dimensional definition, a crystalline solid can be porous (i.e. has porosity) if it contains pores and/or is permeable to fluids moving in or out of the material.

Owing to the complexities surrounding the sorption of chemicals into any material, several important interpretations have now been expressed with regard to what constitutes a porous material. In the important book on zeolites by Breck,[54] it is stated that gas or vapour sorption experiments of a variety of compounds revels what kind of porosity a compound has. Both S. Kitagawa[34] and L. J. Barbour[55] have reiterated in recent review/perspective papers that "porosity" has to be demonstrated, normally by means of gas sorption isotherms, for a compound to be termed "porous". In conclusion, the mere occurrence of interstitial space, with or without included guests, does not warrant the compound being descried as porous. Furthermore, for an "open framework" to be defined as porous, it is required that permeability to fluids (gases or liquids) in both directions be demonstrated.

Why study porosity in crystalline materials in the first place? The pores that are generally found in crystals are at the nanometer scale and therefore tend to induce novel chemical and physical phenomena when chemical species are trapped within such small spaces. Consequently, the many applications associated with porous materials include catalysis (mainly due to the large surface area), molecular storage, molecular separation, and molecular sensing. All of these technologically relevant applications have long been associated only with zeolites or activated carbons. However, crystal engineering has given rise to novel materials such as organic crystals for separation,[56] inorganic materials such as metal phosphates,[57] as well as the now very important coordination polymers.[18,19,34,50,58-61]

Although porous materials have a large number of potential applications, gas sorption and separation will be the main focus of the study of these materials in this thesis. Clathrates of gases represent some of the earliest studies of clathrate chemistry and include such examples as the gas hydrates and β-quinol H_2S clathrate. Supramolecular chemistry of gases is a well recognised field of study.[62] A resurgence of gas storage and separation materials' studies has occurred in the last decade, primarily as a result of two significant events. The first event was the increase in the need for a satisfactory storage method for both natural gas (methane) and hydrogen

gas.[63] These two gases are envisioned as being replacement fuels of the future as the supply of crude oil dwindles. However, at present the methods of storing and transporting these gases are both inefficient and dangerous. The second event concerns the phenomenal increase in reports of open network coordination polymers (MOFs).[34,64]

The surge in studies of gas sorption by crystalline materials has necessitated the formulation of rigid rules to describe the concept of crystal porosity.[55] The rules set out by Barbour are as follows. *Virtual porosity* most often occurs by deletion of selected atoms (usual candidates include counter ions, solvent guest molecules and sometimes even the ligands bridging two metal ions) from a file containing the asymmetric unit of a crystal structure. This is closely related to the concept of an open structure: henceforth a compound that clearly shows a framework that contains guests is described as an open network (or framework) structure that has the *potential* to show porosity. *Transient porosity* (or porosity "without pores") refers to the phenomenon of gas and liquid permeability within crystals that possess lattice voids but have no obvious atomic-scale channels leading to these voids. Closely related to this phenomenon is the concept of "gating" within some porous systems.[45,65] Gating occurs in structures when pores are temporarily formed as a result of a particular stimulus (e.g. application of an external gas pressure above the "gate opening" pressure). *Conventional porosity* refers to the standard occurrence of fluid permeability within a crystalline material and is best emphasised by a type I sorption isotherm.[34]

Objectives and Results

The main objective of this study is the exploration, by crystal engineering, of the design features required for the formation of porous crystalline materials. This is mostly focused on the supramolecular aspects of packing within crystals to yield void space. As a consequence of this, most of the materials studied here are organic. However, two discrete coordination complexes were also studied as these compounds do not conform to the commonly investigated coordination polymer materials. Furthermore, the packing modes are reminiscent to those of organic molecular crystals (i.e. packing due to intermolecular interactions other than coordination bonds). A significant component of this study concerns seemingly nonporous porous

materials as a different class of compounds with respect to conventional porous materials.

As a continuation of a preexisting study of calixarene-based porous materials, two calixarenes (Scheme 1) were investigated. The first, *p-tert*-butylcalix[4]arene (TBC4), is a well-known organic host in the solid-state.[45] The sublimated phase of this compound was investigated for its ability to absorb gases and small molecules, even though no "pores" can be discerned within the structure - only interstitial void space is apparent.[66] Experiments aimed at understanding the mechanism by which the molecules diffuse within the crystal were performed. The second calixarene compound is 5,11,17,23-tetra-*tert*-butyl-25,26,27,28-tetramethoxy-2,8,14,20-tetra thiacalix[4]arene (MeOTBCS).[67] Sublimation experiments yielded two different phases of the pure compound. One of these phases possesses intriguing sorption abilities even though, once again, no "pores" are obvious.

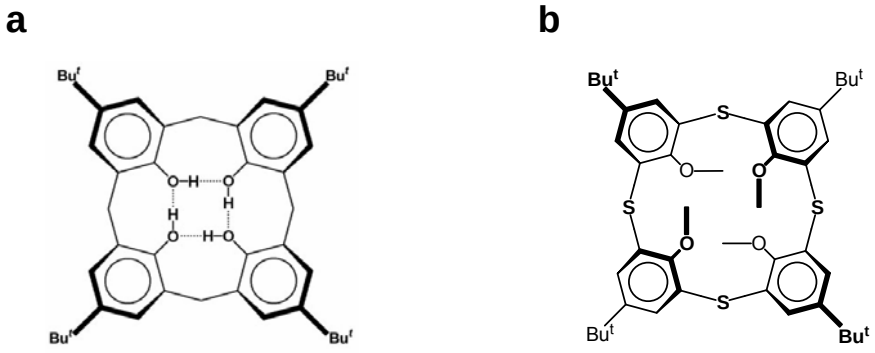

Scheme 1. a) *p-tert*-butylcalix[4]arene (TBC4) b) 5,11,17,23-tetra-*tert*-butyl-25,26,27,28-tetramethoxy-2,8,14,20-tetrathiacalix[4]arene (MeOTBCS)

Another approach to forming open networks in the organic solid-state is to use the high directionality properties of the hydrogen bond. The prototypic organic host that uses both hydrogen bonds and "odd-shape" is Dianin's compound (Scheme 2).[28] This classical host was reinvestigated for new host:guest chemistry.[68] Although the sublimed "empty" phase of Dianin's compound is well-known, its gas sorption potential has never been explored before, and have therefore been investigated here.

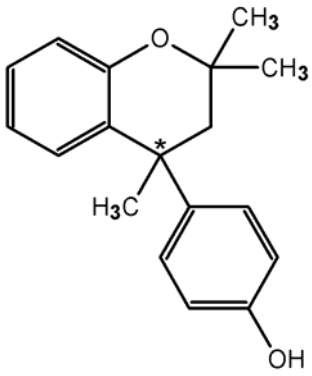

Scheme 2. Dianin's compound (* denotes the chiral center of this compound).

F. Toda and coworkers have extensively investigated the rigidity of a diacetylene bridging group when functionalised with hydroxyl groups.[69] In a related study, our work on the crystalline diol 2,7-dimethylocta-3,5-diyne-2,7-diol (Scheme 3a) containing a diacetylene bridging group lead to the serendipitous discovery of new and intriguing host:guest chemistry. The system possesses both polarity and chirality simultaneously and exemplifies a well-characterised case of self-inclusion.[43] Owing to a lack of porosity, modification (i.e. crystal engineering) of the host was undertaken. This resulted in the structural characterisation of 2-methyl-6-phenylhexa-3,5-diyn-2-ol (Scheme 3b) with a structure analogous to that of 2,7-dimethylocta-3,5-diyne-2,7-diol.

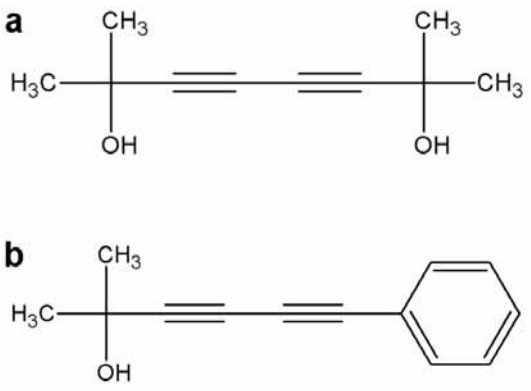

Scheme 3. (a) 2,7-dimethylocta-3,5-diyne-2,7-diol. **(b)** 2-methyl-6-phenylhexa-3,5-diyn-2-ol.

Utilisation of discrete metallocycles represents the next step in designing a porous material. "Donut-shaped" molecules that cannot interdigitate naturally form

void spaces when packed together. As a result, the two dinuclear "donut-shaped" complexes (Scheme 4) were synthesised in collaboration with Dr. Liliana Dobrzańska.[70] Desolvation of the crystals occurred by single-crystal to single-crystal transformation, allowing a detailed study of the resulting porous compounds.

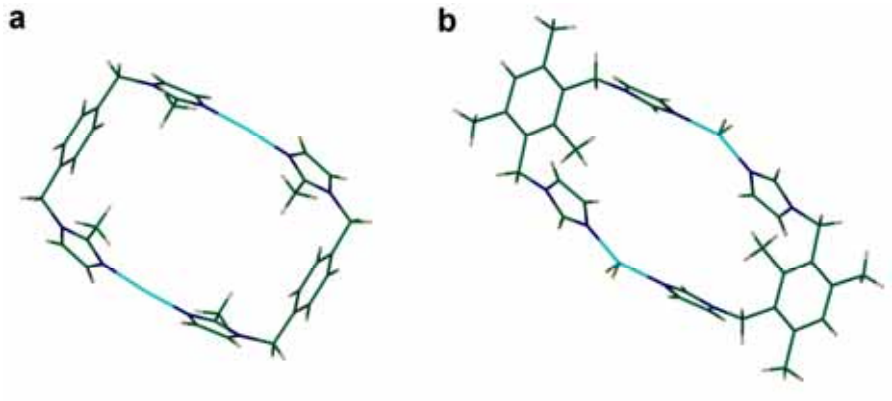

Scheme 4. a) $[Ag_2IMID_2]^{2+}$ donut-shaped complex. b) $[Cu_2(BITMB)_2(Cl)_4]$ metallocycle

All of the porous crystalline materials were further investigated for their gas sorption properties using equipment and methodology developed as part of these studies. These include accurate determination and visual representation of void space and pore dimensions using Connolly's MSROLL software, which was interfaced with Barbour's X-Seed program.[55] A method for investigating the thermodynamic parameters associated with gas sorption into a porous system is presented here and is used to help provide insight into the phenomenon of "nonporous" sorption.

2. Synthesis

5,11,17,23-tetrakis(1,1dimethylethyl)-25,26,27,28-tetrahydroxycalix[4]arene (abbreviated as *p-tert*-butylcalix[4]arene)

The general 'one-pot" procedure using the base (NaOH) catalysed reaction optimised by Gutsche *et al,*[71] and described in the book *Macrocyclic synthesis, A practical approach,* edited by David Parker,[72] was used to synthesise *p-tert*-butylcalix[4]arene.

MeOTBCS

MeOTBCS was synthesised using the literature method of reacting *t*-butyl phenol with elemental sulphur using a base catalyst.[7] Methylation of the OH groups was carried out using cesium carbonate as described in the book *Macrocyclic synthesis, a practical approach*.[72]

1,4-bis(2-methylimidazol-1-ylmethyl)benzene (IMID)

2-Methylimidazole was reacted with a unimolar quantity of α,α-dichloro-p-xylol (in a 10:1 molar ratio) in 100ml of methanol under reflux for 15 hours. Purification was carried out by removing the solvent under vacuum, and then dissolving the residue in a saturated solution of potassium carbonate. The product precipitated from this solution and was washed with water.

1,3-bis(imidazol-1-ylmethyl)-2,4,6-trimethylbenzene (BITMB)

The same procedure used for the synthesis of IMID was used for BITMB except that a 10 molar quantity of imidazole and a unimolar quantity of 2,4-bis(chloromethyl)-1,3,5-trimethylbenzene were used. Purification was carried out by removing the solvent under vacuum, and then dissolving the residue in a saturated solution of potassium carbonate. The product precipitated from this solution and was washed with water.

2,7-dimethylocta-3,5-diyne-2,7-diol and 2-methyl-6-phenylhexa-3,5-diyn-2-ol

Oxidative coupling of acetylenes utilising Cu(I)Cl was performed to synthesise 2,7-dimethylocta-3,5-diyne-2,7-diol from 2-methyl-3-butyn-2-ol. 2-Methyl-6-phenylhexa-

3,5-diyn-2-ol was synthesised using the same method, but reacting 2-methyl-3-butyn-2-ol with bromoethynyl benzene.

Dianin's compound

The condensation of phenol with mesityl oxide in acidic conditions, as outlined in the original paper[28a] written in Russian, and optimised by Dr. Bredenkamp, was used to synthesise Dianin's compound.

General procedures for growth of crystals.

In nearly all cases, crystals were grown by slow evaporation of a solution. In the cases of the coordination compounds, appropriate molar quantities of metal salt and ligand were dissolved in a solvent or solvent mixture. This was effected in new glass vials after using compressed air to blow out dust that might act as nucleation sites. The vials were then sealed with parafilm or polytops, with a few holes to allow slow evaporation of the solvent. The slow vapor diffusion technique was used on coordination compounds when the diacid ligands needed to be deprotonated by an amine base introduced slowly via the vapor phase. For organic compounds, a small quantity of compound or compounds (+50mg) was also dissolved in solvent and slow evaporation of the solvent yielded crystals. The vial and perforated lid system was used. Sublimation under vacuum was also used for crystallisation of organic compounds. This was done in a commercially available glass oven supplied by Büchi.

3. Instrumentation and Experimentation

Many routine experimental techniques were used during this study and will only be described briefly as the literature abounds with the theory and practice of these methods. No attempt will be made to direct the reader to specific references or general background provided on the techniques. However, a few non-standard techniques and instruments were developed and refined for the work to be undertaken effectively. These will be described in more detail in later chapters and, where possible, background information will be given.

Single-Crystal X-ray Diffraction Analysis

When suitable crystals were found to have good morphology and extinguished plane polarised light uniformly, they were cut, when necessary, and placed on the end of a glass rod using paratone oil. A Bruker-Nonius SMART Apex single-crystal x-ray diffractometers, equipped with an Oxford cryostream cooling system, was used to collect diffraction data.

Thermogravimetric Analysis

Using a TA Instruments Q500 thermogravimetric analyser, samples of 10-25 mg were heated from ambient temperature to 450-500^{o}C at a constant heating rate of 5 ^{o}C/min.

Differential Scanning Calorimetry

Using a TA Instruments Q100 differential scanning calorimeter, samples of 5-20 mg were heated from ambient temperature to 450-500^{o}C at a heating rate of 5 ^{o}C/min.

Hot Stage Microscopy

A hot stage was constructed locally. It consists of a circular copper heating plate with a small hole of approximately 1mm diameter in the centre. The heating element was connected to a variable voltage supply and temperature was monitored using a k-type thermocouple. The polarising stage of the microscope was removed and replaced with the hot stage. A thin glass cover slide was used to support the crystals such that they could be visually inspected during heating.

Nuclear Magnetic Resonance Spectroscopy

Samples were dissolved in deuterated chloroform and ^{1}H and ^{13}C NMR spectra were recorded using a Varian Unity INOVA 400 MHz spectrometer.

Infrared Spectroscopy

Crystalline samples were analysed using a Nicolet Avatar 330 FT-IR instrument with an ATR (attenuated total reflection) accessory (Smart Performer).

Connolly Surface Package for Structural Analysis

The program MSROLL by Michael Connolly,[76] originally designed for use in protein cavity studies, was incorporated into X-Seed to allow the analysis of void spaces and pore dimensions. MSROLL maps the free volume available to a spherical probe, whose radius can be specified. The original software calculates the *contact* surface of the probe. As determination of pore size requires calculation of an *accessible* surface, the software was modified to give the option of mapping either type of surface. This modification is simple, yet effective – the specified probe radius is added to the van der Waals radii of each of the atoms involved, the probe radius is then given as zero and the accessible surface is the "contact" surface traced by the centre of the probe. The permeable radius of a circular pore can be determined by systematically increasing the probe radius until the accessible surface does not extend beyond the centre of the pore.

The gas sorption instrument and methodology will be described in Chapter 5.

4. Host:Guest Chemistry and Crystal Structures

There has been significant recent interest in the study of porosity and gas sorption by materials such as carbon nanotubes, zeolites, silicates, graphite and coordination polymers.[58b,64,75] However, given the emphasis placed on optimising sorption capacity as percentage gas uptake by weight, it is rather surprising that the solid/gas supramolecular chemistry of purely organic crystals has received only limited attention. It is self-evident that substituting heavier elements with lighter analogs can enhance weight percentage values for a given topology. To date this approach has yielded some success as exemplified by the construction of zeolite mimics that incorporate carbon-based spacer ligands.[58b,19] But the tide seems to be turning, as purely organic crystals are now beginning to receive increasing attention in the quest for new porous gas sorbing materials.[45,76]

The study of porous organic materials has a long history, originating in the host:guest chemistry of crystalline solvates.[52b,77] In particular, in more recent times Wuest has reported impressive results using compounds with hydrogen bonding functional groups such as aminotriazine and pyridinone. These materials exhibit porosity at the solid/liquid interface.[78] With regard to gas sorption, the work of Sozzani *et al.* has demonstrated that tris-o-phenylenedioxycyclo-triphosphazene crystals can be used for gas storage.[76b] Through the work of Atwood and Barbour, calixarene-based organic crystals have emerged as materials exhibiting intriguing gas sorption capabilities and host:guest chemistry.[45,56,69a,79] Some of the organic crystalline materials described here build on the work cited above and involves the use of both classical and non-classical systems in an attempt to better understand porosity in organic crystals. The structural aspects of the crystal forms employed in the gas sorption experiments are described in this chapter, while discussion of the sorption experiments is deferred to Chapter 5.

Crystals capable of gas sorption can be categorised as either “porous” or “seemingly nonporous”. The host:guest chemistry of two systems that can be defined as porous are investigated. These are the helical structures of 2,7-dimethylocta-3,5-diyne-2,7-diol and 2-methyl-6-phenylhexa-3,5-diyn-2-ol, and Dianin’s compound. The helical structures are newly described whereas Dianin’s compound is well-known as a classical organic host system. In the case of Dianin’s compound, new host:guest

chemistry is described. The structural aspects of two nonporous systems involving *p-tert*-butylcalix[4]arene and 5,11,17,23-tetra-*tert*-butyl-25,26,27,28-tetramethoxy-2,8,14,20-tetrathiacalix[4]arene are also described. These two sets of studies will help to better understand the counterintuitive diffusion of small molecular species into nonporous crystalline materials.

Finally the structure and properties of discrete metallocyclic compounds will be presented. The first example consists of a cationic silver complex crystallised to form a one-dimensional channel-type porous crystal. The second compound consists of a neutral copper complex that represents the first metal-organic member of the seemingly nonporous porous family of crystalline materials.

Helical host systems

Diol host systems constitute a mainstay of solid-state supramolecular chemistry.[47,69b] Hydrogen bonding of the alcohol groups is crucial to the understanding of the clathration abilities of these hosts. In some cases, helical host lattices are formed by alicyclic diols through intermolecular hydrogen bonding of the hydroxyl groups to create a host framework with voids space for guests.[47] If the diol host is sterically bulky, for example 1,1,6,6,-tetraphenyl-2,4-hexadiyn-1,6-diol (Scheme 5),[69b] hydrogen bonding is utilised to bind the guest.

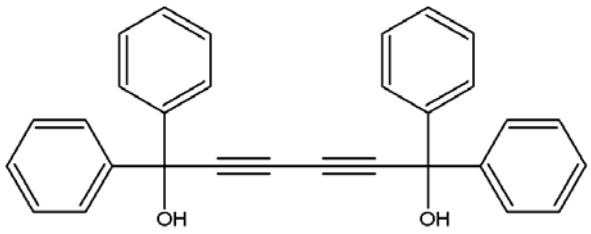

Scheme 5. 1,1,6,6,-tetraphenyl-2,4-hexadiyn-1,6-diol

A serendipitous discovery of a crystalline byproduct yielded the crystal structure of 2,7-dimethylocta-3,5-diyne-2,7-diol (Compound **1**, Scheme 6). The structural similarity between 1,1,6,6,-tetraphenyl-2,4-hexadiyn-1,6-diol and compound **1** is not reflected in the crystal packing mode of the two compounds: **1** behaves more like the alicyclic diols reported by Bishop.[47] A literature survey of **1** shows that it is a common byproduct of acetylenic coupling reactions involving 2-methyl-3-butyn-2-ol

but there is only one structural report of its (possible) host:guest chemistry,[80] namely a dichloromethane clathrate. However, as will be shown below, this structure report may be erroneous.

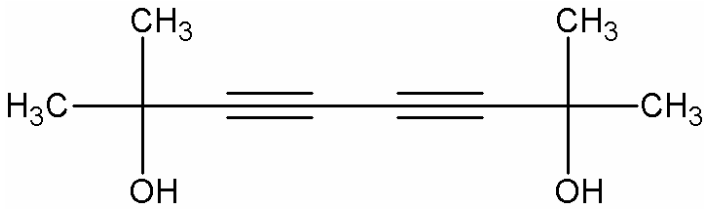

Scheme 6. 2,7-dimethylocta-3,5-diyne-2,7-diol

The structural report of compound **1** describes a tubular (Figures 3 and 4) clathrate of dichloromethane (thought to be highly disordered). Precisely the same host structure is apparent in all the structures elucidated in this project. This suggests that **1** might form the basis of one of the few examples of a host system where the same framework persists with different guests.[45] Compound **1** crystallises in the space group *R*3. Owing to the three-fold symmetry of the framework, it was thought that a guest with the same symmetry would alleviate the problems associated with disorder that inherently occur when a minor component does not match the overall symmetry of the structure. For this reason carbon tetrachloride (CCl_4) was used. A small amount of **1** was dissolved in warm CCl_4 and allowed to cool. Rod-shaped needles, suitable for SCD analysis, grew from this solution.

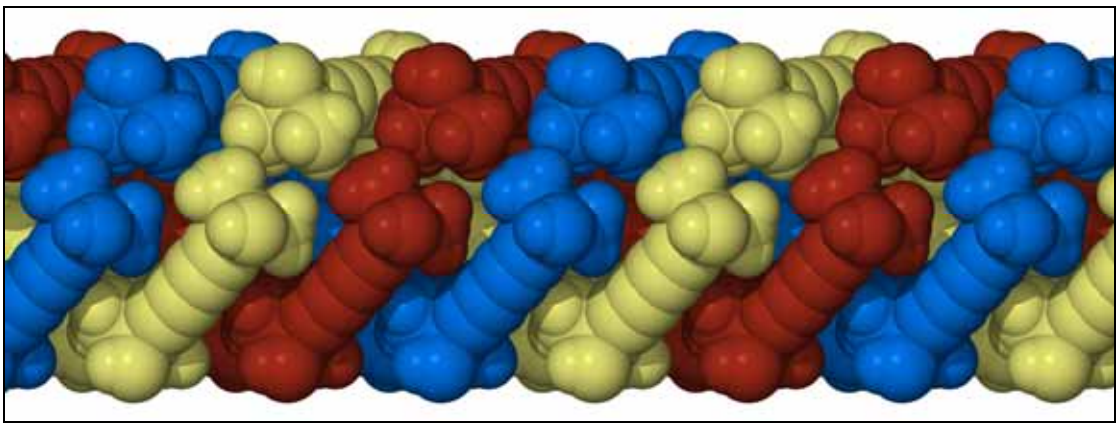

Figure 3. Triple helical "tube" found with host system of **1**. Atoms are shown in spacefilling representation. Guests included in the tube have been removed for clarity.

SCD analysis reveals that the CCl_4 is enclathrated as expected. Moreover, the resulting structure, also in the *R*3 space group, possesses no disorder. The host forms triple helical tubes (threefold stacks of eclipsed molecules) that are hydrogen bonded to each other via their hydroxyl groups (Figures 3 and 4).

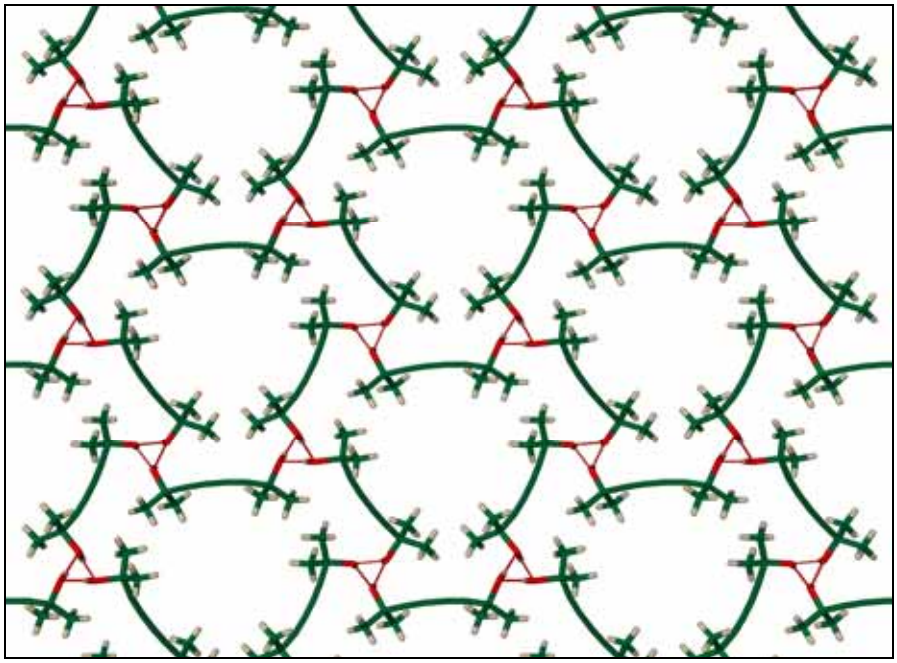

Figure 4. Packing of the triple helical tubes stabilised by the hydrogen bonded association of hydroxyl groups. Molecules shown in capped-stick representation and guests are removed for clarity. Red dashed lines represent hydrogen bonding.

The hydrogen-bonded spiral, termed "the spiral chains of hydrogen bonds to produce a spin" by Bishop, is a well-recognised motif available for the association of hydroxyl groups by hydrogen bonding (Figure 5).[47] The CCl_4 is trapped inside the void space formed within the helical tubes of **1** (Figure 6). This enclathration of CCl_4 is interesting with regard to the formation of *polar* chiral crystals. Note that the CCl_4 molecules are all oriented in the same direction within a channel. Indeed, this is also that case throughout the crystal structure. Therefore, the crystal structure is both chiral (helical tubes) and polar (CCl_4 guests oriented all in the same direction). The generation of polar, chiral crystals has potential applications such as second-harmonic generation (SHG) in non-linear optics. The directionality of the CCl_4 is related to the shape of the void space in which the CCl_4 is located. Although spacefilling representations appear to depict the channel of the helical tube as uniform in width,

this is not the case (Figure 6b). The channel is punctuated by regularly spaced bottlenecks resulting from the positioning of the host methyl groups of **1**. This predisposes the CCl_4 molecules to be positioned in the wider spaces of the channel.

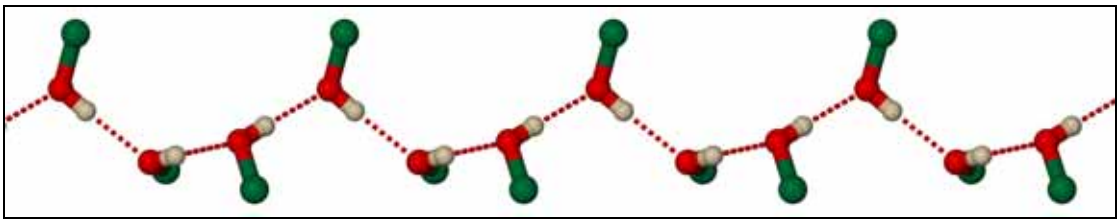

Figure 5. The hydrogen bonded single helical motif formed by the host hydroxyl groups in structures of **1**. Atoms are shown in ball-and-stick representation. Dashed lines represent hydrogen bonding. Only the carbon atom bonded to the hydroxyl groups and the hydroxyl groups themselves are shown for clarity.

Thus, once one CCl_4 is oriented in a particular direction within the channel, its direction will determine the direction of all the other CCl_4 molecules within the same channel. This is due to the manner in which the CCl_4 molecules need to be situated within the bulges of the channel in order to effectively occupy the space available. However it is less easy to rationalise why there appears to be a form of "communication" between neighbouring channels with regard the observation that the CCl_4 orientation *throughout* the crystal is unidirectional. It is also interesting that there appears to be some van der Waals overlap between the guest chlorine atoms and the host carbon atoms. The Cl···C distance is 3.271 Å, which is well within the sum of the van der Waals radii of 1.7 Å and 1.8 Å, respectively. This can be clearly seen from Figure 6b: The van der Waals surface of the CCl_4 guests protrude through the Connolly surface. This possible overlap of electron clouds is perhaps due to the ellipsoidal shape of the chlorine atoms and the carbon atoms, and not because of true van der Waals overlap (such as occurs in a hydrogen bond).[22-26]

The helical packing of **1** is similar to that of the helical host lattices formed by the alicyclic diols. Interestingly, if one follows the six structural membership rules defined for the alicyclic diol series, compound **1** matches exactly except, of course, that it is not alicyclic.[47] Also of interest is that **1** can now be considered to be one of the few small molecules known to form hydrogen bonded helical host structures (i.e. such as members of the urea family).[81]

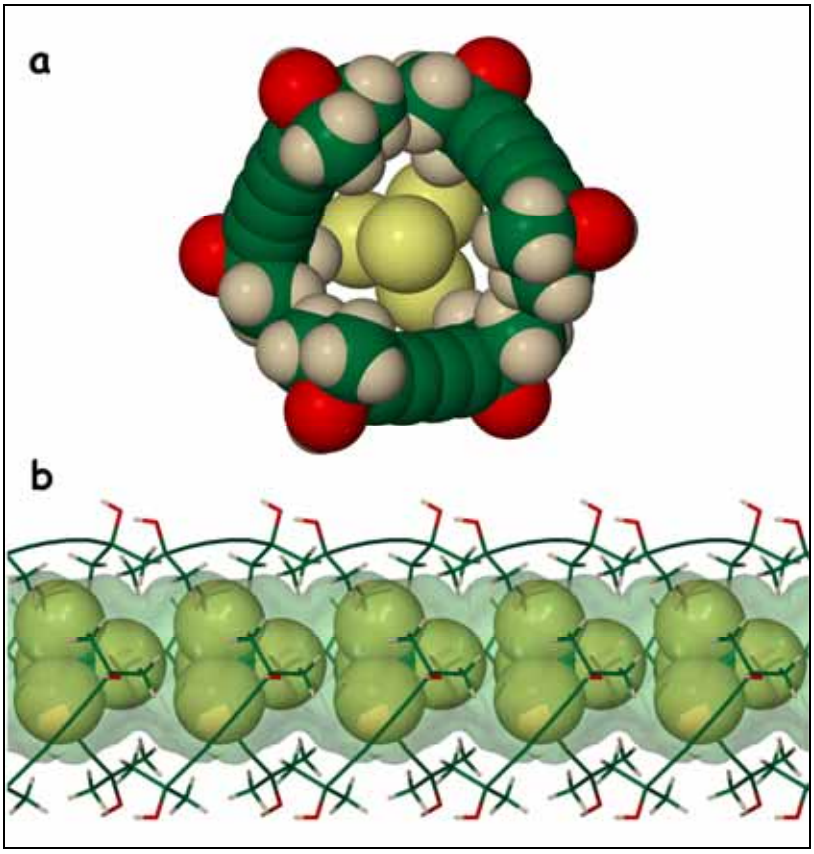

Figure 6. a) Enclatharation of CCl_4 in helical tubes formed by host **1**. All molecules are shown in spacefilling representation. **b)** Diagram showing the polar orientation of the CCl_4 molecules in the helical tubes of **1**. A Connolly surface (probe radius of 1.17 Å) of the interior of the helical tube is shown at 0.7 % transparency (lime green) to allow visibility of molecules behind and within the surface. Molecules of **1** are shown in capped-stick representation and CCl_4 molecules are shown in spacefilling representation.

The host:guest chemistry of **1** was studied further by dissolving **1** in several solvents to investigate possible enclathration. Interestingly most of the common solvents such as water, all of the "small" alcohols, alkanes (branched and linear), acetonitrile, acetone and toluene did not form solvates. The structures of the crystals grown from these solvents appeared to be either empty, or filled with disordered solvent. NMR and IR studies of the crystals revealed that solvents were not present in these cases. Compound **1** gives rise to two proton NMR peaks at 3.47 and 3.95 ppm and four carbon NMR peaks at approximately 30.9; 65.5; 66.3 and 84.0 ppm, as might be expected. The solid-state IR spectra are relatively simple and the elucidation of the solvent guest peaks was accomplished by comparing the sublimed crystals with solvated crystals, and by referencing against solvent peaks found in the Aldrich

Library of Infrared Spectra (Spectra given in Appendix B).[82] Sublimed **1** is used as a reference spectrum to compare with the solvate or suspected solvate crystals. The solvate crystals were allowed to dry in order to exclude any surface solvent on the crystals from interfering with the analysis. The only exception to the solvents that are not enclathrated is benzene. It should be noted that TGA of several solvates indicated that the solvent is only released when the host compound sublimes. TGA is therefore not a useful method of characterising these systems.

The benzene enclathrated crystals differ from the other solved crystals in that the guest is significantly different in shape. This disparity causes difficulties in locating and refining the benzene guest well and it was therefore constrained to conform to a hexagonal shape. The host structure is the same as previously observed and it orients the benzene into discrete pockets along the channel of the helical tubes (Figure 7). However, the benzene is not orientationally polarised as in the case of the CCl_4 structure.

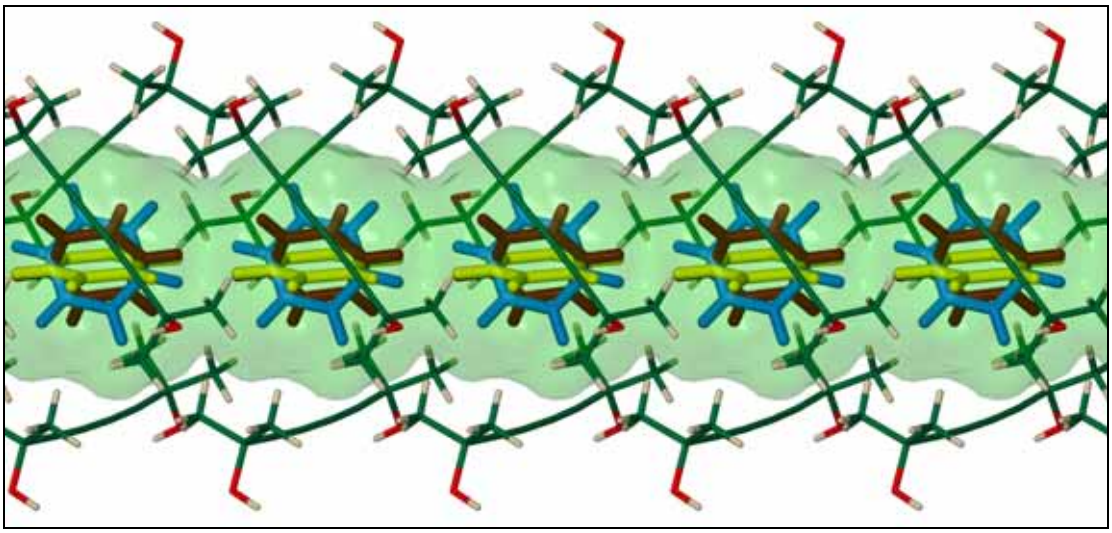

Figure 7. The structure of the **1**$_3$·Benzene clathrate showing the positions of the disordered benzene guests within the helical tubes. The three symmetry-related positions of benzene are shown in blue, yellow and brown. All molecules are shown in capped-stick representation

To investigate whether the crystals that appeared to be empty were indeed porous, the crystals were exposed to iodine vapours. None of these crystals changed colour, thus implying that iodine had not been adsorbed. Although this does not constitute proof of no porosity, it can still be viewed as a negative result. The

enclathrated crystals were also tested after the crystals had been allowed to dry for a few days. Interestingly the benzene-included crystals absorbed iodine as evidenced by their tips changing colour. The dark red tip of a crystal was cleaved and subjected to x-ray diffraction analysis to reveal an iodine clathrate. The $\mathbf{1}_3 \cdot I_2$ crystal structure is interesting in that the host system is identical to those investigated thus far. The iodine does not pack in a linear fashion along the channel as observed for the conducting tris(o-phenylenedioxy)cyclotriphosphazene$\cdot I_2$ adduct.[83] In our case the iodine is disordered, owing to the symmetry, in the discrete pockets of the channel and is orientated at an angle of ~75° relative to the axis of the channel (Figure 8). As with the benzene-included structure, the iodine guest is not orientationally polarised within the channels of the helical host.

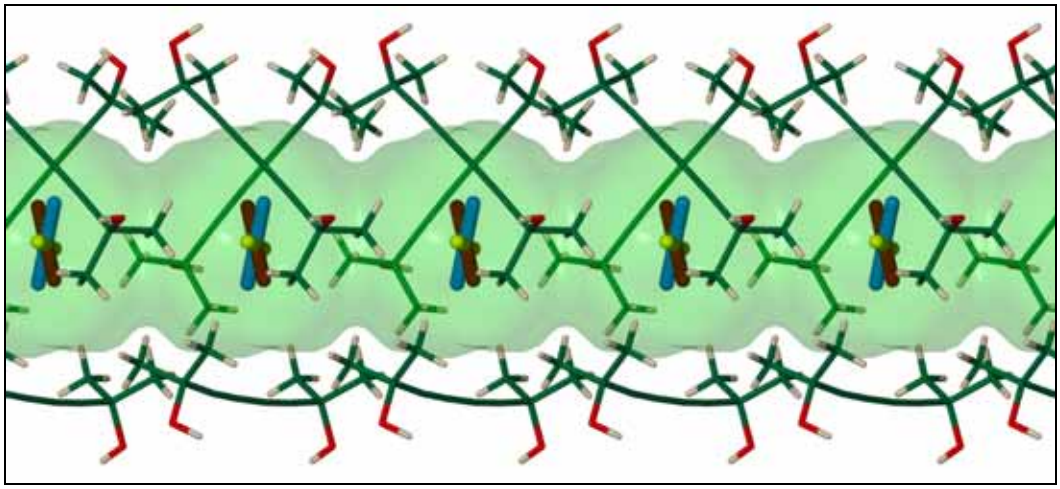

Figure 8. $\mathbf{1}_3$·Iodine adduct structure showing how the iodine molecule is disordered within the widest part of the channel. The three possible orientations of iodine are shown in yellow, blue and brown. All molecules are shown in capped-stick representation.

Based on this result, it was hoped that this system could be used for gas sorption studies. However, such experiments revealed almost no gas sorption for both the apparently empty crystals and the evacuated clathrate samples. This implies that the crystals form a well-packed system upon guest loss, or when guest is not encapsulated. Vacuum sublimation is an obvious technique that can be used to produce guest-free crystals. Sublimation of **1** revealed what once again appeared to be an empty host with the same host framework. Although some electron density was apparent within the channel, NMR revealed that only **1** is present in the crystals. Gas

sorption was attempted again and once more the results were negative. This led to a detailed crystallographic analysis of the "empty" crystals in an attempt to account for the mysterious electron density within the channels. The highest electron density peaks were modeled as partial-occupancy carbons and the structure was expanded to reveal the possible identity of the "guest". Surprisingly, the "guest" resembled disordered **1** (Figure 9). Thus these crystals, and possibly the reordered phase after guest loss, can be described in terms of molecular self-inclusion. In the literature, self-inclusion has been used to describe systems where a framework of crystal structure can be defined and the same compound is found in this framework in a different orientation or configuration. Examples of this phenomenon include trimesic acid hydrate[84], the self-inclusion of one of the helical tubuland family exo-2,exo-6-dihydroxy-2,6-dimethyl-9-oxabicyclo(3.3.1)nonane (another diol)[85], and 4,4-bis(4-hydroxyphenyl) cyclohexanone.[86] However, in none of these examples of self-inclusion has it been fully shown that the "host system" forms the same framework when a different guest is included. In the two examples of the trimesic acid monohydrate structures, the "framework" possesses subtle differences. The layers that constitute the host framework are aligned exactly in the case of the picric acid structure whereas in the self-included example the layers are misaligned. As well as the framework being different the fact that two components are needed to make the framework means self-inclusion is inappropriate as only one of the two components is included in the host framework. In both of the other two cases of self-inclusion, only the so-called self-inclusion structure has been found and no other "guest" has been included. In the case of compound **1** the host system is exactly the same whether the included guest is the host molecule itself, or another molecule all together.

This form of "true" self-inclusion exhibited by compound **1** therefore appears to the first of its kind. The overall disorder of included **1** is not just due to the threefold symmetry of the system but also due to possible staggering within neighbouring channels. Figure 9 shows how the disorder can be visualised. In any particular channel within a crystal there is probably no disorder of the guest molecules except for the threefold disorder of the methyl and hydroxyl groups. The disorder is due to how the guests in neighbouring are oriented in relation to the visualised channel. The disorder dictates that the neighbouring channel's guests can be located in two different, but overlapping positions, and there is an even chance of either possibility within a given

channel. This is in contrast to CCl_4 crystal structure where the channels and their contents are all identical according to the crystallographic model.

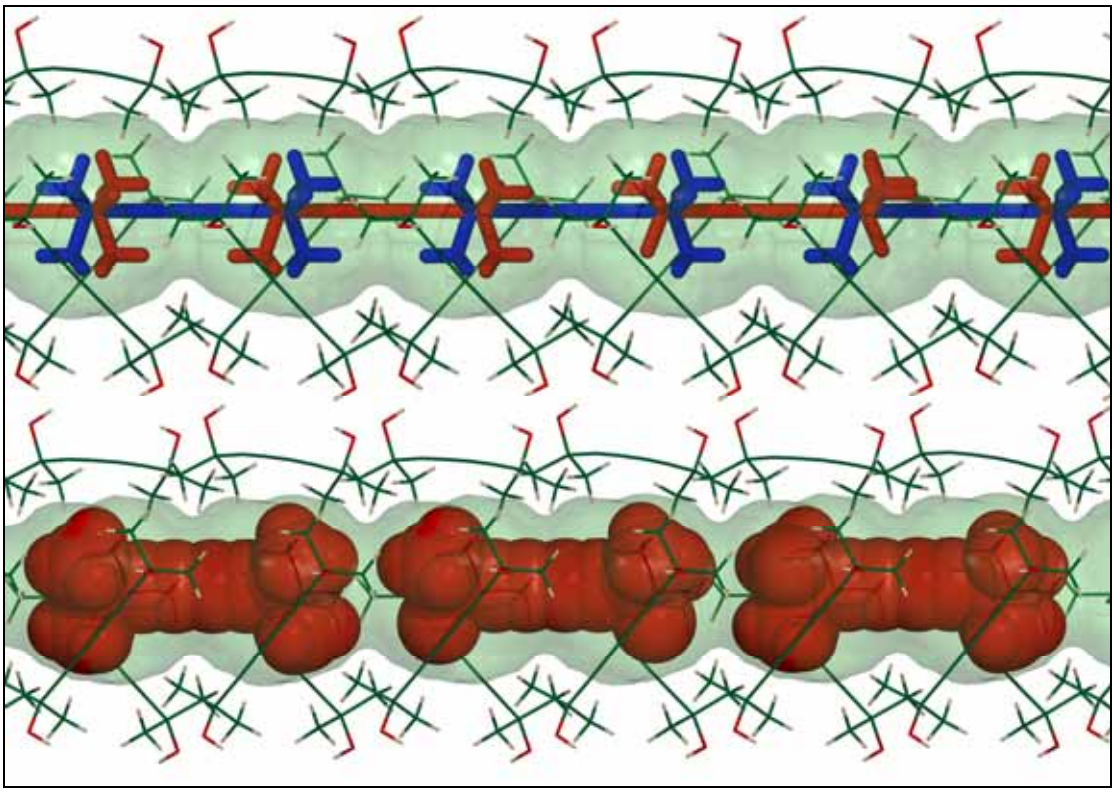

Figure 9. Self-inclusion of **1**. Two adjacent channels showing the positions of the "guest" molecules of **1** in red as observed in the ordered structure. It can be seen that the guest molecules are positionally staggered with respect to those of the neighbouring channels. The blue molecules shown in the top channel indicate the alternative positions of the guest molecules in the disordered structure. Therefore, in the disordered structure, the molecules within each channel are most likely stacked end-to-end in an ordered fashion, but bear no relation to the ordering in the neighbouring channel. Ultimately, the disorder observed is a reflection of the average structure with respect to the relative guest positions in neighbouring channels.

Our characterisation of the self-included structure sheds light on the structure report of $\mathbf{1}_3 \cdot CH_2Cl_2$ mentioned earlier.[80] The paper reports a dicloromethane clathrate, but after many attempts to reproduce this result, it appears that this report is incorrect. IR, NMR and x-ray analyses show that dichloromethane is not enclathrated and that the crystals grown from a dichloromethane solution are always self-included. It appears that the electron density of the self-included **1** was mistaken to be disordered

dichloromethane. This "honest mistake" shows that x-ray analysis is not infallible and that it is advisable to ensure that the structural model is consistent with results obtained from supporting analytical measurements.

In total only a few solvents were found to be included by **1**. These are benzene, CCl_3Br, CCl_3CN, CCl_4, $SiCl(CH_3)_3$. The I_2 adduct could only be produced by exposing dried $\mathbf{1}_3$·benzene crystals to iodine vapour. Compositions were also confirmed by IR and NMR analysis of these clathrates since x-ray diffraction analysis can be problematic. It is interesting to note that the trichloromethyl and trimethylsilyl moieties seem to be facilitate inclusion into **1** whereas the *tert*-butyl moiety does not. This indicates that the host system is highly selective. The adducts of CCl_3Br, CCl_3CN, CCl_4, $SiCl(CH_3)_3$ all feature polar alignment of the guest within the chiral host channel (Figure 10).

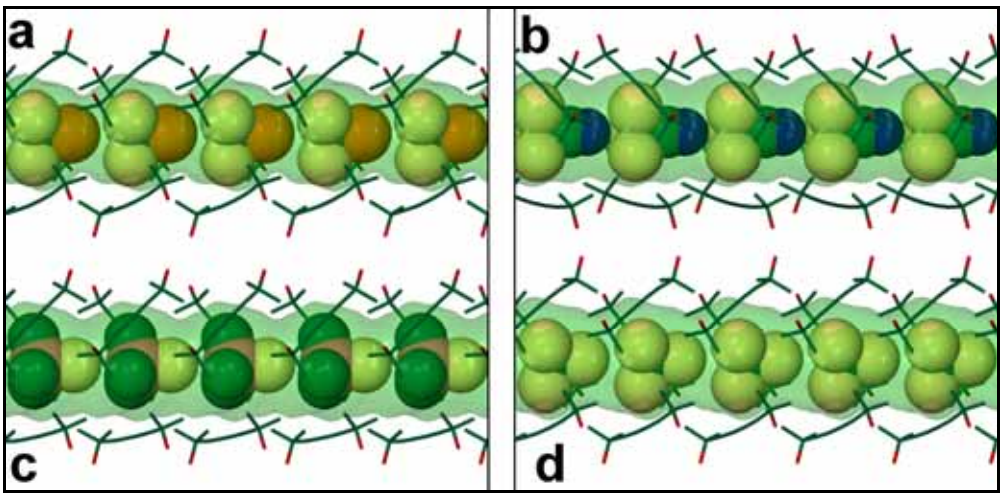

Figure 10. Polar alignment of the four guest compounds CCl_3Br **(a)**, CCl_3CN **(b)**, $SiCl(CH_3)_3$ **(c)** and CCl_4 **(d)** shown in van der Waals representation inside the channels (transparent green surface) produced by the host framework (shown in capped-stick representation). The helices are left; right; left; left for the structures a to d, respectively. All structures are viewed down the *b* axis.

This is an interesting result in that the crystals are both *polar* and *chiral*. This suggests that these crystals could be useful for second order non-linear optics. Second order non-linear optical materials are required to be non-centrosymmetric. Theoretical considerations dictate that polarity is also a very important aspect of such materials.[87] For these reasons, the non-linear optical properties were measured. For technical

reasons a full study of these properties could not be undertaken, but it was found that these crystals possess significant non-linear optical properties.

The findings associated with compound **1** led to the investigation of the possibilities for crystal engineering with a view to designing a porous material. As compound **1** was discovered during the synthesis of 2-methyl-6-phenylhexa-3,5-diyn-2-ol (compound **2,** Scheme 7), a phenyl derivative of **1**, the crystal structure of **2** was determined to see what effect the phenyl substitution has on the packing.

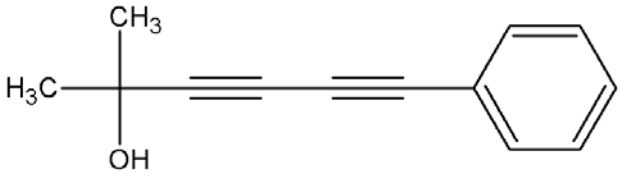

Scheme 7. 2-methyl-6-phenylhexa-3,5-diyn-2-ol

Interestingly, the helical motif is present once again. However, in this case the space group is $P3_2$ (or $P3_1$). Compound **2** forms a quadruple helix instead of the triple helix formed by **1** (Figure 11). In addition to the helical relationship between the two structures, it can be seen that neighbouring tubes are similarly aligned next to one another (Figure 12). However, since the *tert*-alcohol moiety of **1** is replaced in **2** by a phenyl moiety, there is a loss of some hydrogen bonding capability. This loss is compensated for by the formation of edge-to-face π-π interactions (also known as C-H···π interactions, H···centroid distance of 2.939 Å).

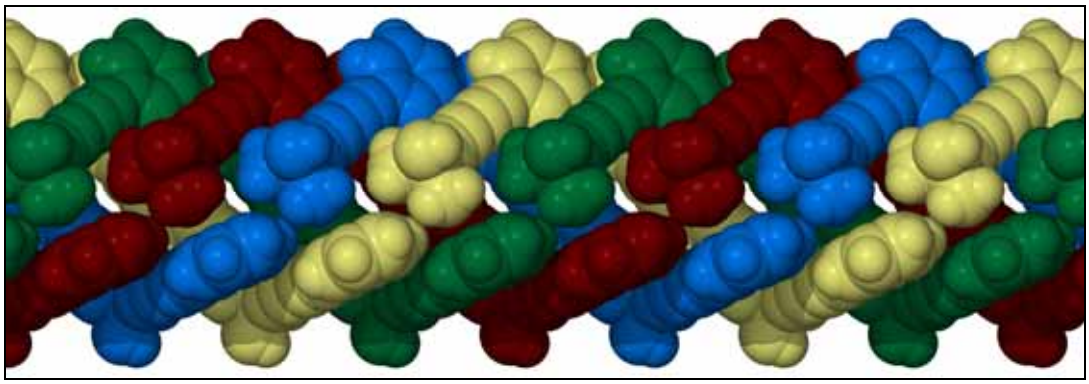

Figure 11. Quadruple helical tube in the crystal system of **2**. Atoms are shown in spacefilling representation.

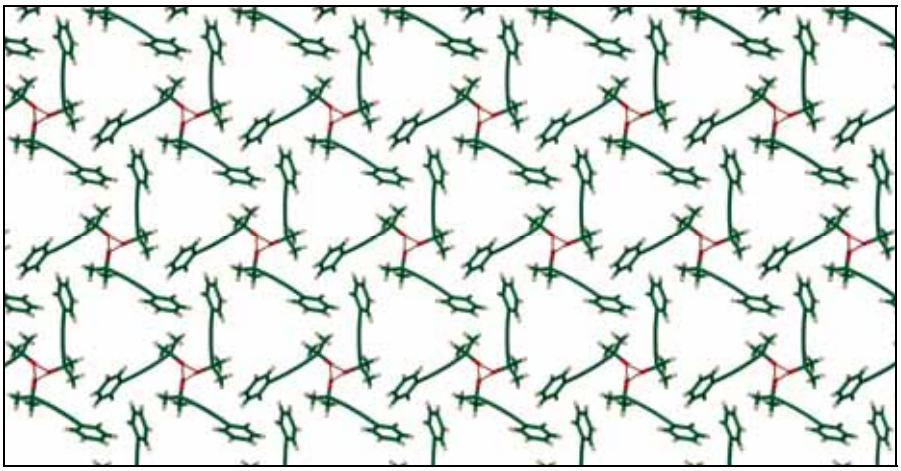

Figure 12. Packing of the quadruple helical tubes *via* the single hydrogen bonded hydroxyl groups and π···π interactions. Molecules are shown in capped-stick representation and guests are removed for clarity. Red dashed lines represent hydrogen bonding.

The replacement of hydrogen bonds by π-π interactions is an interesting crystal engineering concept. It was hoped that, owing to the bulky size of the phenyl moiety, the occurrence of self-inclusion would be impaired. Sublimation of compound **2** results in the desired structure, without any apparent self-inclusion. This is evidenced by the total lack of any appreciable electron density (largest peak of 0.27 $e^-/Å^3$) in the open space within the quadruple helical tube. Unfortunately both the I_2 and gas sorption failed, implying that the sublimed material lacks any appreciable porosity. This does not necessarily mean that there is no chance of porosity, as the single-crystal structure apparently indicates large open channels and a low density of 0.91 g/cm^3, but rather that bulk production of a porous phase of this material is more difficult than anticipated. The possibility of polymorphism of the powdered sample used for gas sorption cannot be discounted either.

A CCDC search for 4-diphenylbutadiyne,[88] and our own determination of its crystal structure, reveals that the natural progression from one phenyl moiety to two leads to a completely new structural packing motif. 4-Phenylbuta-1,3-diynylbenzene crystallises in the space group $P2_1/n$ and packs (not surprisingly) in a herringbone motif. There are two known adducts of this compound involving pentafluorobenzoic acid and 1,4-bis(perfluorophenyl)butadiyne.[89] These two structures both crystallise in the space group $P1$, and are structurally similar, but share no similarities with the two

helical structures formed by compounds **1** and **2**. Another possible modification of compound **1** that is the replacement of the methyl moieties with protons to form hexa-2,4-diyne-1,6-diol. There is a structural report dating from 1971 that refers to this molecule packing in the $P2_1/c$ space group, but the coordinates are unfortunately not available.[90]

Other crystal engineering modifications could be made to the helical host systems formed by compounds **1** and **2**, other than those mentioned above. One of the foremost goals of host:guest research is the creation of chiral host systems. This could easily be introduced synthetically into the compounds **1** and **2** by using 3-butyn-2-ol instead of 2-methylbut-3-yn-2-ol. 3-Butyn-2-ol is chiral and is available commercially in its resolved form, or as a chiral mixture. This may allow an extensive synthetic and crystallographic study by using molecules analogous to those shown in Scheme 8. Chiral acetylenic alcohols have a long history of inclusion chemistry, especially as demonstrated by Toda.[69a]

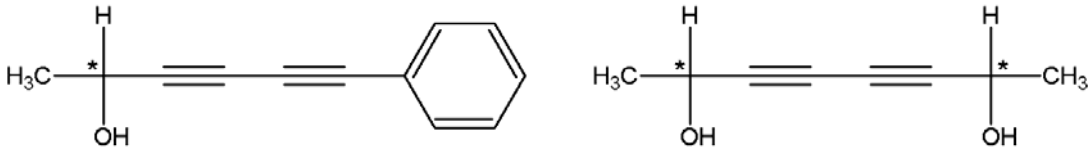

Scheme 8. Two possible chiral molecules that could produce frameworks analogous to those of compounds **1** and **2**.

Dianin's Compound

The inclusion behaviour of Dianin's compound (4-*p*-hydroxyphenyl-2,2,4-trimethylchroman) (Scheme 9) is arguably one of the most recognised archetypes of solid-state supramolecular chemistry. Since its discovery nearly a century ago by Russian chemist A.P. Dianin,[28a] many crystal structures involving Dianin's compound as a host have been reported.

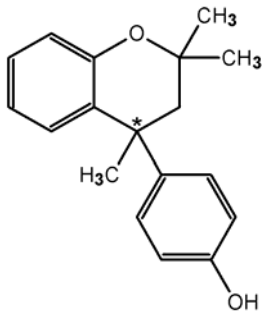

Scheme 9. Dianin's compound. * denotes a chiral carbon atom.

The most remarkable feature of these structures is that they comprise a homomorphic series with regard to the skeletal framework formed by the host compound, i.e. they are isoskeletal.[28b,43] The chiral molecules crystallise as a racemate with six molecules situated about a site of 3 symmetry to form a cyclic, hexameric arrangement of O–H···O hydrogen bonds between phenolic groups of alternating R and S stereoisomers (Figure 13a,b). Three like-isomers project above the plane of the hydrogen-bonded ring of oxygen atoms while their enantiomers are directed below the plane (Figure 13a,b). The reason behind the up/down arrangement of the phenol groups in all these cases is recognised as being the sterics of the aromatic rings. The hydrogen bonded hexamers are stacked into one-dimensional columns perpendicular to the hydrogen bonded ring such that the R and S components of adjacent units interdigitate to form a relatively large hourglass-shaped interstitial cavity of approximately 240 $Å^3$ (Figure 13c). The van der Waals, puzzle-like packing of these columns completes the crystal lattice.

The hydrogen bonded hexagonal ring is clearly recognised as a major structure-directing feature of this system. Indeed, this packing mode persists despite synthetic modifications such as thiolation of the phenolic group,[91] removal of one of the 2-methyl groups[92] and replacement of the oxygen heteroatom by S[93] or Se.[94] Of more general interest, this particular packing mode involving the hexameric arrangement of hydrogen bonds is found in other host systems such as β-hydroquinone and phenol. Together these host systems form the hexahost family of compounds and are the inspiration for a host design strategy championed by MacNicol.[10,95] The analogy is based on the idea of using a hexasubstituted benzene analogues instead of the hydrogen-bonded hexamer.

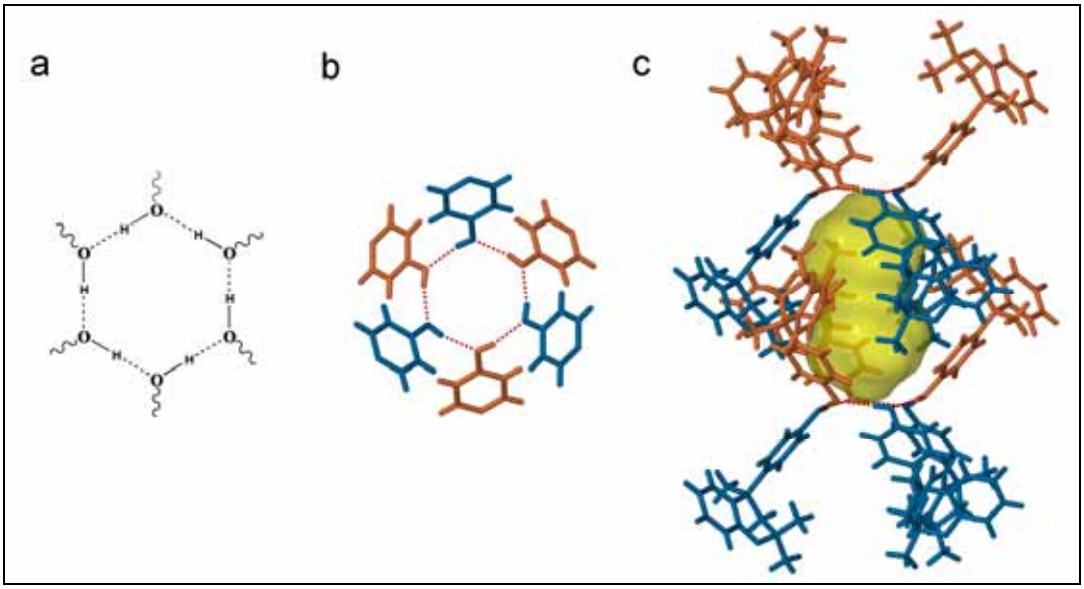

Figure 13. (a) A schematic of the cyclic, hexameric arrangement of O–H···O hydrogen bonds. **(b)** The hydrogen bonding of the phenolic groups of alternating R and S stereoisomers to form the up/down, cyclic, hexameric arrangement. **(c)** Interdigitation of opposite stereoisomers to form the hourglass-shaped interstitial cavity (semi-transparent yellow surface). All molecules are shown in capped-stick representation.

To date Dianin's compound has only been observed to crystallise in the trigonal space group *R*3, which has necessitated modeling of guest molecules as disordered owing to symmetry constraints. The α (apohost) or guest-free phase has an identical (isoskeletal) framework in which the hourglass cavity is maintained and shrinks only slightly to ~231 $Å^3$ (probe radius of 1.55 Å). The guest-free compound can be synthesised by either crystallising from dodecane or tetradecane, or by subliming under vacuum at ~250°C. Owing to this ability to crystallise with comparatively large voids, we have studied the gas sorption properties of the guest-free compound, and these results are presented in Chapter 5.

Although it is well-known that resolved Dianin's compound does not form clathrates and crystallises in the space group $P2_12_12_1$, no structural reports or data deposits have been made at the CCDC.[10,95,96] For this reason the resolved *S*-Dianin's compound was investigated to elucidate its structural motifs.[68b] Instead of the known hydroxyl hydrogen bonded motif associated with Dianin's compound, the hydroxyl groups are hydrogen bonded to the chromen bridging oxygen, with an O-H···O donor···acceptor distance of ~2.96 Å (Figure 14).

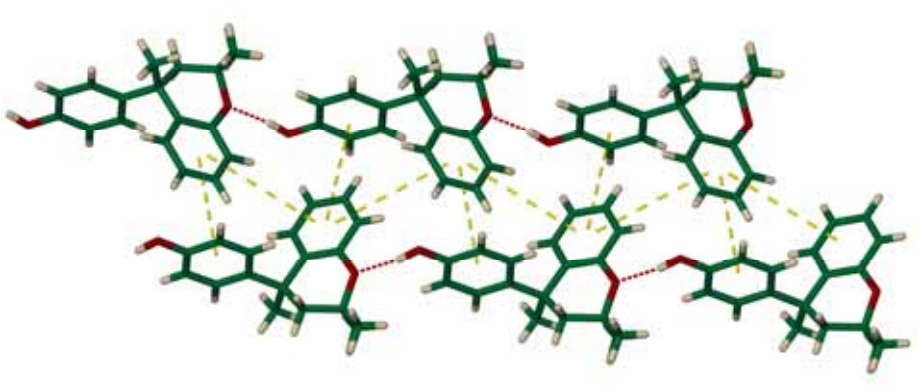

Figure 14. The crystal packing in *S*-Dianin's compound in capped-stick representation, showing the hydrogen-bonded chains and the π-π interactions between adjacent chains. Intermolecular hydrogen bonding is shown as red dashed lines and intermolecular π-π interactions are shown as yellow dashed lines.

These hydrogen bonds arrange the Dianin's compound molecules into infinite chains running along [100]. Two adjacent chains are held together strongly by edge-to-face π-π interactions to form double strands (centroid-to-centroid distances of 5.781 and 5.021 Å) (Figure 14). Within a double strand, the two individual chains are related by a 2_1 axis. These double strands further pack in a herring-bone motif (Figure 15).

A serendipitous discovery of an interesting new host:guest system between Dianin's compound and morpholine led to the investigation of the inclusion properties of amine guests in Dianin's compound clathrates. The discovery can be described as induced salt formation by partial host-to-guest proton transfer during the morpholine enclathration by Dianin's compound.[68a] Slow evaporation of a concentrated solution of Dianin's compound in morpholine yielded crystals suitable for single-crystal x-ray structural analysis. The asymmetric unit of the *P*1 structure consists of six molecules of Dianin's compound (two deprotonated anions and four neutral molecules) and two morpholinium cations. Structures with such relatively high Z' values are reasonably rare and warrant further investigation with regard to the possibility of a misassigned space group.[97] Two similar sets of molecules, each comprised of two neutral Dianin's compounds, a deprotonated Dianin's compound anion and a morpholinium cation, can easily be distinguished.

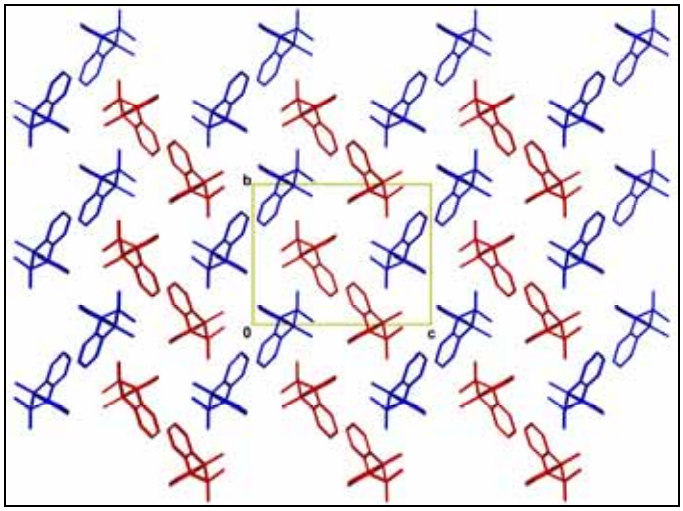

Figure 15. Herring-bone packing of the double strands of *S*-Dianin's compound. Molecules are shown in capped-stick representation and viewed along [100]. Hydrogen atoms have been removed for clarity. Double strands are coloured red and blue to emphasise the herring-bone-type packing arrangement.

Each set of four molecules forms the basis of a crystallographically unique one-dimensional column aligned parallel to [100] (one situated along x, 0, 0 and the other along x, ½, ½). A detailed analysis reveals that the latter column can be exactly mapped onto the former by an inversion operation through ¼, ¾, ¼, followed by a threefold rotation about (100). However, the crystal cannot be reassigned to a higher symmetry space group and the apparent symmetry can reasonably be considered as non-crystallographic. Furthermore, it should be noted that the unit cell parameters are remarkably close to being assignable to a monoclinic system. However, the necessary symmetry is not present (i.e. there is an apparent threefold and not a twofold rotation). Even with deprotonation of the two of the Dianin's compound molecules in the asymmetric unit, the overall structure is surprisingly similar to the previously reported structures of Dianin's compound clathrates. Unlike the previously reported clathrates of Dianin's compound, the guests in these crystals are not disordered. It must be also noted that the deprotonation of Dianin's compound in a solid-state structure has not been reported to date. The characteristic hourglass cavity shape already described is retained and encapsulates two morpholinium cations (Figure 16).

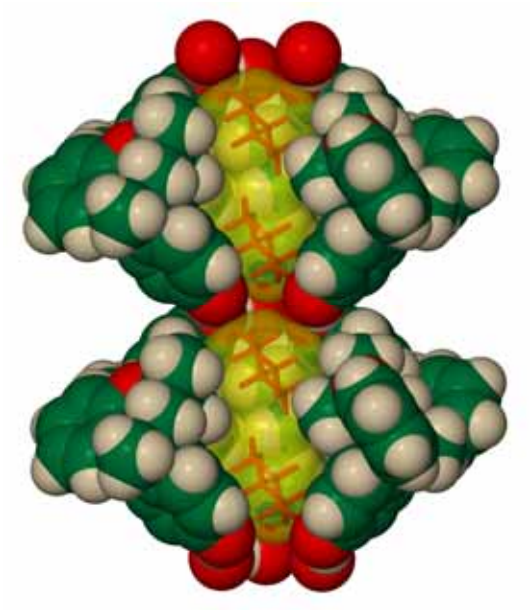

Figure 16. Molecular cages (semi-transparent yellow surfaces) formed by Dianin's compound encapsulate the protonated morpholinium cations (orange, capped-stick). The Dianin's molecules are shown in spacefilling representation and those nearest the viewer have been removed in order to reveal the contents of the cavities.

The feature of interdigitation by enantiomers of Dianin's compounds to form this cavity is retained as well. This therefore leads to the formation of the now familiar one-dimensional columns and, consequently, its corresponding puzzle-like packing arrangement. The most significant difference between this structure and that of the neutral host is the considerable perturbation of the hydrogen bonding hexameric motif that forms the nodes of the one-dimensional columns (Figure 17).

The cyclic hydrogen bonded motif, considered critical for the stabilisation of the neutral host structure, is interrupted as a result of deprotonation of two of the phenolic hydroxyl groups. Instead of six intermolecular host···host hydrogen bonds, only four are now formed (Figure 17b). The loss of two energetically important hydrogen bonds is compensated for by the formation of a total of four new hydrogen bonds from the protonated amines of two morpholinium guests to the phenolic oxygen atoms of deprotonated and neutral Dianin's compound molecules (Figure 18). This occurs on both sides of the nodes of the one-dimensional column of host molecules such that a hexameric hydrogen bonded chair [···O–H···O(···H–O)···H–N–H···O–H···O(···H–O)···H–N–H···] is formed. The two morpholinium guest ions that participate in this cyclic hydrogen bonded pattern are situated in adjacent interstitial cavities.

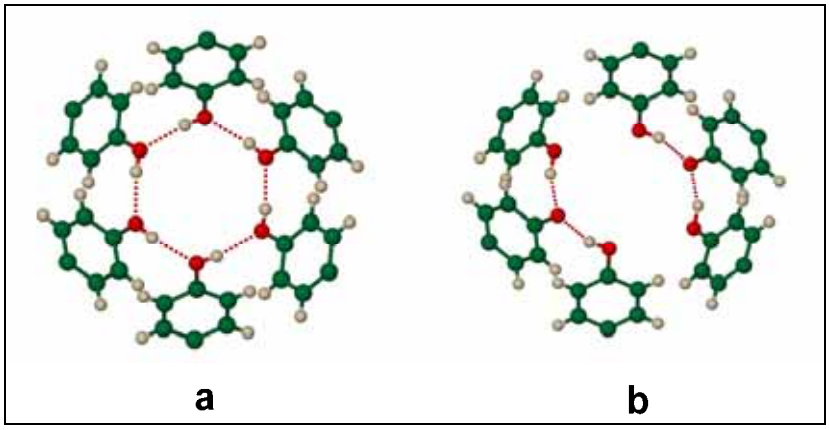

Figure 17. (a) Ball-and-stick representation of the hexagonally hydrogen bonded phenolic OH groups characteristic of neutral Dianin's compound host systems and **(b)** a distorted "hexagon" showing how two Dianin's compound molecules hydrogen bond to the nearest deprotonated molecule in the anionic host system.

An important aspect of the morpholinium enclathration by Dianin's compound is the host:guest (H:G) ratio. The H:G ratio is best rationalised by considering the static volumes of the guest molecules (or disordered molecules where applicable) as well as the free volumes of the interstitial cavities. A H:G ratio of 6:1 implies one guest molecule per cavity whereas a ratio of 3:1 implies two guest molecules per cavity.

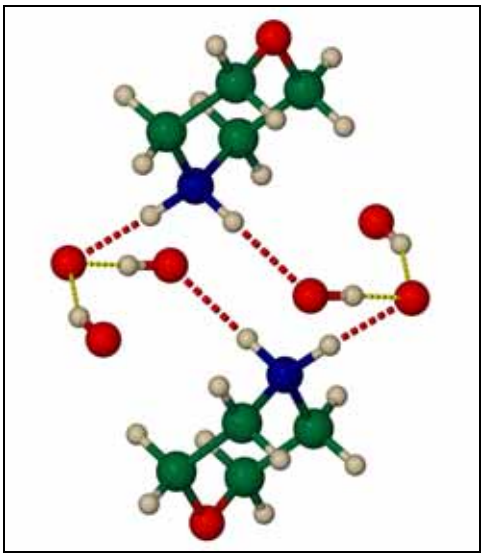

Figure 18. Hydrogen bonded network formed between the six phenolic groups (only O–H and O^- shown for clarity) and the morpholinium guests. Hydrogen bonds between OH and O^- are shown as yellow dotted bonds. The red dotted bonds indicate hydrogen bonds associated with the protonated amine group of morpholine.

For example, the formic and acetic acid clathrates[98] have H:G = 3:1 while the carbon tetrachloride,[99] chloroform,[100] propionate[101] and p-xylene[102] clathrates have H:G = 6:1. The two smallest organic acids form hydrogen-bonded dimers within the lattice voids. However, the cavity space is presumably not large enough to accommodate the other types of guest molecules in pairs (it must be noted that complementarity of shape is also important). Since morpholinium is larger than $CHCl_3$ and comparable in size to CCl_4 (Figure 19), it is at first surprising that the morpholinium clathrate structure has H:G = 3:1.

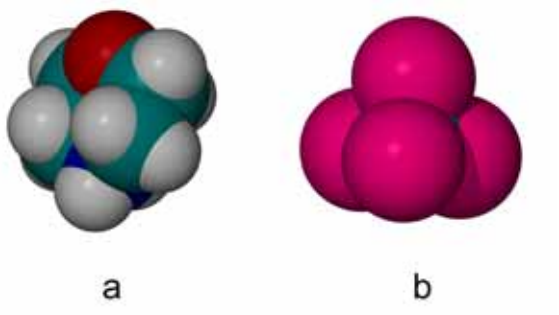

Figure 19. Size–shape comparison of **(a)** morpholinium and **(b)** carbon tetrachloride shown in van der Waals representation.

As noted above, the morpholinium cations are hydrogen bonded to the phenolic host oxygen atoms and there is thus some van der Waals overlap between host and guest. It is interesting to note that disruption of the hexagonal hydrogen bonded motif normally observed in Dianin's compound structures results in no significant change in the shape or volume of the interstitial cavity (Figure 20). There is also some van der Waals overlap between the two morpholinium ions in each cavity (Figure 20d). A relatively short C–H···O hydrogen bond (C···O = 3.11 Å and ∠C-H···O = ca 128^o) is formed between the two guest molecules. This close contact allows the two morpholinium anions to form a compact dimer which fills the cavity with a high packing efficiency of approximately 73.5%. Such close packing between host and guest is likely to contribute significantly towards minimisation of the overall lattice energy.

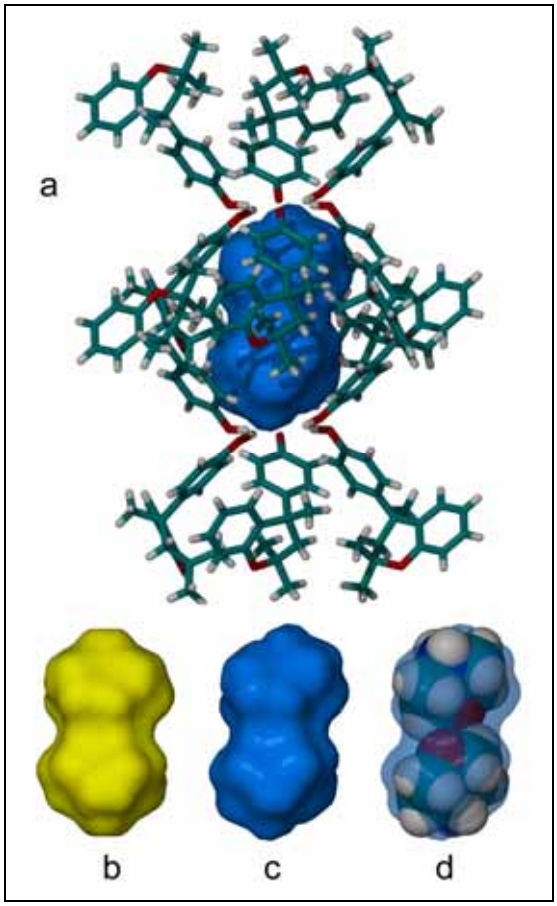

Figure 20. Surfaces representing the molecular cavities in Dianin's compound structures: **(a)** columnar packing of the host, **(b)** the cavity formed by the CCl_4 clathrate, **(c)** corresponding view of the cavity containing morpholinium and **(d)** the cavity occupied by two morpholinium molecules shown in van der Waals representation. The calculated cavity volumes are 237 $Å^3$ for the morpholinium clathrate and 238 $Å^3$ for the CCl_4 clathrate using a probe radius of 1.2 Å.

As a continuation of this study, the literature on Dianin's compound was surveyed to ascertain whether any other peculiar results had been reported on the clathration of amines by Dianin's compound. All the structural reports of Dianin's compound to date have shown that the crystalline space is always trigonal or, as in our case, a close approximation. With this information in hand it can easily be understood that the cavity of the host is composed of exactly six Dianin's compound molecules and that the host:guest ratios must be either 6:1; 3:1(6:2); 2:1(6:3); 3:2(6:4); 6:5 or 1:1(6:6) when considering the condition that all cavities must be crystallographically equivalent in a structure. It is therefore surprising to find reported host:guest ratios of 4:1 and 1:1 when the guest is relatively large.[102] There are two possibilities for these

strange results: they might be incorrect or, alternatively, the reported crystalline materials may not belong to the same structural family.

A systematic study was made of other amines (preferably those that are liquids at room temperature) that would also deprotonate the host in the same manner as morpholine. Five other amines, *viz*. propylamine, isopropylamine, *sec*-butylamine, allylamine and piperidine, were found to have a similar effect on the symmetry of the Dianin's compound host. Interestingly, four of these are primary amines, and one is a secondary amine like morpholine. This indicates that variation is possible for the amine type of the guest that causes distortion of the hexagonal ring of hydroxyl groups. The structures are in essence similar to that of the morpholine structure in terms of the host framework, but the deprotonation phenomenon is slightly different. Despite the deprotonation phenomenon being different in these cases, the hexagonal hydrogen bonded ring is still altered, therefore precluding 3 symmetry.

The main difference between the primary amine structures and the morpholine structure relates to the fact that the protonated amine group is primary. This means that, after transfer of a proton, the amine has three possible hydrogen bond donor groups (Figure 21). However, it seems the third possible hydrogen bond is too sterically hindered to be significantly strong (donor to acceptor distance of 3.121 Å, and N-H···O angle of 159.7^{o} in the case of the propylamine structure).

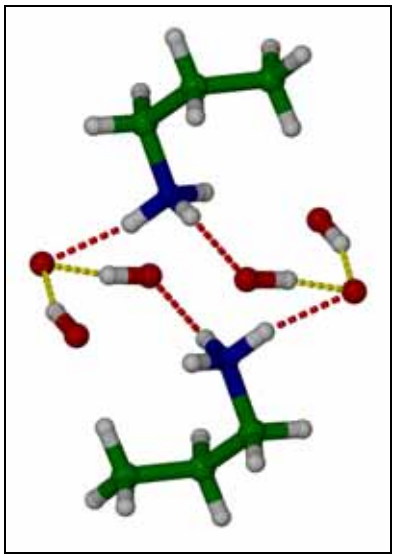

Figure 21. Primary amine hydrogen bonding of propylamine in the Dianin's compound clathrate structure. Atoms are shown in ball-and-stick representation.

The allylamine and piperidine structures are different in that there appears to be some disorder and the deprotonation is not as symmetrical as in the other examples. An interesting aspect of the allylamine clathrate is the possibility of [2+2] photodimerization under UV light as the two enclathrated guests per cavity are self-assembled well enough to satisfy Schmidt's rule (the C···C distance is 4.2 Å which is the same as Schmidt's limit for photodimerization) (Figure 22).[15]

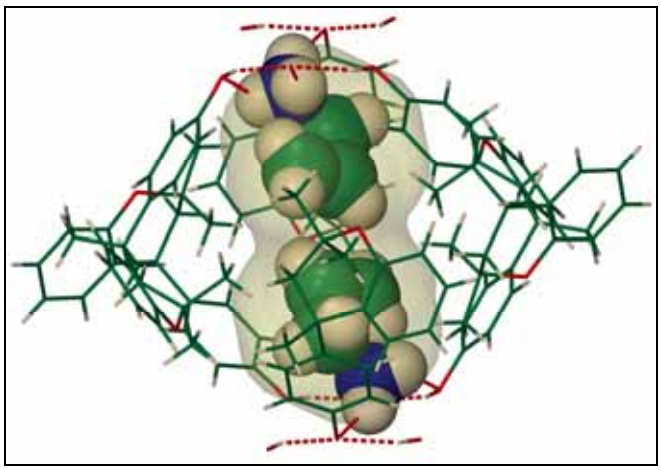

Figure 22. Self-assembly of the two guests within the cavity of the Dianin's compound clathrate of allylamine. Allylamine guest atoms are shown as spheres of 0.7 times their van der Waals radii to highlight the excellent alignment of the double bonds for [2+2] photodimerization.

Owing to ordering of the guest within the cavity of the Dianin's host by virtue of deprotonation compared to the usual *R*3 host structures, there exists a strong possibility for studying photodimerization by single-crystal to single-crystal transformation.

To further test the flexibility of the deprotonation phenomenon, ethylene diamine was also investigated as a guest. Surprisingly, the space group for this structure is *R*3. (unit cell : *a*, *b* = 53.599 Å; *c* = 11.00 Å). This unit cell appears to be exactly doubled along the *a* and *b* axes with respect tot the "normal" Dianin's compound clathrates. The asymmetric unit consists of four Dianin's compound molecules, three normal and one deprotonated, and two ethylene diamine guests. However, the two guests are in two very different environments. One of the guest instances appears to be located in a niche exactly the same as that found in the

triclinic systems described above. Each ethylene diamine molecule within a cavity has deprotonated one Dianin's compound molecules as seen before. This part of the structure possesses only crystallographic inversion centres. The other amine guest type is unexpectedly different. It is located on the threefold axis and is therefore best described as reminiscent of the well-known trigonal Dianin's compound clathrate guests (it is disordered and could not be fully modelled). This implies that the two known columnar arrangements of Dianin's compound are present as supramolecular entities cocrystallised together in a 3:1 ratio (Figure 23).

A systematic search for the larger trigonal structure within the five amine structures (propylamine, isopropylamine, *sec*-butylamine, allylamine and piperidine) led to the surprising discovery that the crystals can be indexed as either the larger trigonal space group (*a*, *b* axis ~ 53.6 Å) or the triclinic space group. In this particular case no metrical relationship exists between these two space group choices. However, the structures with morpholine and ethylene diamine can only be described in the original manner, i.e. triclinic and larger trigonal, respectively. These observations have thus far resisted a satisfactory explanation.

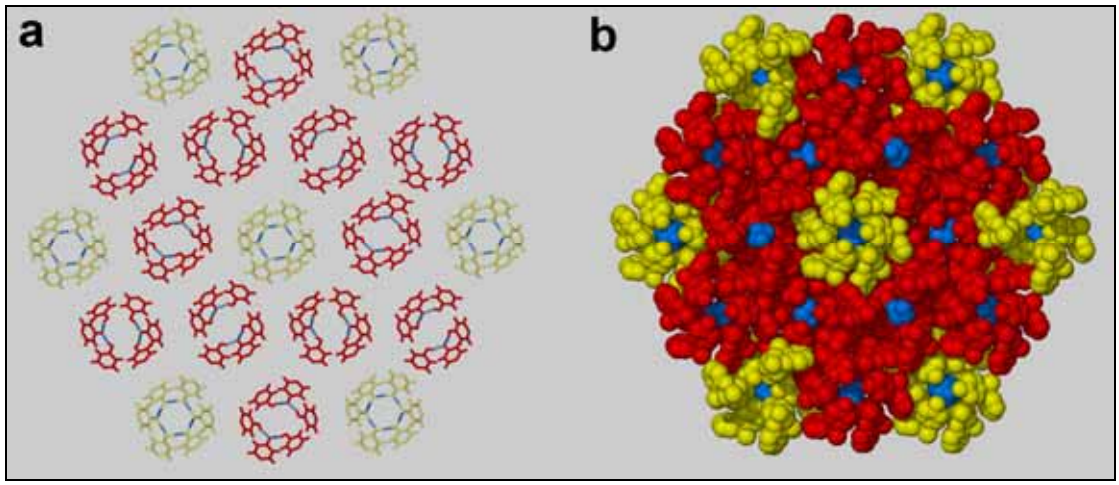

Figure 23. (a) A scheme showing the ensemble of different hydrogen bonding arrangements in the Dianin's compound : ethylene diamine host–guest system viewed along [001]. **(b)** The columns, shown in spacefilling representation, formed by the different packing motifs. The yellow columns contain disordered guest molecules whereas the red columns contain ordered ethylene diamine molecules due to proton migration between host and guest. Ethylene diamine guests are shown in blue.

Two Dianin's compound clathrates of piperidine, i.e. triclinic and trigonal, have now been found. A third phase of these two compounds has been reported in the literature, almost incidentally.[102] It was shown and accepted that the piperidine/Dianin's compound host guest ratio is 1:1, but this rather unusual result has never been explained in terms of the well-known Dianin's compound structures. Since two adducts of these two compounds have been described here, the 1:1 structure was elucidated as well. The space group is $P2_1/c$ and the asymmetric unit consists of one Dianin's compound and one piperidine. Deprotonation does not appear to have occurred, but the x-ray analysis is not conclusive. As deprotonation normally does not often occur in amine-alcohol mixed crystals, this structure was modelled as having no proton transfer. Only neutron diffraction analysis or solid-state NMR would be able to confirm this assumption unequivocally. The packing of this structure involves hydrogen bonding between OH groups of two enantiomers of Dianin's compound and the secondary amine groups and two piperidine molecules to form a four-membered adduct (Figure 24). Here it is useful to use graph set analysis to define the adduct as $R^4_4(8)$.

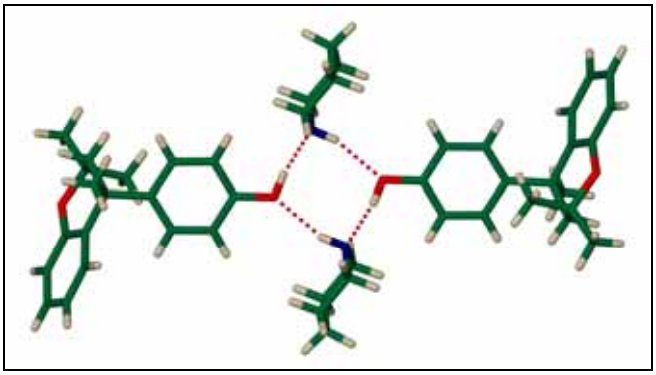

Figure 24. Adduct formed between Dianin's compound and piperidine in the ratio 1:1. Molecules are shown in capped-stick representation.

The synthon shown is relatively rare and could only be found in five other cases.[103] The jigsaw-like packing ability of Dianin's compound is once again evident in this structure. The four-membered adduct shown above is the supramolecular building block of this structure. These building blocks form two-dimensional layers running along the *bc* plane. The jigsaw-like ability of Dianin's compound observed in the foregoing structures is well illustrated in these two-dimensional layers, as there are

no apparent weak interactions (other than van der Waals) that can orchestrate the interplay between the building block synthons. The images in Figure 25 show how the adduct blocks interdigitate with one another to form two-dimensional layers that are in van der Waals contact with one another.

The most fascinating aspect of this structure is that it exists at all. It is normally presumed that Dianin's compound only forms clathrates when it packs forming a cavity composed of six Dianin's compound molecules. In this case the well-known motif is disrupted by the formation of a robust four-membered adduct involving strong hydrogen bonds between two amines and the phenolic groups of the *S*- and *R*-Dianin's compound molecules. This alternative motif therefore raises several questions: (1) what other amines would disrupt the packing of Dianin's compound? (2) what would happen if a chiral compound were introduced? (3) as Dianin's compound is chiral, could it be used to separate chiral amines or could it be resolved itself by crystallisation with a resolved chiral amine? These possibilities may well represent the future of solid-state supramolecular studies of Dianin's compound.

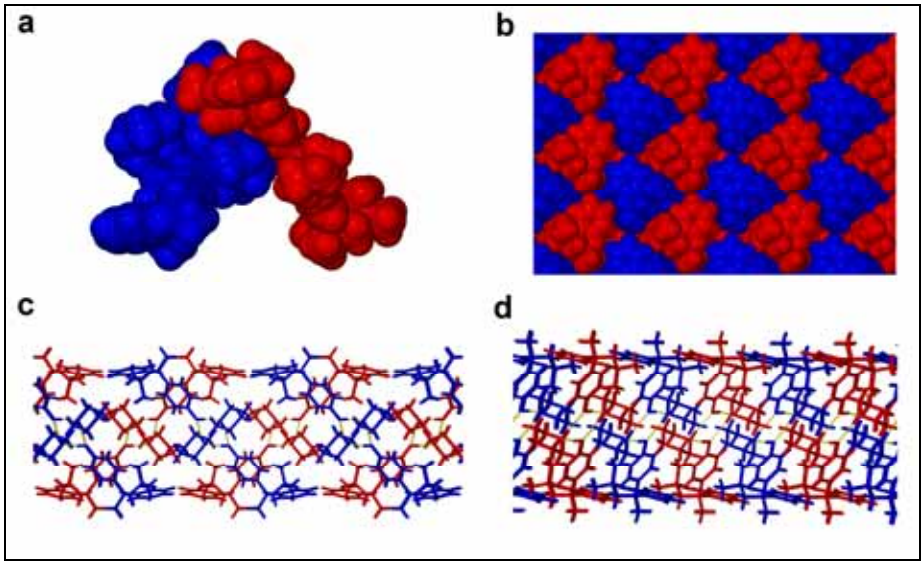

Figure 25. (a) Two supramolecular building blocks (each an adduct consisting of Dianin's compound and piperidine in a 2:2 ratio) are hooked into each other like jigsaw pieces. **(b)** Spacefilling diagram of the packing of the two-dimensional layer viewed perpendicular to the *bc* plane. **(c)** View along the *b* axis of the supramolecular building blocks showing how they are perpendicular to one another (i.e. red and blue coloured fragments at 90° to each other). **(d)** The two dimensional layer viewed down the *c* axis showing how the perpendicular bricks are packed one on top of the other.

p-tert-Butylcalix[4]arene

p-tert-Butylcalix[4]arene (Scheme 10) has proven to be a fascinating and controversial compound. The main concern of this study relates to the structural characteristics of the sublimed, low-density form owing to this material's ability to absorb gas. Atwood *et al.* first reported the ability of this low-density material to absorb small molecules even though there are no discernable pores in the structure. The extraordinary single-crystal transformation that occurs when vinyl bromide is absorbed sparked renewed interest in this compound.[79b,104]

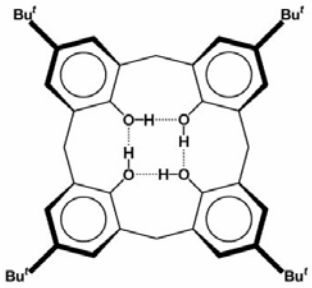

Scheme 10. *p-tert*-butylcalix[4]arene

Ripmeester showed that a dense structure of pure *p-tert*-butylcalix[4]arene can be crystallised over three days from a tetradecane solution heated to 70 ^{o}C for several hours.[105] The structure consists of a close-packed arrangement of van der Waals dimers of calixarenes – each calixarene inserts one of its *tert*-butyl groups into the cavity of its partner, and *vice versa*. With increasing interest in this compound and its properties, it became important to test whether the low-density sublimed structure could be obtained by other means. Indeed, it was not known which, if any, of the two published apohost phases might result from removal of guest from the well-known toluene clathrate.[106] It was then established that the low-density form can be produced by heating the toluene solvate at 220^{o}C under reduced pressure for three hours.[107] A subsequent report by Ripmeester *et al.* then showed that a complex relationship exists between the various polymorphic forms of pure *p-tert*-butylcalix[4]arene with regard to desolvation of its inclusion compounds.[108] In the same report it was also shown using DSC evidence that the sublimed form undergoes a reversible phase change at around 92^{o}C. From this experimental result Ripmeester *et al.* concluded that "the phase that Atwood *et al.* found upon sublimation is in fact not the same phase for

which they determined the structure". For this reason it was decided to investigate these temperature dependant changes by single-crystal x-ray diffraction in order to determine which structure was most relevant when studying the gas sorption properties.[66a]

The crystal structures of the low-density form of *p-tert*-butylcalix[4]arene were determined at three different temperatures, –100°C, 20°C and 130°C. Each of these structures conforms to the space group $P2_1/n$ with the asymmetric unit consisting of a complete *p-tert*-butylcalix[4]arene molecule. The *p-tert*-butyl calix[4]arene molecules are stabilised in the cone conformation by the cyclic network of intramolecular hydrogen bonds between the hydroxyl groups at one end of the molecule. The three structures each have the recognisable **abcd** bilayer structure, and layers of facing *p-tert*-butyl calix[4]arenes are in van der Waals contact with one another by virtue of their *tert*-butyl groups (Figure 26).[79b] The facing *p-tert*-butylcalix[4]arene molecules do not interdigitate at all, causing the formation of a reasonably sized unoccupied cavity of ~234 $Å^3$ (using a probe radius of 1.45 Å and the atomic coordinates of the -100 °C structure) (Figure 27). In terms of packing, all three sublimed crystal structures therefore have little in common with the high-density structure.

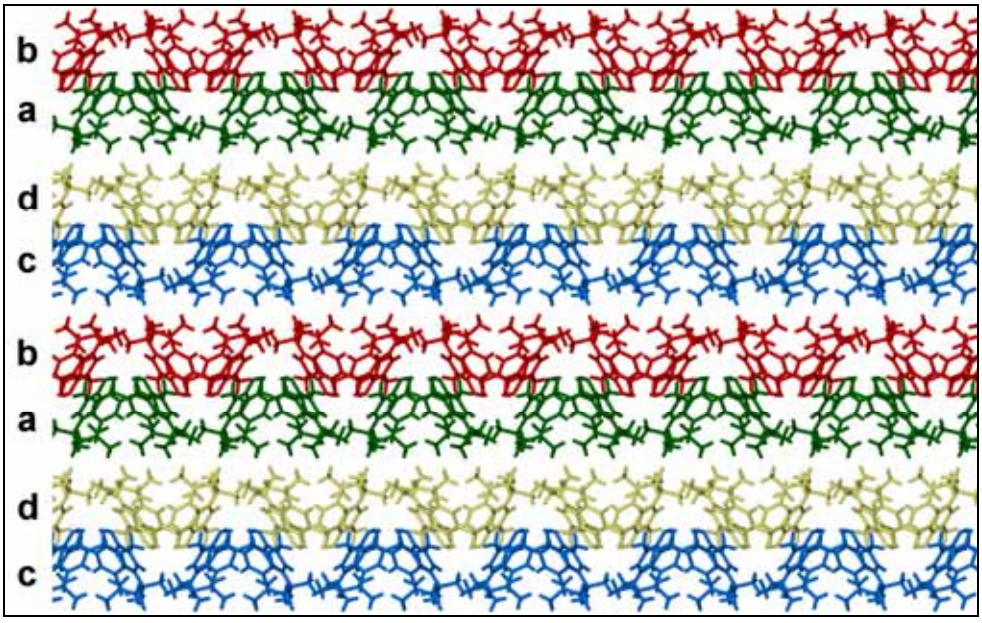

Figure 26. The **abcd** bilayer structure of *p-tert*-butylcalix[4]arene as viewed along [010]. Two distinct bilayers, **ab** and **cd**, can be distinguished. Layers **abcd** are coloured yellow, green, red then blue respectively. Molecules are shown in capped-stick representation.

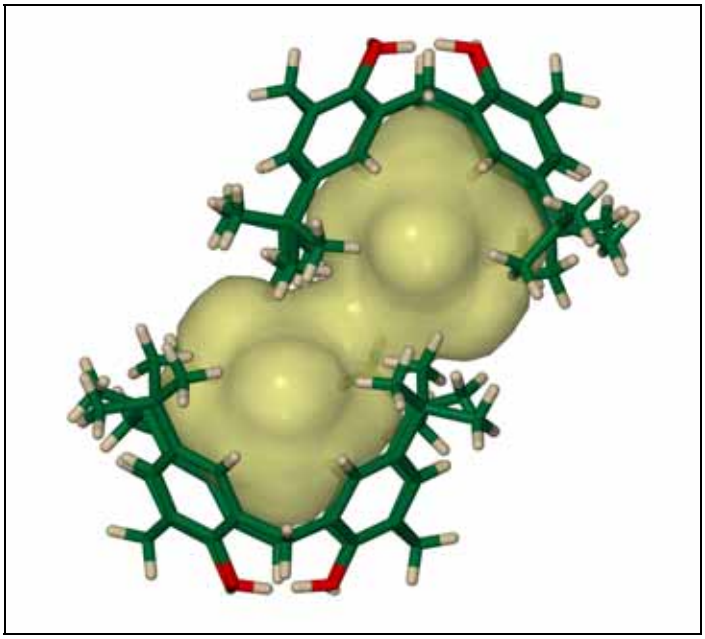

Figure 27. The cavity enclosed by two facing *p*-*tert*-butylcalix[4]arene (yellow surface, 1.45 Å probe radius, -100°C structure). Half of the disordered *tert*-butyl groups have been removed for clarity.

Figure 28a shows that only one of the four *tert*-butyl groups is disordered over two positions at -100°C. At this temperature each of the ordered *tert*-butyl groups is approximately positioned between two proximal *tert*-butyl groups of a facing calixarene embedded in an adjacent layer. The disordered group is located in the midst of four *tert*-butyl groups, each belonging to a separate calixarene of the facing layer, and thus has more freedom of rotation about the Csp^2–Csp^3 single bond. Figure 28b shows that the packing mode of facing layers relative to one another is largely the same at 20°C as at -100°C. However, all four *tert*-butyl groups are disordered over two positions at 20°C. This observation can easily be rationalised since the bilayers are stacked along the crystallographic *b* axis, which elongates by 0.55 Å upon warming from -100°C to 20°C, implying that the layers are more partitioned. Thus all of the *tert*-butyl groups are bestowed with more freedom of rotation.

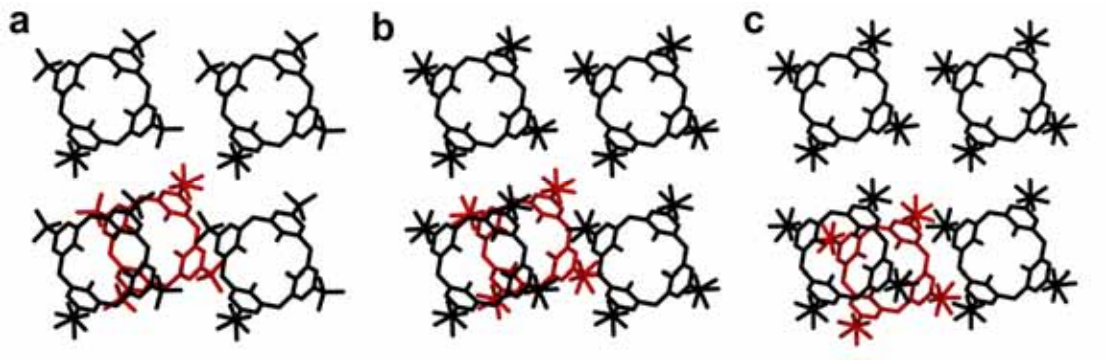

Figure 28. Comparison between structures of sublimed *p-tert*-butylcalix[4]arene determined at **(a)** -100°C, **(b)** 20 °C and **(c)** 130 °C (viewed along [010]). In each case, four calixarenes (black) belonging to the same layer are shown with their cavities facing away from the viewer. There is almost no variation in the relative positions of the molecules within each layer as the temperature is increased. One calixarene from the adjacent, facing layer is shown in red to highlight the subtle differences in the relative placement of neighbouring layers.

The crystallographic *b* axis of the 130°C structure is elongated by 0.50 Å in comparison to that of the room temperature structure. Although the relative positions of the *p-tert*-butylcalix[4]arene molecules within a layer remain seemingly unchanged upon heating to 130°C, a lateral shift by 2.34 Å of one layer occurs with respect to its adjacent, facing layer (Figures 28c and 29). This shift has a profound effect on the geometry of the lattice void between offset, facing calixarenes. In the –100°C and 20°C structures, the approximately hourglass-shaped voids have diameters of ~ 2.42 Å at there narrowest points. In the 130°C structure, a *tert*-butyl group of one of the calixarenes guards the opening of the other such that the diameter of the narrowest point of the void between the two molecules shrinks to ~1.74 Å. On the atomic scale, the two calixarene cavities effectively become isolated from one another at higher temperatures (> ~92 °C) whereas they are merged at lower temperatures (Figure 30).

In summary, the sublimed crystals do indeed appear to undergo a temperature-dependent phase change as shown by the DSC work of Ripmeester *et al*. The previously unknown high temperature phase has now been described. This has some importance in the gas sorption properties of the sublimed phase as several questions still need to be answered. For example, why does the sublimed material only absorb one mole of carbon dioxide per cavity when there is sufficient space for at least two CO_2 guests?

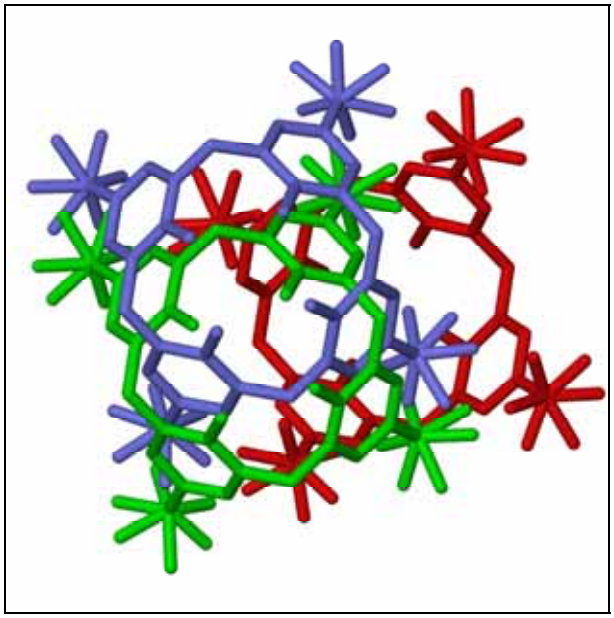

Figure 29. Overlay of the void-forming calixarene dimers at 20°C (red/ green) and 130°C (red/blue). The molecule shown in red is common to both structures. The difference in location between the blue and green molecules represents a lateral shift of 2.34 Å upon heating the crystal from room temperature to 130 °C.

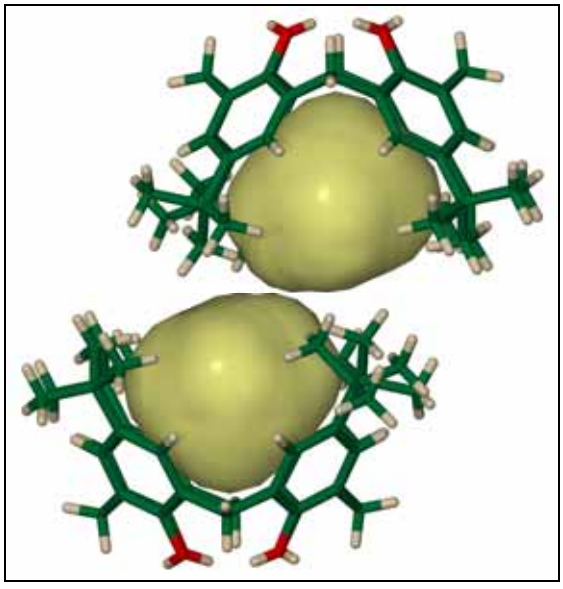

Figure 30. The cavities generated by two facing *p-tert*-butylcalix[4]arene molecules in the 130°C structure (yellow surface, 1.74 Å probe radius. This probe radius was used to clearly show the two cavities. A probe radius of 1.45 Å also generates two cavities, but in the image the cavities are not clearly separated). Half of the disordered *tert*-butyl groups have been removed for clarity.

MeOTBCS

The simple notion of molecular transport through any matrix implies the presence of suitably sized channels defined and bounded by van der Waals surfaces. For example, molecular-scale hydrodynamics is only expected to occur if the narrowest site of the channel is at least wide enough to admit a single water molecule. However, the groundbreaking work of Atwood and coworkers with *p-tert*-butylcalix[4]arene has given rise to questions concerning the transport of small, mobile molecular species in solid media and has shown that the conventional conception of crystal porosity may be flawed.[79b] Water transport across cell membranes in biological systems is significantly enhanced by the presence of aquaporins,[109] proteins that associate as tetramers to form cylindrical transmembrane pores which are 2 to 3 nm long and about 0.3 nm wide at their narrowest point. Water travels through these channels at bulk diffusion rates,[110] presumably as single-file, hydrogen-bonded chains consisting, at any instant, of about seven to nine water molecules.[111] While interest in the transport properties of aquaporins has mainly focused on their selectivity for water over protons,[112] the influence of the channel size on water permeation has also received significant attention.[112f,113] The shape, dimensions, and electrostatic profile of biological pores are considered to be the major determinants of their function. In this light it will be shown how diffusion occurs in and out of a simple organic crystal, which can be considered to be nonporous in a conventional sense. This will be shown by the elucidation of the guest-free crystalline polymorphs of the organic molecule, as well the iodine included polymorph structures and finally by showing that the diffusion of water and iodine into the physically porous guest free polymorph is possible.

Crystals of pure 5,11,17,23-tetra-*tert*-butyl-25,26,27,28-tetramethoxy-2,8,14,20-tetrathiacalix[4]arene (**3**) (Scheme 11) were prepared by sublimation at 240^{o}C under reduced pressure. Visual examination of the crystals revealed two different morphologies: primarily parallelepipeds (**3a**), interspersed with a relatively small number of square plates (**3b**). The paucity of the more interesting square plate crystals is unfortunate since a sufficient quantity of these crystals could not be prepared to allow determination of thermodynamic and kinetic properties of this crystal form. The structures of both crystal forms were elucidated by single-crystal x-ray diffraction analysis and found to be polymorphs of one another. In both cases the calixarene

assumes the *1,3-alternate* conformation, and the molecule is approximately box-shaped, with estimated dimensions of 10 x 10 x 14 Å.

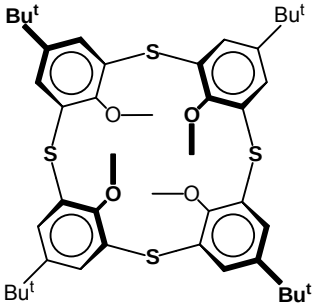

Scheme 11. 5,11,17,23-tetra-*tert*-butyl-25,26,27,28-tetramethoxy-2,8,14,20-tetrathiacalix[4]arene (compound **3**).

The space group of polymorph **3a** is *C*2/*c* and the asymmetric unit consists of a complete molecule of **3**. The calixarene has the 1,3-alternate conformation, which differs from that in the previously reported structure of the pure compound.[114] In the previously reported structure, obtained from large bulky solvents such as isopropanol and *p*-xylene, the calixarene is found in the *1,2-alternate* conformation and the space group is *P*1. The molecules in this new monoclinic structure are arranged within the structure in two distinct orientations, each with the principal molecular axis canted at an angle of 83^{o} with respect to the other. This structure is very dense and is of no further interest to this study.

The space group of polymorph **3b** is $P42_1m$ and the structure possesses two crystallographically unique molecules of **3** (Figure 31). One of the molecules (**3b$_1$**) is situated on the intersection of the two mirror planes at (110) and (-110) while the other (**3b$_2$**) straddles a position of 4 site symmetry at 0,0,0 (Figure 31). All of the calixarene molecules in the crystal are aligned with their principal molecular axes parallel to [001] and the extended structure consists of columns of **3b$_1$** and **3b$_2$** stacked end-to-end along this direction. Although **3b$_1$** and **3b$_2$** have the same overall conformation, remarkably subtle, yet ultimately critical metric differences exist between them. This is best emphasised by comparing this structure with the known inclusion structures of **3**.[114] In these structures the space group is *Pnmm* ($a \approx 12$, $b \approx 13$, $c \approx 15$ Å) with the molecules packed one on top of the other. The subtle differences in the two crystallographically unique molecules of **3** are best shown when

viewing five neighbouring columns of **3** to illustrate how one column is slightly twisted (**3b$_2$**) relative to the surrounding columns (**3b$_1$**) (Figure 32).

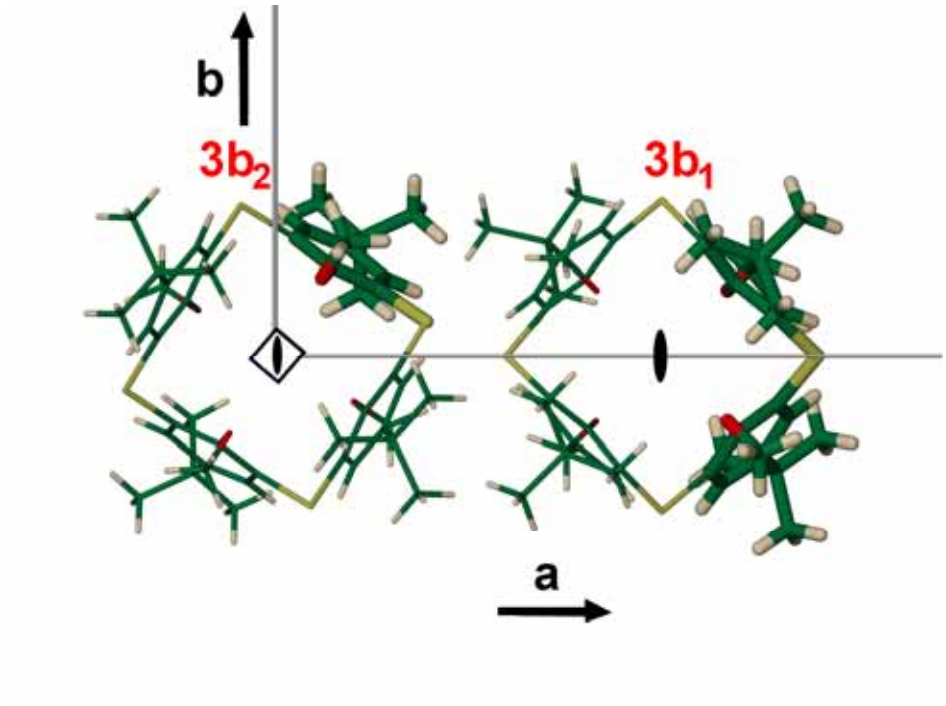

Figure 31. Perspective view of structure **3b** projected along [001]. The space group is P42$_1$*m* (no. 113) with *a*=*b*=19.494(2), *c*=12.102(1) Å. Two crystallographically unique molecules are shown in capped-stick representation and the thicker bonds indicate the asymmetric unit in each case. As indicated, molecule **3b$_1$** resides on a 2*mm* axis while **3b$_2$** occupies a position of 4 site symmetry.

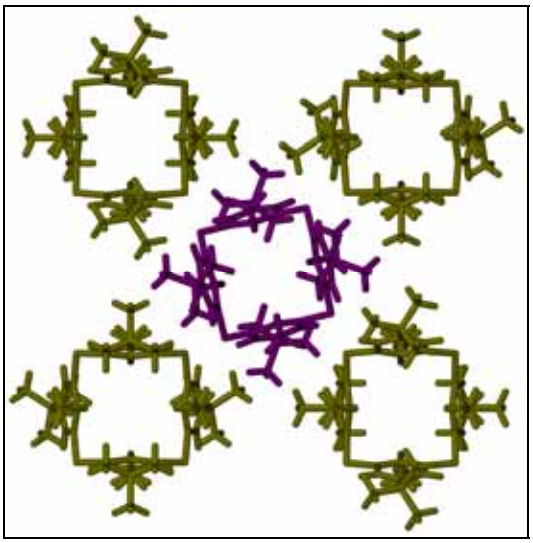

Figure 32. Packing mode of structure **3b** illustrating the twisting of molecules **3b$_2$** (center, purple molecule) with respect to molecules of **3b$_1$** (outer, green molecules).

Each pair of distal aromatic rings in the 1,3-alternate conformation of **3** forms a pincer-like arrangement. At each extremity of the molecule along its principal axis the "pincer" enfolds a small cleft with a narrow entrance guarded by two *p-tert*-butyl moieties. It is interesting to note that **3b** contains two crystallographically distinct molecules of **3**, with three of the four clefts unique. As a consequence of its 4 site symmetry, both clefts of $\mathbf{3b_2}$ are identical, and the dihedral angle between the distal rings is 26.08°. Two unique clefts are present in $\mathbf{3b_1}$ and the dihedral angles between their distal rings are 20.78° and 35.68°. This observation implies that one cleft is significantly larger than the other. The radius of the largest sphere capable of mapping a channel through to the centre of $\mathbf{3b_2}$ along its principal axis is 0.97 Å and the corresponding value for $\mathbf{3b_1}$ is 0.89 Å (note that the van der Waals radius of a hydrogen atom is often taken to be about ~1.17 Å).

After collection of x-ray diffraction data, the crystal of **3b** was immersed in water for 8 h. Data were then recollected, and yielded structure **3c**. The space group of **3c** is also $P42_1m$ ($a=b$=19.516(2), c=12.096(1) Å) and structure solution reveals the same arrangement and relative conformations of the calixarene moieties (correspondingly designated $\mathbf{3c_1}$ and $\mathbf{3c_2}$) as observed in **3b** (distal ring dihedral angles are 26.48° for $\mathbf{3c_2}$, and 20.28° and 35.08° for $\mathbf{3c_1}$). FT-IR (Appendix B) analysis of carefully dried crystals, after similar treatment with water, indicated the presence of water molecules in **3c** and an overall calixarene:water ratio of 1:1 was determined by thermogravimetric analysis. In accordance with these results, least squares refinement of **3c** yielded difference electron density peaks consistent with the presence of water oxygen atoms in the structure. Each of the two clefts of $\mathbf{3c_2}$ contains a water molecule at 50% site occupancy. The larger of the two clefts of $\mathbf{3c_1}$ contains one water molecule, while the smaller cleft remains unoccupied. A lower-symmetry structure of an inclusion complex of **3** with both water and dichloromethane has previously been published.[114]

The structure of **3b** is most likely dictated by complex packing considerations that do not favour a more symmetrical arrangement containing a single, unique conformation of **3**. Our experimental results show unequivocally that exposure of single crystals of **3b** to liquid water results in water molecules becoming lodged within some of the pincerlike clefts of the calixarenes. The water uptake is stoichiometric and the lattice structure remains otherwise unchanged. It appears that

the three crystallographically different but similar molecular clefts exhibit remarkably subtle degrees of selectivity towards the guest water molecules. Figure 33 shows the two unique clefts of **3c$_1$** represented as Connolly contact surfaces. The *tert*-butyl groups guarding the mouth of the smaller of the two clefts (Figure 33a) are rotated such that the cleft volume is maximised.

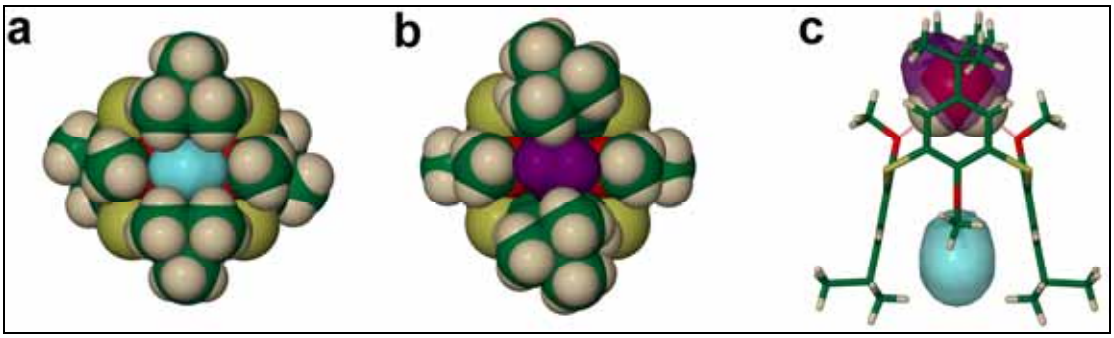

Figure 33. Molecule **3c$_1$** with its two clefts shown as Connolly surfaces. A probe radius of 1.4 Å was used to calculate the surfaces representing the voids. **(a)** At one extremity of the host molecule, the unoccupied void (16.1 Å^3) is shown as a light blue surface. **(b)** The fully occupied void (35.8 Å^3) at the other end of the molecule is shown as a purple surface. **(c)** A side-view of **3** showing a section through the two cavity surfaces. The water molecule within the larger cavity is shown in van der Waals representation. Hydrogen bonds are indicated as dashed red lines.

Although the void is large enough to accommodate a water molecule, it remains unoccupied in **3c** (Figure 33c). The cleft at the other end of the calixarene (Figure 33b) is larger, as a result of the greater angle between its distal aromatic rings. The two *tert*-butyl groups at this end are each disordered over two distinct positions. Four combinations of positions of these groups relative to one another are possible, but only two are geometrically unique (the combination defining the maximal void space is shown in Figure 33). This cleft accommodates one water molecule, while the water donates two hydrogen bonds (O···O=2.998 Å) to the methoxy oxygen atoms at the base of the cleft (Figure 33c).

The two molecular clefts in **3c$_2$** (shown as Connolly surfaces in Figure 34) are equivalent in size and shape, and each is barely large enough to accommodate a single molecule of water (ca. 19.7 Å^3) in a hydrogen-bonded environment (assuming that hydrogen bonding involves a small amount of van der Waals overlap of molecules).

The *tert*-butyl groups do not appear to be disordered, and are positioned relative to one another so as to minimise the total void volume as well as the opening to the cleft. In the final crystallographic model, **3c$_2$** acts as host to only one water molecule that is disordered equally over the two possible sites (Figure 34b). The water molecule donates two hydrogen bonds (O···O=2.995 Å) to the calixarene methoxy oxygen atoms.

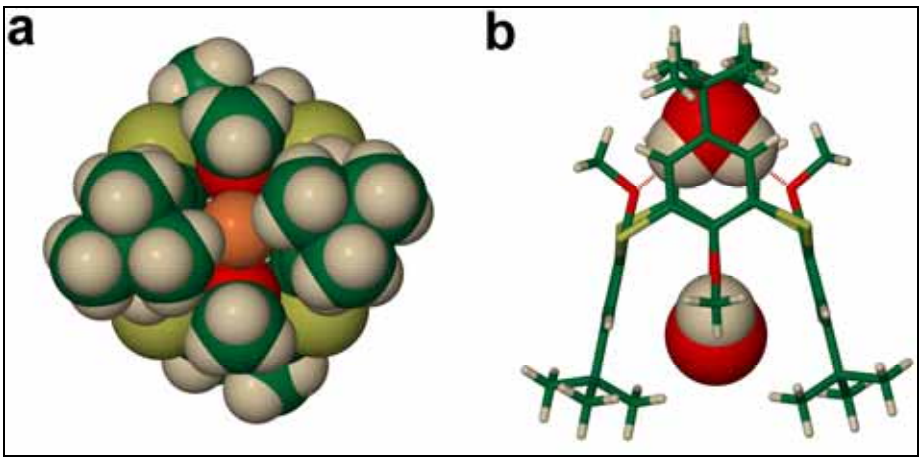

Figure 34. Connolly surfaces (orange) representing the two symmetry related clefts (13.5 Å^3 each) in **3c$_2$**. **(a)** A view along the principal axis of the host molecule shows that the mouth of the cleft is guarded by two *tert*-butyl groups. **(b)** A side-view of **3** showing two water molecules, each at 50% site occupancy, in space-filling representation.

From thermogravimetric and x-ray structural analyses it can be inferred that any molecule of **3** can only accommodate a maximum of one water molecule, even though there is enough space for two. Indeed, repeated soaking experiments lasting from eight hours to several days yielded consistent host:guest ratios of 1:1. The two distal *tert*-butyl groups at the mouth of each cleft are too close to one another to allow a water molecule to enter without conformational distortion of the calixarene. The water uptake appears to occur through a complex mechanism involving rotation of the *tert*-butyl groups, with concomitant flexing of the host molecule whereby the distal aromatic rings lining the target cleft move apart. Such flexing most likely occurs as rotation about the C-S bonds of the thioether linkages. The flexibility can easily be rationalised as the *1,2-alternate* conformation of **3** is also found. Thus the aromatic rings of the remaining cleft would be required to pinch closer together to compensate energetically for the bond strain. Once a water molecule is admitted into the cleft, the

host molecule can return to its original conformation. The water molecule now finds itself in a favourable environment were it is stabilised by two hydrogen bonds to symmetrically placed methoxy oxygen atoms. According to this assumption, the incorporation of a water molecule into one of the calixarene clefts inhibits uptake of water by the remaining cleft. The water molecule serves as a steric brace to the pinching motion that is required to open the opposite cleft of the host in order to capture a second water molecule. One of the voids of **3c$_1$** is significantly larger than the other and is also guarded by rotationally compliant *tert*-butyl groups. Hence, it is plausible that water uptake by this void is kinetically favoured over that of the other, and the crystallographic model with a single water molecule at only one end of **3c$_1$** seems reasonable. Since both of the host cavities of **3c$_2$** are equivalent, we propose that a water site occupancy of 50% in each cavity implies that each molecule of **3** only captures one water molecule, but that the two cavities are equally favoured.

Although the possible mechanism by which water molecules enter the voids of isolated host molecules has been discussed, careful scrutiny of the packing mode of the calixarene molecules reveals that the host framework is nonporous. This observation raises the intriguing question of how the water molecules diffuse through the lattice before becoming lodged within the calixarene cavities.

Since structures **3b** and **3c** were determined using the same crystal, we can disregard the possibility of a water-inclusion process involving crystal dissolution and regrowth. Indeed, compound **3** is highly hydrophobic with no discernable water solubility, even in boiling water. The calixarene molecules are stacked in columns parallel to [001]. Connolly surface plots (Figure 35a) reveal lattice voids (shown in green) embedded within bundles composed of four nearest-neighbour calixarene columns. These voids are isolated from one another by *tert*-butyl and methoxy methyl groups and do not merge to form channels. Assuming that the *tert*-butyl groups can rotate in a concerted fashion during water uptake, it is possible to construct a model in which the lattice voids can be extended maximally towards one another along [001] (Figure 35b).

However, there appears to be no set of orientations for the *tert*-butyl groups that allows the lattice voids to transform into channels. Therefore, no rational pathway can be traced whereby water molecules might be transported through the crystal lattice. Moreover, with the exception only of the location between the two methoxy oxygen atoms embedded within each calixarene cleft, the entire host framework presents a

highly hydrophobic environment. In summary of the above, the molecular clefts of the host molecules constitute the only hydrophilic regions of the crystal structure, and there are no channels leading to these clefts.

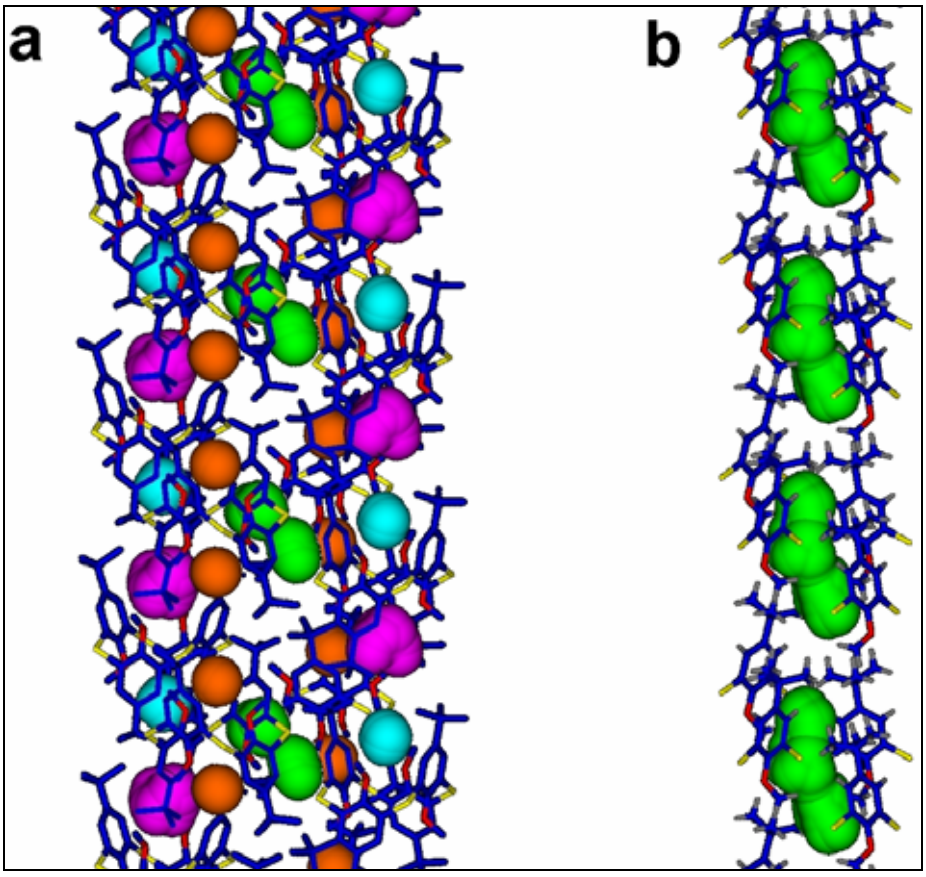

Figure 35. Four adjacent columns of **3** in **3c**, viewed perpendicular to [001]. (a) The Connolly surfaces of the molecular clefts in **3** are shown in blue, purple, and orange (see Figures 33 and 34). The lattice voids between the calixarene atoms are shown in green (45.6 $Å^3$). Hydrogen atoms are omitted for clarity. **(b)** The *tert*-butyl groups of **3** have been rotated to allow maximum extension of the lattice voids (91.4 $Å^3$) along [001]. Only the parts of the calixarenes defining the lattice voids are shown.

The uptake of an individual water molecule can be simplified as a two-step process involving diffusion through the lattice, followed by complexation by the host molecule. While water molecules travel through the nonporous hydrophobic lattice with seemingly little concern for van der Waals surface constraints, they appear to be quite selective with regard to the size, shape, and electrostatic profile of their final resting places. Carbon nanotubes have been studied extensively as model systems for small hydrophobic channels by using molecular dynamics simulations.[112f–h,115] These

studies indicate that water can be transported quite rapidly through such channels in single file. However, for diffusion to occur, it is generally understood that the channels must be of a suitable diameter (as defined by the van der Waals surfaces of the constituent atoms) to allow free passage of the water molecules. Indeed, this is taken to be a universal requirement for the diffusion of any substance through any matrix.[116] These results imply that the classical view of diffusion might be inappropriate when applied at the atomic scale. We have shown that water molecules have the ability to burrow through a rigid medium such as a crystal without the clear presence of suitable channels. It must be said that the lattice and molecular voids in the structure of **3b** are essential to the diffusion process. Although these voids do not merge to form channels, they are situated relatively close to one another at the atomic scale. In such cases, it is perhaps possible for water molecules to exploit the voids as "stepping stones" to travel through the lattice. The water-transport mechanism would thus involve water molecules hopping between voids until a thermodynamically favourable location can be found. The implications of these findings are that, either crystals are not as rigid as generally presumed, or that van der Waals surfaces do not behave as classical barriers to small molecules in motion.

In continuation of the study of the porous characteristics of **3b**, iodine sorption experiments were conducted. Exposing sublimed crystals to iodine vapour resulted in some of the crystals changing colour. It is relatively difficult to separate the two polymorphs from each other visually and the iodine sorption provides a means of identifying crystals that are "porous" by eye, as the polymorph **3a** does not absorb iodine. If the crystal is initially colourless and absorbs iodine, its colour normally changes to a shade of red. Only a few of the crystals became red. Inspection of the shape of these crystals indicated that they were likely to be the **3b** polymorph and this was confirmed by single-crystal x-ray analysis. Of more interest is that the iodine could be easily removed from these crystals by placing them under vacuum for several hours to again yield the "empty" **3b** structure, thus proving that these crystals are fully porous as evidenced by their ability to absorb and release guests. The structure of the iodine clathrate (**3d)** is important to the study of water absorption because the iodine absorption sites provide some insight to the possible movement of molecular species through the lattice voids. The iodine molecules cannot reside within the small clefts of the calixarenes and are instead located in the "stepping stone" lattice voids between the calixarene molecules. The host:I_2 ratio is 2:1.

Owing to the low yield of the polymorphic **3b** structure by means of sublimation, it was hoped that an inclusion compound of iodine grown from solution might provide the appropriate structure that could be converted to the 'empty' porous phase by simple evacuation. To this end iodine was dissolved in acetyl acetate together with compound **3** - it is known that compound **3** forms phase **3a** from a solution of acetyl acetate.[116] The formation of red crystals indicated that iodine had been successfully integrated into the crystal (**3e)**. However, x-ray diffraction analysis revealed that this was instead a new phase. This solvent-induced iodine inclusion compound crystallises in the orthorhombic space group *Pnma* and the host:guest ratio is 1:1. The calixarene methoxy groups are disordered over two positions in order to allow more space to include the iodine. An iodine···O (methoxy) interaction is implied by van der Waals overlap (see Figure 36). These adducts of **3**·iodine are stacked one next to the other to form one-dimensional rows. The adducts are packed in an up/down fashion translated half the dimension of the adduct in all three directions of space. This structure is virtually the same as those found for the chloroform and dichloromethane/water clathrates reported in the literature.

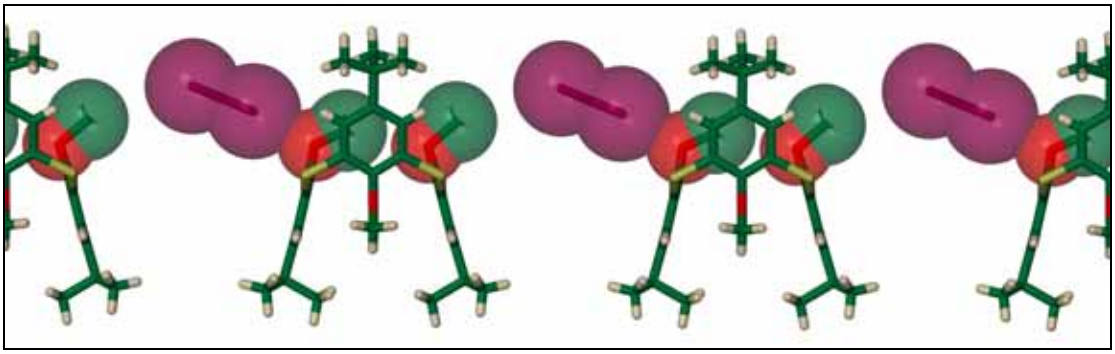

Figure 36. Iodine-included structure **3e** with a host:guest ratio of 1:1.

The physical behaviour of the crystal phase **3e** is also different from that of the vapour exposed crystals. When placed under vacuum the orthorhombic phase does not release the iodine.

It appears that a solvent-based approach to the crystallisation of phase **3b** may not be feasible. It may be that the solvent-based crystallisation of this calixarene is a thermodynamically controlled crystallisation process that favours lower symmetry (Figure 37). The sublimation process may well interfere with this process, sometimes

facilitating the formation of a metastable phase (i.e. **3b**) by means of kinetic crystallisation.

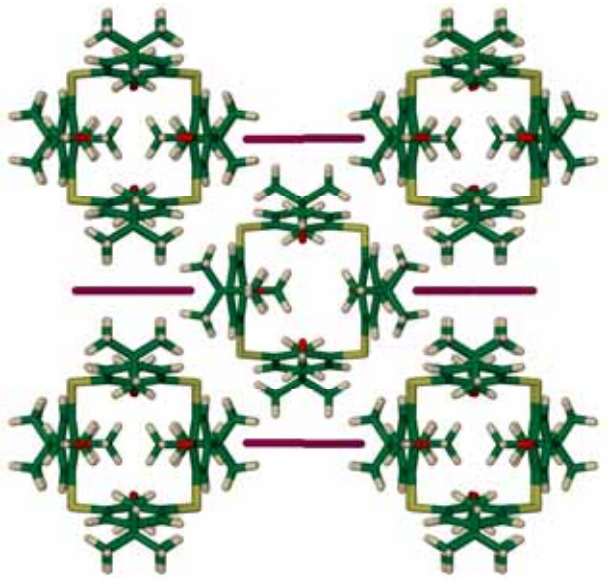

Figure 37. The lower symmetry of the calixarenes found in **3e**.

Metallocycles

One of the aims of this study was to find novel forms of porous structures as well as to study known forms of porous crystalline structures. Much focus has been placed on coordination polymers mostly due to the success of O. M. Yaghi, M. Kitagawa, G. Férey and many others.[18,19,34,50,57-61,64] In keeping with our overall interest in the inherently inefficient packing of *discrete* cavity-containing, discrete complexes incorporating the ligands 1,4-bis(2-methylimidazol-1-ylmethyl)benzene (IMID) and 1,3-bis(imidazol-1-ylmethyl)-2,4,6-trimethylbenzene (BITMB) are reported here. They represent a divergent design strategy for producing porous structures. Instead of forming rigid, stable coordination polymers, these discrete coordination compounds pack very much like organic crystals, in that supramolecular interactions play a large part in the formation of void space.

Silver-IMID Metallocycle

Compound **4** :- $[Ag_2(IMID)_2](BF_4)_2 \cdot (CH_3CN)_2$

Compound **5** :- $[Ag_2(IMID)_2](BF_4)_2$

Slow evaporation of an equimolar solution of $AgBF_4$ and 1,4-bis(2-methylimidazol-1-ylmethyl)benzene (IMID) in acetonitrile (methanol can also be used) yielded single-crystals suitable for x-ray diffraction analysis (Figure 38).[70a]

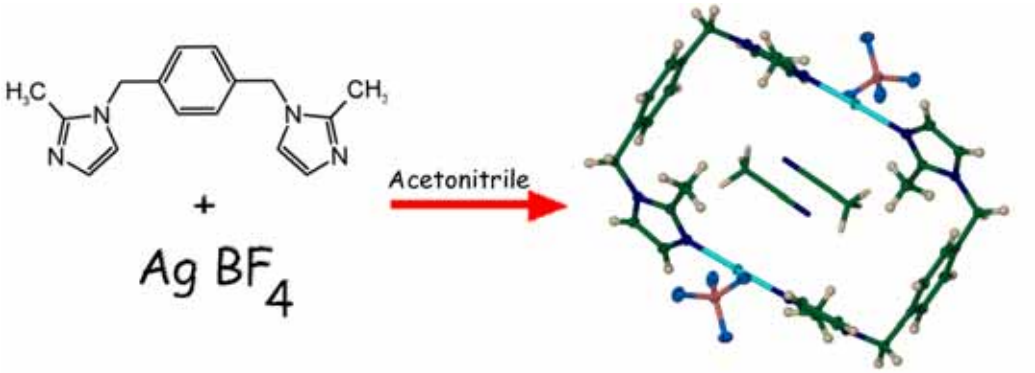

Figure 38. Scheme showing the formation of $[Ag_2IMID_2](BF_4)_2 \cdot 2CH_3CN$.

The crystallographic study reveals a discrete rectangular complex composed of two linearly coordinated silver ions doubly bridged to one another by means of two IMID ligands. The ring-like complexes are stacked along the crystallographic *c* axis to form one-dimensional channels (Figure 39). Acetonitrile solvent molecules occupy the channels, while the BF_4^- anions are situated between adjacent columns of stacked $[Ag_2IMID_2]^{2+}$ complexes. The BF_4^- anions also provide part of the wall of the one-dimensional channel when a small enough probe radius is considered. The acetonitrile guest does not interact with the BF_4^- anions. Each column is in van der Waals contact with six neighbouring columns (Figure 40) to form a "brick wall" packing motif as viewed along [001]. This arrangement is stabilised by intermolecular offset π-π interactions between the imidazole rings along [010] (interplanar distance = 3.454 Å) and benzene rings along [100] (interplanar distance = 3.52 Å).

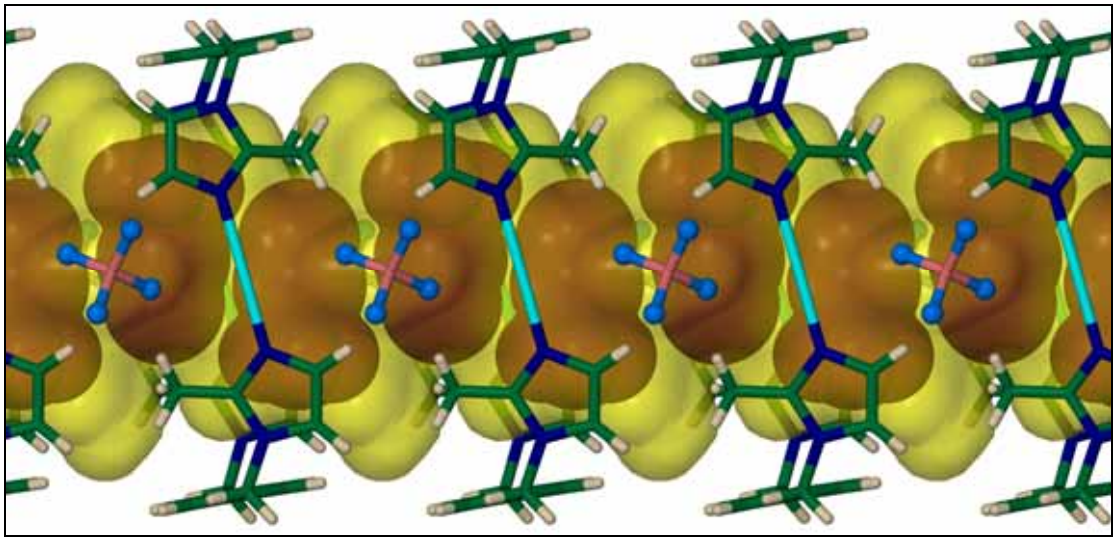

Figure 39. Perspective view perpendicular to a one-dimensional channel (semitransparent yellow surface, probe radius of 1.17 Å) defined by a column of cyclic $[Ag_2IMID_2]^{2+}$ complexes. The complex ions $[Ag_2IMID_2]^{2+}$ are shown as capped-sticks, the BF_4^- ions as balls-and-sticks, and the acetonitrile molecules are shown in the van der Waals metaphor. Colours: carbon, green; hydrogen, white; nitrogen, dark blue; silver, light blue; boron, pink; fluorine, ocean blue; acetonitrile; brown.

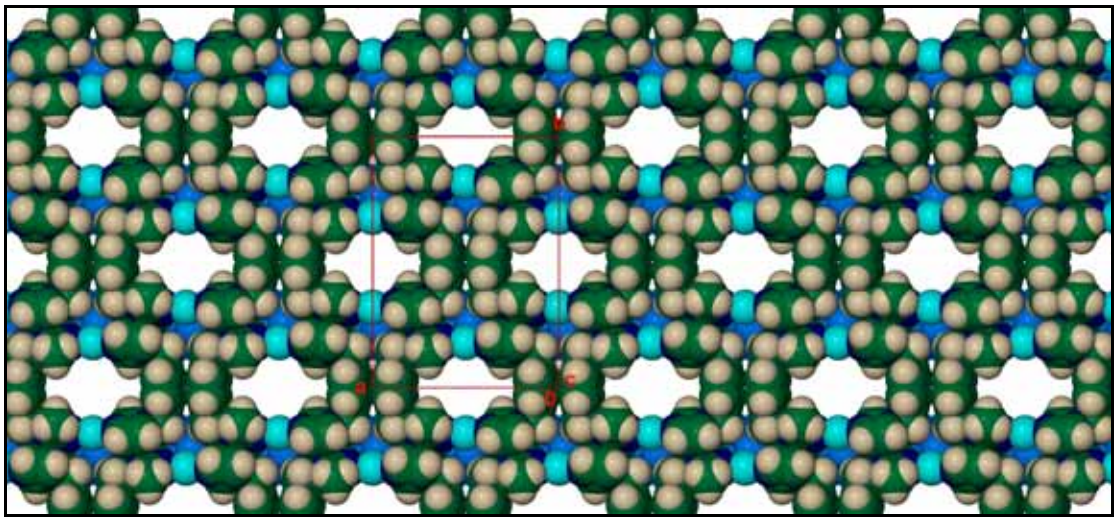

Figure 40. Space filling projection showing the packing arrangement of the rectangular $[Ag_2IMID_2]^{2+}$ host complexes to form channels along [001]. Acetonitrile guests have been removed for clarity. Colours: carbon, green; hydrogen, white; nitrogen, dark blue; silver, light blue; fluorine, ocean blue.

Thermogravimetric analysis of this compound shows that the acetonitrile guest molecules can be removed completely by heating the crystals to > 80°C. Two

acetonitrile molecules per complex were found, which is consistent with the x-ray structure. Using hot stage microscopy, crystals heated to 80°C were observed to remain intact and transparent. A crystal thus treated was therefore subjected to single-crystal x-ray diffraction analysis (at 100K) (compound **5**), which showed that no significant rearrangement of the host lattice takes place as a result of the thermally induced desolvation. No electron density peaks were located within the channels previously occupied by the acetonitrile guests. The structure was also determined at room temperature as gas sorption experiments are conducted under these conditions. The vacant channels are approximately rectangular in cross-section with internal van der Waals dimensions of ca 4.9 x 7.5 Å. The unoccupied space in the crystal is estimated to be approximately 22% of the total volume.

Seemingly Nonporous Cu-BITMB Metallocycle

Compound **6** :- $[Cu_2(BITMB)_2Cl_4]\cdot CH_3OH\cdot H_2O$

Compound **7** :- $[Cu_2(BITMB)_2Cl_4]$

Compound **8** :- $[Cu_2(BITMB)_2Cl_4]\cdot I_2$

Slow evaporation of a methanolic solution of $CuCl_2\cdot 2H_2O$ and the *exo*-bidentate ligand 1,3-bis(imidazol-1-ylmethyl)-2,4,6-trimethylbenzene (BITMB) in a 1:1 molar ratio afforded single crystals suitable for x-ray diffraction analysis (compound **6**).[70b] A discrete cyclic dinuclear complex $[Cu_2(BITMB)_2Cl_4]$ is formed as shown in Figure 41.

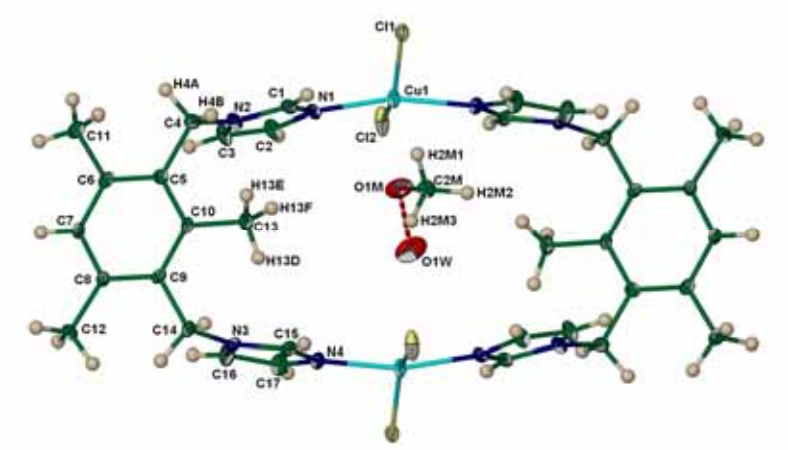

Figure 41. The discrete cyclic dinuclear complex $[Cu_2(BITMB)_2Cl_4]$. Atoms shown as 50% probability ellipsoids. Labelled atoms represent the asymmetric unit.

Each copper ion is coordinated to two chloride anions and two BITMB ligands in a distorted square planar arrangement with like ligands *trans* to one another. The rings are canted at an angle of approximately 40º with respect to the crystallographic *a* axis along which they are stacked one above the other to form linear columns. The space within the complex ring is occupied by a hydrogen bonded (O···O = 2.769(8) Å) two membered adduct consisting of one water molecule and one molecule of methanol (Figure 42a). The adduct is disordered equally over two positions across a crystallographic inversion centre and the methanol oxygen atoms are weakly associated with the copper ions at a distance of 2.461(3)Å and situated at the apex of a pseudo square pyramid. Thermogravimetric analysis of the crystals reveals that solvent loss occurs readily, even at room temperature. Heating of the crystals at 60ºC under vacuum for one hour results in complete removal of the solvent molecules while the crystals show no visible signs of mechanical stress. X-ray diffraction analysis (compound **7**) confirms that no significant change of the structure occurs on desolvation except that the space previously occupied by solvent molecules becomes devoid of any appreciable electron density (Figure 42b).

It is interesting to note that, after desolvation, the crystals do not appear to absorb water even after exposure to the atmosphere for three weeks. The empty structure is interesting in that when using the Connolly package to investigate the porosity of the compound, no significant pore size is found. In fact a comparison of the "pore" sizes between the empty and solvate structure shows that the empty structure has a maximum static pore size of r_{pore} = 0.961 Å and the solvate structure has a maximum of r_{pore} = 1.327 Å (where r_{pore} is the radius of the probe).

In order to probe the permeability of solvent-free crystals, a desolvated single-crystal was exposed to iodine vapour in a sealed vial for 25 hours. After exposure, the colour of the crystal changed from green to brown with no discernible degradation of its single crystallinity. X-ray analysis of the new clathrate (compound **8**) reveals the presence of iodine in the guest pockets (Figure 42c). Each iodine molecule is disordered equally over two positions with a total site occupancy of one within each pocket. In the disordered model, one of the iodine atoms is situated on a crystallographic inversion centre and at a distance of 3.458(1)Å from each copper ion. Although too long to be considered a coordination bond, this distance, and thus the consistent location of an iodine atom at this site, is likely due to a weak Cu···I

electrostatic interaction. The I–I bond length is 2.648(1) Å and is in the slightly low to normal range. The arrangement of the host complexes in the iodine clathrate is essentially identical to that in methanol·water solvate and solvent-free compound. In the iodine clathrate a probe with r_{probe} < 1.242 Å is required in order to map an open channel, i.e. a maximum static pore size (note that the van der Waals radius of iodine is generally taken to be approximately 1.98 Å).[117]

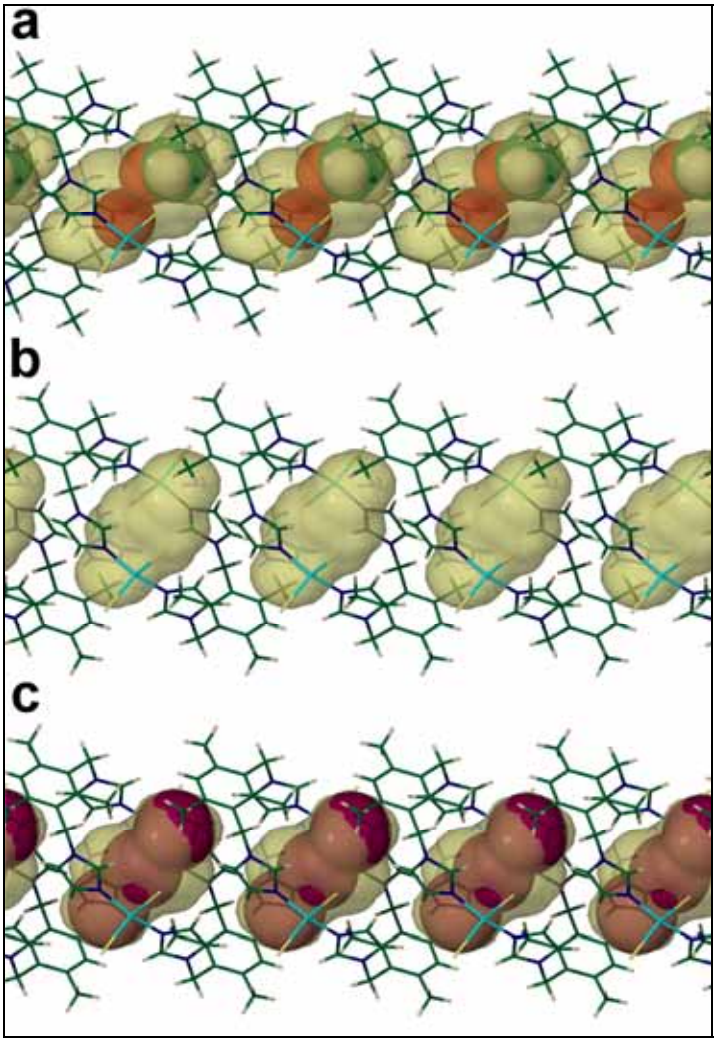

Figure 42. Void space (yellow semi-transparent surface, r_{probe} = 1.4 Å) resulting from the packing arrangement of the complexes one on top of the other. **(a)** Solvent cavities occupied by the methanol:water adduct in **6** (cavity volume ≈141.7 Å^3). **(b)** Empty voids after removal of the methanol:water adduct from **6** by heating to form **7** (structure elucidated under vacuum) (void volume ≈109.6 Å^3). **(c)** The disordered I_2 situated in the cavity of **8** (cavity volume ≈129.8 Å^3). Protrusion of the iodine van der Waals surface beyond the Connolly surface implies the presence of weak intermolecular interactions in these regions.

The mapping of a channel to connect the voids not only indicates that the structure is changing slightly but that the overall structure does not possess channels. The structure also appears to "swell" when accommodating the guest. For example a simple measurement of the Cu···Cu distance indicates that the distance for the empty structure is 6.598 Å and swells to 6.621 Å in the methanol:water solvate, swelling even further to 6.916 Å in the case of the I_2 complex. The overall flexibility of the coordination complex may therefore allow "transient" porosity to arise, allowing the guest to enter the voids without much of a penalty in energetic terms.

Discussion

The main aim of this study was to produce porous crystalline solids. The materials investigated here further extend the concepts unearthed following the initial discovery of diffusion into the *p-tert*-butylcalix[4]arene structure, i.e. the concept of porosity without the need for obvious pores. Classical aspects of host:guest chemistry, one of the fundamental concerns of supramolecular chemistry and crystal engineering, of all these systems were also studied.

Compounds **1** and **2** produced exciting results involving mostly host:guest chemistry. The high selectivity of the framework created by **1**, which binds a small number of molecules, is rare. The helical tubes formed within these structures represent an addition to the helical host families of urea and the acyclic diols. The non-centrosymmetric structures also promise possible applications and further studies in non-linear optics as most of the guests are bound in polar arrays. Within the realm of host:guest chemistry, the persistent retention of the host structural framework is an uncommon phenomenon. The discovery of a well-definable case of self-inclusion necessitates an adjustment in the way organic crystals can be viewed - just because a compound crystallises pure does not necessary mean that it cannot exhibit host:guest properties. Indeed, Toda *et al.* have stated that **1** does "not show any inclusion ability."[70] The lightweight host framework of **2** also provides hope of producing a porous structure which has a high density of small pores, but is light enough to allow useful weight percentages of guest to host.

Dianin's compound is undoubtedly one of the archetypal organic molecular hosts. Our interest in Dianin's compound stems from its ability to form an empty host with appreciably sized voids connected by easily characterised pores. This phase, grown by sublimation under vacuum, was studied for its gas sorption properties. The

host:guest chemistry of Dianin's compound has been studied for nearly a full century, yet it surprisingly still yielded significant new paradigms during this study. This includes the deprotonation phenomenon by morpholine guests resulting in a lowering of symmetry to triclinic, along with ordering of guest species. This result adds to the well-studied collection of guest types bound within Dianin's compound clathrates. Owing to the ordering of the guest within the void spaces of the framework of Dianin's compound, the possibility of supramolecular ordering for the catalysis of a chemical reaction can be envisioned in the form of the allylamine clathrate. The deprotonation of the host framework of Dianin's compound also results in supramolecular cocrystallisation when ethylene diamine is used as a guest. The two host systems, i.e. the deprotonated form and the neutral form, cocrystallise as a large trigonal system reminiscent of the neutral host. The two structural types discovered in this study differ crystallographically from the *R*3 clathrates only in the hydrogen bonded sextet of hydroxyl groups. The skeletal structure of Dianin's compound essentially stays the same, indicating that the hydrogen bonded sextet of hydroxyl groups is not necessarily the driving force for the formation of Dianin's compound clathrates. These results represent the supramolecular variation in the Dianin's compound clathrates, rather than a molecular variation as conducted by MacNicol and co-workers. However, this is partially contradicted by the finding that piperidine can induce the formation of any of the two new structural types, as well as forming a known 1:1 host to guest complex which crystallises in the monoclinic space group. It appears that if there is a strong enough driving force in the form of a stable hydrogen bonding motif, Dianin's compound can be induced to not crystallise with a guest in 3 symmetry. The relevantly new concept of cocrystals could be used to uncover a wealth of new clathrate chemistry for Dianin's compound. For such an "old" compound, Dianin's compound has a healthy future.

p-tert-Butylcalix[4]arene is a very elegant, simple cup-shaped molecule that appears to form one of the most counterintuitive and complex porous materials. The phase changes that occur within this structure due to thermal changes serve to illustrate how the overall structure is malleable enough to allow significant changes at the atomic level without loss of mosaicity at the micro scale. Cooperativity between the individual neighbouring molecules, and indeed layers of molecules at the supramolecular scale, is evidenced to the extreme by these structural changes. These

changes may lead to the improved understanding of the mechanism of sorption not just of gas molecules, but larger organic solvents.

The double-ended host molecule **3** features two pincerlike clefts, each defining a void approximately the size of a single water molecule. Encapsulation of water at one extremity of the molecular receptor appears to inhibit guest inclusion at the other end. This observation is easily rationalised in terms of conformational flexibility of the host molecule during guest complexation, as well as by our comprehension of van der Waals interactions. However, conventional wisdom does not explain why water molecules display seemingly little regard for van der Waals constraints during the dynamic diffusion process: it is only when they finally come to rest that the water molecules appear to obey spatial restrictions imposed by van der Waals surface contacts. Our results imply that the classical view of diffusion might be inappropriate when applied at the atomic scale and has shown that water molecules have the ability to burrow through a rigid medium such as a crystal without the clear presence of suitable channels. It is our belief that the lattice and molecular voids in the structure of **3b** are essential to the diffusion process. Although these voids do not merge to form channels, they are situated relatively close to one another at the atomic scale. In such cases, it is perhaps possible for water molecules to exploit the voids as "stepping stones" to travel through the lattice. The water-transport mechanism would thus involve water molecules hopping between voids until a thermodynamically favourable location can be found.

This idea of "stepping stones" is visualised by the absorption of iodine molecules into precisely these voids when the empty crystals are exposed to iodine vapour. Once again, this takes place with total disregard for the van der Waals constraints. The discovery of an inclusion complex, synthesised from a solvent mixture of iodine and **3**, shows how important the subtleties of molecular structure can be in conferring large changes in macro-physical properties such as porosity. These findings have potentially important implications for both theoretical and experimental studies of water-transport phenomena, particularly across biological membranes. The implications of these findings are also that crystals might not be as rigid as generally presumed, and/or that van der Waals surfaces might not behave as classical barriers to small molecules in motion.

Overall, the discovery of new host:guest chemistry has illustrated the complexity of achieving porous phases of molecular crystals. New paradigms such as

self-inclusion illustrate once again how nature abhors a vacuum, even within the close-packed and ordered environment of the crystal. Despite these "negative" results, the porous states of sublimed Dianin's compound and *p-tert*-butylcalix[4]arene were found to be amenable to gas sorption studies. In addition, a sublimated polymorph of 5,11,17,23-tetra-*tert*-butyl-25,26,27,28-tetramethoxy-2,8,14,20-tetrathiacalix[4]arene provided a new member to the short list of seemingly nonporous porous solids. Most important of all is how these relatively few compounds illustrate that there are a multitude of fascinating phenomena still waiting to be discovered by exploring the realm of organic crystalline solids.

The two complexes in the structures **4** and **6** produced crystals that are porous and therefore could be investigated using gas sorption experiments. Compounds **4** and **5** are salts that have a cyclic cationic complex that encloses void space. The stronger electrostatic potentials of the cationic species surrounding the void space provides an instrument for unlocking degrees of gas:solid interactions. The complexes forming structures **6**, **7** and **8** are neutral. It is interesting that they represent the first coordination compounds to be added to the young family of seemingly nonporous porous crystalline materials that contain discrete lattice voids (thus far calixarenes provide the only other examples).

5. Gas Sorption and Separation

Studies of porous crystalline materials have almost exclusively been concerned with the naturally-occurring zeolites for a relatively long time.[54] However, over the last decade these studies have evolved to include organic compounds[45,55,56,66b,76,79a] and coordination polymers.[19,58,59,64,65,75i] The many applications associated with porous materials include catalysis,[118] molecular storage,[28b,30,38,58b,62] molecular separation,[56,119] molecular sensing,[120] electronics,[83,121] and ion exchange.[122] This chapter is mainly concerned with the storage and separation of gases.

Nitrogen, carbon dioxide, methane, oxygen and hydrogen are the most commonly encountered and utilised gases, as summarised in Table 2. The recent surge in interest in gas storage and separation is a direct result of the much fêted "Hydrogen Economy".[63] The effort devoted to the search for alternative fuels has increased substantially with heightening awareness of dwindling fossil fuels supplies. The availability of methane and hydrogen in abundant supplies of natural gas and water has resulted in these two gases leading the race to be proclaimed the best alternative fuel.

Table 2. Common gases and their uses.

Gas	Uses
Nitrogen (N_2)	80% of earth's atmosphere, nitrogen cycle in nature
Carbon dioxide (CO_2)	most recognised greenhouse gas (pollutant), photosynthesis, main product of combustion of carbon-based fuels
Methane (CH_4)	natural gas, possible replacement for fossil fuels
Oxygen (O_2)	combustion, respiration, reactant in hydrogen fuel cells
Hydrogen (H_2)	basis of the hydrogen economy, reactant in hydrogen fuel cells, believed to be the best alternative to fossil fuels

One of the most significant problems associated with using these two gases as fuels relates to the difficulties associated with their storage and transport.[63] Gases stored even under high pressure (considered dangerous as well) do not contain as much energy per unit weight as conventional fuels such as gasoline. One of the most

promising approaches to solving this problem involves the reversible sorption into porous materials.[75g] Separation of the five gaseous compounds listed above from one another and other gases, especially sulphur containing compounds, is also an extremely important concern.[56,123] At the current level of technology, H_2 is produced commercially *via* the two reactions, steam reforming of natural gas and the water-gas shift reaction (see below).

$$CH_4 + H_2O \rightleftharpoons CO + 3H_2$$

$$CO + H_2O \rightleftharpoons CO_2 + H_2$$

The final product, H_2, requires substantial purification by removing impurities such as CO, CH_4, H_2O, any impurities within the natural gas and, primarily, CO_2. Both the design and implementation of separation technologies has improved to such an extent that any improvement in gas separation necessitates the development of new adsorbent materials.[56]

Substantial effort with regard to the development of adsorbent materials has focused on porous metal-organic frameworks (coordination polymers). The three leading personalities in this area are O. M. Yaghi, S. Kitagawa and G. Férey. Yaghi uses the concept of reticular synthesis to design MOFs that possess promising sorption properties.[19,64,75i,119] Kitagawa focuses on characterising these compounds and has directed the field towards dynamics and flexibility.[34,124] Férey has used experience gained from studying porous metal phosphates to design complex porous coordination polymers with high surface areas.[57,58]

Porosity studies of crystalline materials, especially of "organic zeolites", are still in their infancy. Is not yet clear how surface area, shape, type of interactions at the gas/solid interface or chemical functionality of the material will improve sorption properties. Thus, this study represents an effort towards gaining insight into the nature of gas sorption phenomena.[125]

A description of the gas sorption apparatus and methodology is given at the beginning of this chapter in order to disclose how the experimental results were obtained. The quantification of the isosteric heat of sorption of CO_2 into the sublimed low-density form of *p-tert*-butylcalix[4]arene (chapter 5.3) follows. Although the

sublimed phase of Dianin's compound (chapter 5.2) is well-known, the selective sorption by this material is presented here for the first time. The gas sorption isotherms of CO_2, N_2, CH_4 and H_2 by compound **5** (desolvated silver-IMID metallocycle, chapter 4) are presented next. Compound **7** (desolvated seemingly nonporous Cu-BITMB metallocycle, chapter 4) is the first coordination compound to be categorised as a seemingly nonporous material that is indeed porous. An attempt at understanding the mechanism of sorption by this material is presented at the end of this chapter.

Gas sorption equipment and methodology

Owing to our lack of a commercial instrument for the measurement of gas sorption by crystalline solids, suitable equipment was designed and constructed locally. Since gravimetric measurements require highly accurate and sophisticated balance mechanisms, it was decided to use volumetric measurements in accordance with our own technical capabilities. The volumetric measurement of the gas sorption isotherms is relatively simple and accurate: high precision electronic pressure transmitters record sorption as a change in pressure while the volume of the system remains fixed.

Figure 43. Volumetric gas sorption apparatus.[79a]

Modular brass Swagelok components were used to assemble the apparatus shown in Figure 43. The entire system is housed in a thermostated cabinet in order to facilitate long-term temperature control and stability. The left-hand chamber serves as

a gas reservoir for the release of a known amount of gas into the right-hand chamber, which contains the sample. The volume of each of the chambers is initially calibrated using N_2 gas (the ideal gas law is applied at relatively low pressures) and an aluminium cylinder of known volume (calculated from its density and weight). The volume of the sample is determined from its weight and density (the latter is known from the single-crystal x-ray structure determination). In a typical isothermal experiment, the chamber containing the sample is first evacuated while the reservoir is pressurised with the gas of interest. The valve dividing the two chambers is opened briefly (normally about one second) and then closed again. If the sample absorbs the gas, the pressure within the sample chamber will continue to drop until equilibrium is reached. From the pressures measured at the beginning of the experiment and at the equilibrium pressures of both chambers, the amount of gas absorbed by the sample can readily be determined. A computer interface allows the experiment to be followed in real-time and records data for the entire experiment. A typical result is shown in Figure 44.

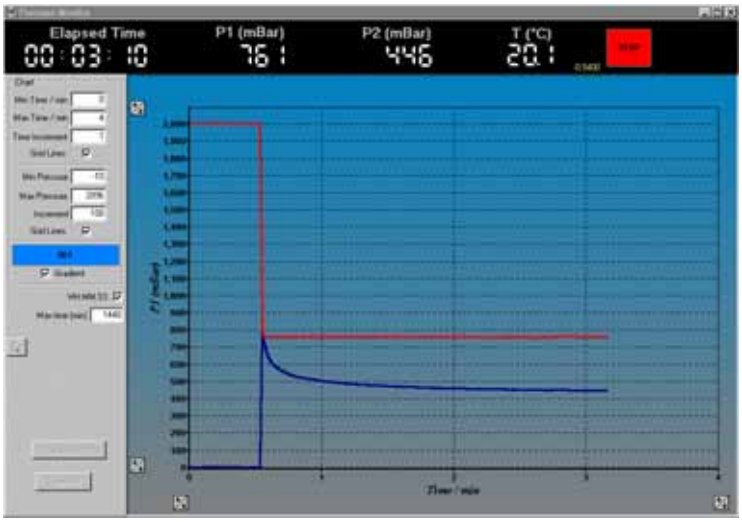

Figure 44. Computer interface for monitoring a gas sorption experiment. Note that the experimental values required for the calculation of the amount of gas absorbed are the initial pressures ($P1 \approx 2000$ mBar and $P2 \approx 0$ mBar at t = 0 min) and the equilibrium pressures ($P1 \approx 761$ mBar and $P2$ has not yet reached equilibrium at t = 3 min).

The amount of gas absorbed can be expressed as mass percentage (g/g), percentage occupancy (%) or moles of gas per gram of substrate absorbed

(mmoles/g). From a cumulative series of sorption experiments it is possible to plot a curve of occupancy as a function of equilibrium pressure.

The isosteric heat of sorption is determined experimentally by recording equilibrium pressure as a function of temperature for a fixed quantity of gas and substrate. The initial part of the experiment involves introducing a fixed quantity of gas and allowing the pressure to equilibrate. The temperature is then ramped at a constant rate (normally 0.2°C per minute) from room temperature to 60°C and then the back to room temperature. The Clausius-Clapeyron equation relates the isosteric heat of sorption to the change in pressure with temperature in the following manner.[126]

$$\mathrm{d}\,(ln\ P)\ /\ \mathrm{d}\,(T) = \Delta H\ /\ RT^2$$

This simple equation can be derived from basic thermodynamic principles. The following equation represents the equilibrium process of gas inclusion/release:

$$m\mathbf{H}_{(s)} \quad + \quad n\mathbf{G}_{(g)} \quad \# \quad \mathbf{H}_m\mathbf{G}_{n(s)}$$

The reaction rate constant can be approximated as

$$K \quad = \quad [\mathrm{H}_m\mathrm{G}_n]/[\mathrm{H}]^m[\mathrm{G}]^n$$

As both the host and the resultant complex are solids the equation simplifies to

$$K \quad = \quad [\mathrm{G}]^{-n}$$

The reaction rate constant is related to the thermodynamic parameters of a reaction by the following equation:

$$\Delta G = -RT\ ln\ K \quad = \quad \Delta H \quad - \quad T\Delta S$$

which then gives the following:

$$-RT\ ln\ K \quad = \quad \Delta H \quad - \quad T\Delta S$$

$$-RT\ ln([\mathrm{G}]^{-n}) \quad = \quad \Delta H \quad - \quad T\Delta S$$

The chemical activity of the gaseous guest can be approximated as its pressure, and the following obtains:

$$-RT\,ln\,[\mathrm{P}]^{-n} \;=\; \Delta H \;-\; T\Delta S$$

$$nRT\,lnP \;=\; \Delta H \;-\; T\Delta S$$

$$n\,lnP \;=\; \Delta H/RT \;-\; \Delta S/R$$

Therefore a plot of ln$P$ as a function of $1/T$ should be linear with a gradient of ΔH/R when the value of n is standardised to one mole of gas. ΔH is then defined as the isosteric heat of sorption (ΔH_{iso}). Although ΔH_{iso} is a negative value, it is reported in the literature, as the isosteric heat of sorption, as a positive value. A typical experiment is shown in Figure 45.

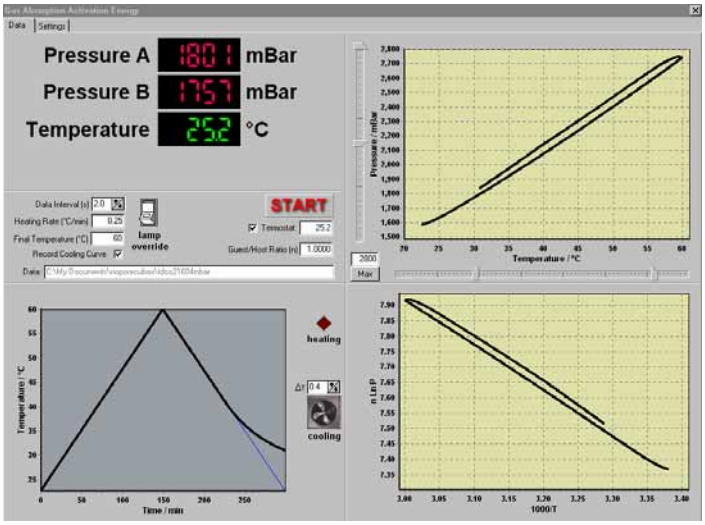

Figure 45. Software interface for the measurement of gas sorption thermodynamics. The bottom right graph can be replotted using Microsoft Excel and the slopes of the heating and cooling curves are averaged to give the isosteric heat of sorption. It is not unusual for the cooling rate (bottom left graph) to deviate from the desired value as the cabinet is well-insulated and cannot cool sufficiently fast at temperatures approaching room temperature.

***p-tert*-Butylcalix[4]arene**

As described earlier, *p-tert*-butylcalix[4]arene forms an inefficiently-packed crystal phase when sublimed at ~275^{o}C under vacuum. The sorption of solvents, first reported by Atwood and Barbour,[79b] revealed that although this phase possesses void space and is able to absorb guests, it does not contain easily-definable conventional pores. The gas sorption capabilities of this material were subsequently reported and it was shown that the material can be used to separate CO_2 from H_2 through selective sorption of the former at relatively low pressure (< 10 Bar).[56] It has been further revealed that this material can absorb a large range of gases such as CH_4, H_2, O_2, N_2 and C_2H_2 to varying degrees, depending on the pressure.[66b,79b,127]

As the sorption of gases by this seemingly nonporous compound appeared to be counter-intuitive, a method of quantifying the sorption parameters was sought with a view to comparing these data with those for conventionally porous and well-understood materials. Using the Clausius-Clapeyron equation, the isosteric heat of sorption (a thermodynamic parameter of a material) for a particular guest (gas) can be determined by means of volumetric experiments as described above. The isosteric heat of sorption can vary with the degree of loading (occupancy) and consequently the determination of thermodynamic parameters as a function of loading can reveal mechanistic information for the material. In this regard, CO_2 was selected as an interesting guest for which to determine isosteric heats of sorption because (i) it is commonly used as a guest for sorbing materials and, (ii) it is selectively absorbed during the separation of CO_2 and H_2, as already stated.[56] The experimental results are given in Figure 46.

Several points of interest are revealed in Figure 46. When the general trend of the curve is extrapolated to zero loading, this value can be compared to potentials measured for other materials. This value is estimated to be approximately 30 kJ/mol (+/- 1). Activated carbons, carbon nanotubes, silicates and coordination polymers generally have isosteric heats of sorption in the range 20-27 kJ/mol.[128] However, the value calculated here falls just in the range of ion-exchanged zeolites, which have values from 30 to 60 kJ/mol.[129] Since the sorption sites within zeolites are associated with coordination of the CO_2 onto metals, it is surprising that TBC4 binds CO_2 comparatively well.

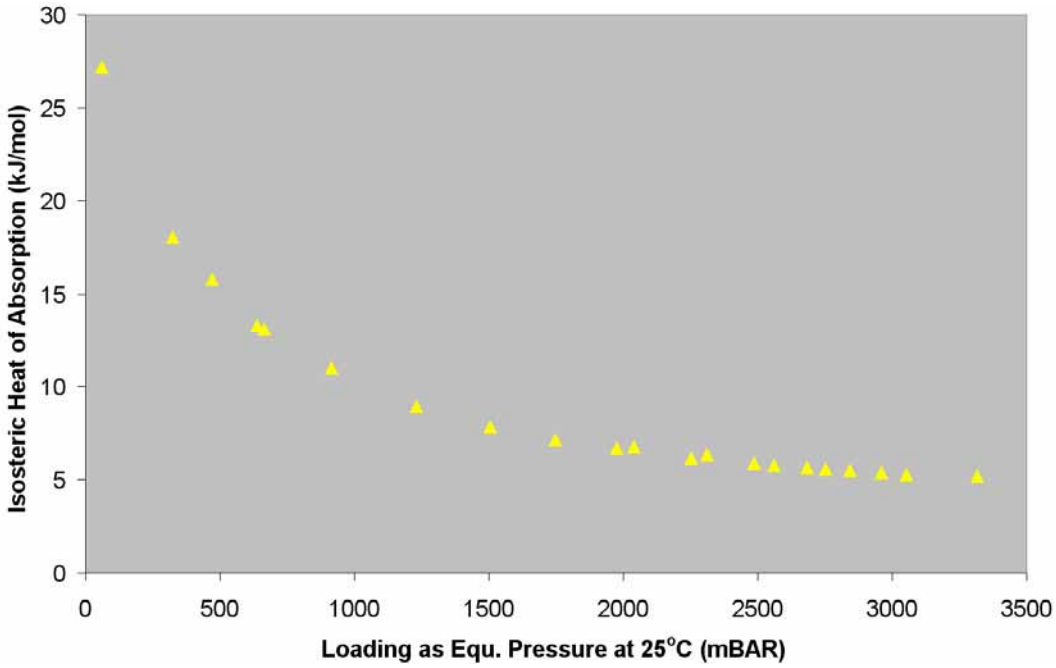

Figure 46. Isosteric heat of sorption versus loading for CO_2 by sublimed TBC4 at 25°C.

As the composition (i.e. organic) of TBC4 is similar to that of activated, the additional binding energy is presumed to be due to the existence of efficient binding sites of the structures i.e. the host:guest binding. As the structure of TBC4 can be regarded as nonporous in the convention sense, the ultimate encapsulation of CO_2 is effected by interstitial van der Waals confinement. This has been shown to improve the stability of highly volatile species, and is termed the "clathrate effect".[45] In summary, the void is relatively small and the confined CO_2 can interact with the host by means of extensive van der Waals contacts.

The change in the isosteric heat of sorption with occupancy implies that the TBC4 structure possesses a heterogenic surface. This is consistent with data from previous studies. The reason for the drop in the isosteric heat of sorption relates to the saturation of the binding sites, inhibiting the transport of guests to open sites. When a mechanism is finally proposed for the diffusion of small molecular species through this host system, this finding should be taken into account. Although there is sufficient space for two carbon dioxide molecules per cavity, dual-occupancy does not occur, even at pressures up to 60 Bar. Increased occupation of the cavities has a substantial negative effect on further diffusion and, consequently, the isosteric heat of sorption of the guest

Dianin's compound

This study was inspired by the desire to understand the dynamics of gas sorption through well-defined pores in simple organic systems. As was revealed by the *p-tert*-butylcalix[4]arene studies, gas sorption does not always require the presence of clearly definable pores in the static structure of a crystalline solid. It is relatively well known that Dianin's compound is one of the few organic compounds that crystallises with some zeolite-like characteristics. That is, it can form a guest-free arrangement that is structurally identical to that of the host in an inclusion compound. This structure is interesting because it has a clearly definable pore. As described earlier, the structure contains a hexameric ring of hydrogen bonded phenolic groups. These form pores which, in turn, lead to the formation of one-dimensional channels (Figure 47). Using a modified version of Connolly's software, the maximum radius of a sphere that could pass through the pore is found to be 1.244 Å (note that this is only marginally larger than the commonly accepted van der Waals radius of a hydrogen atom, and smaller than the van der Waals radius of the next-largest atom, helium (1.4 Å)).

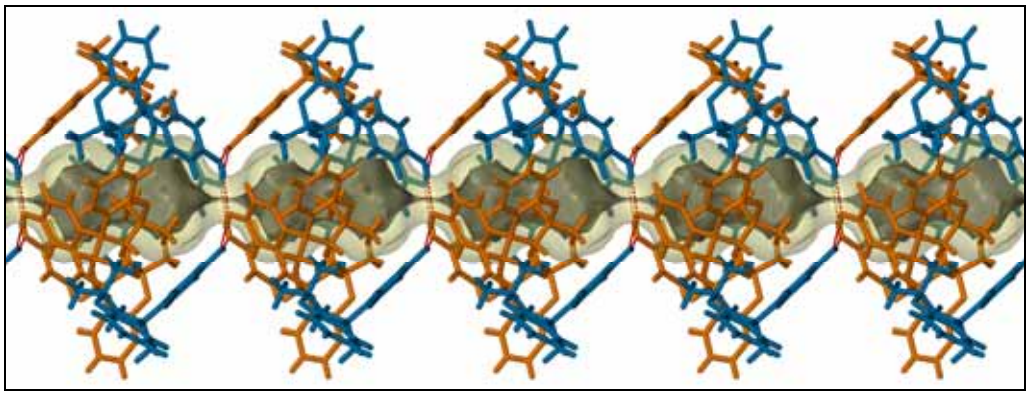

Figure 47. One-dimensional channels formed by sublimed Dianin's compound. The transparent yellow surface represents the contact surface of a probe of radius 1.2 Å, i.e. the volume that a hydrogen molecule could sweep out. The grey accessible surface represents the volume swept out by the centre of a probe of radius 1.2 Å.

Conventional wisdom dictates that, in accordance with van der Waals radii of various gases, only hydrogen gas should be able to pass into the larger cavities of Dianin's compound and therefore be absorbed. However, this assumption assumes that the pore is static which, presumably, is not the case. Thus, to investigate whether

pore dimensions of static crystal data can be used to predict gas selectivity of crystalline solids, the sorption behaviour of several gases was tested.

Of the five gases tested (N_2, CO_2, CH_4, He and H_2), it was found that only hydrogen gas was absorbed. This is an important result in that Dianin's compound shows absolute selectivity for hydrogen gas based on pore dimensions alone, an unprecedented finding. Potentially, this can facilitate the separation of hydrogen gas from any mixture.

One of the prerequisites of a useful sorption substrate is that it is both cheap and efficient. Because the cyclic array of hydrogen bonding produces a pore that exhibits high selectivity required for separation of hydrogen gas, alternative materials exhibiting the same type of pore were sought. Dianin's compound is a member of the extensive hexahost family of compounds (owing to the hexameric arrangement of the phenol groups) and constitutes the basis of finding a 'better' crystalline solid.[10] Phenol cannot be used, as its vacant host framework has not been produced to date. On the other hand, two β-hydroquinone vacant host framework structures are well-known.[27] This structure contains relatively little free volume but possesses the same type of pore as Dianin's compound. Whether this structure can easily be reproduced so that the gas sorption parameters can be measured is a question for further study. Indeed, a literature survey of some early studies reveals that the α-phase, formed by the sublimation of hydroquinol, does absorb a variety of gases, implying that it is not selective towards hydrogen gas. A recent paper reports propargylic alcohols as new additions to the hexahost family.[130] These compounds pack to form the same network of OH bonds. At yet no α-phase has been found and so the gas sorption properties are still unexplored.

An important aspect of these studies relates to the disparities between van der Waals radii and kinetic radii, and the implications of these parameters with regard to gas sorption. The majority of the literature uses kinetic radii to explain the selectivity for gases observed from sorption isotherms at various temperatures and define pore size within a structure using sorption parameters. The most cited reference for this work is the book on zeolites by Breck.[54] The selectivity of the Dianin's compound appears to contradict these results as the kinetic radii of dihydrogen is larger than the pore dimensions. This implies that a re-evaluation of the importance of kinetic versus van der Waals radii may be required.

Silver-IMID Metallocycle

Many porous coordination polymers have been discovered and investigated. However, the use of discrete metallocyclic complexes is relatively unexplored with regard to porosity studies. The discovery of compound **5**, formed by the desolvation of compound **4**, naturally progressed to gas sorption experiments. The vacant channels, formed by the one-dimensional stacking of the $[Ag_2IMID_2]^{2+}$ rectangular complexes, are approximately rectangular in cross-section with internal van der Waals dimensions of ca. 4.9 x 7.5 Å. The unoccupied space in the crystal is estimated to be approximately 22% of the total volume. A disadvantage of this material is that the metal node has a relatively high molecular weight, causing the entire complex to be heavy in relation to the space available within the crystal structure. The density of the crystalline solid is 1.425 g/cm^3. This precludes this material from being practical for hydrogen storage as the molecular weight ratio of hydrogen:silver is 2:107.87, approximately 2% by weight. Therefore a substantial amount of gas would need to be bound per complex in order to yield a useful result. Nevertheless, the sorption isotherms were determined (Figure 48).

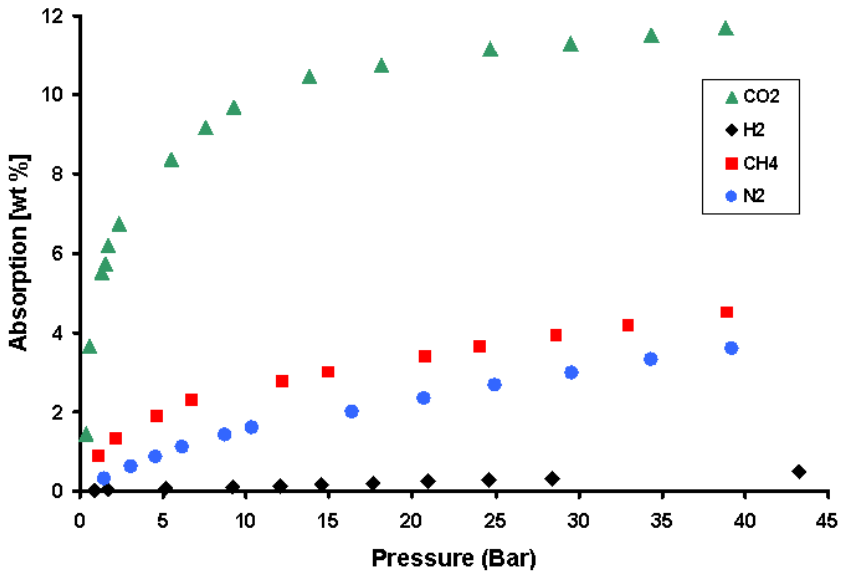

Figure 48. Gas sorption isotherms (weight % versus pressure) of **5** solid with CO_2, H_2, CH_4 and N_2.

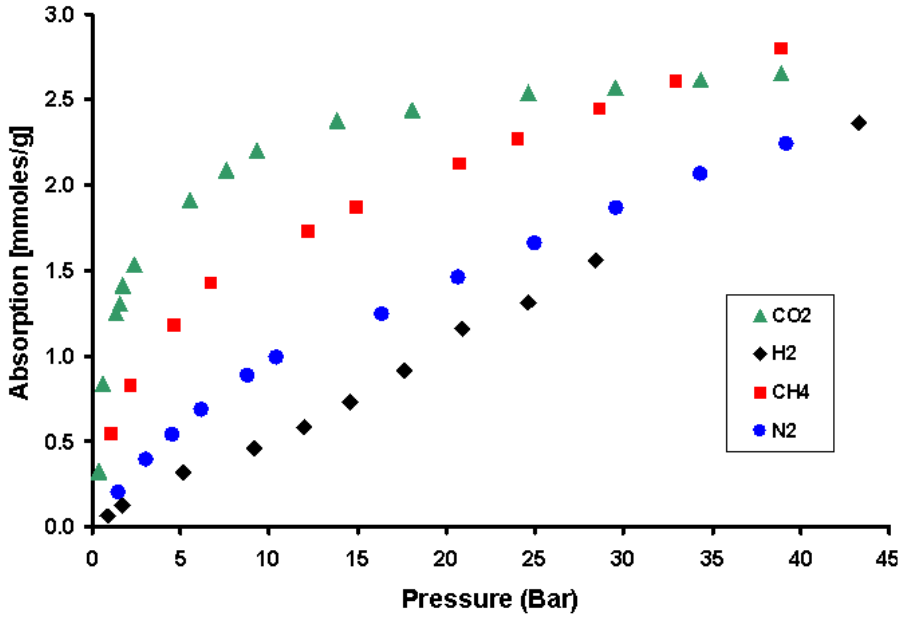

Figure 49. Gas sorption isotherms (mmoles/g versus pressure) of **5** with CO_2, H_2, CH_4 and N_2. Note that at approximately 45 Bar the molar quantities of gas absorbed for the different gases are similar.

Not unexpectedly, the gas sorption isotherms indicate that the binding strength for the gases is in the order $CO_2 > CH_4 > N_2 > H_2$. As the free volume of the solid is low (22%) and the pore size small, saturation occurs at the relatively low pressure of ca 45 Bar. Even with the large differences in size between these four gases, the molar quantity of gas absorbed at the saturation pressure appears to be approximately constant (Figure 49). A respectable weight percentage of ~1% was achieved for the sorption of hydrogen gas at 78 Bar and 30°C.[131] This result compares favourably with other reported values at room temperature.

Seemingly Nonporous Cu-BITMB Metallocycle.

As a continuation of the studies on metallocyclic compounds that crystallise to form porous solids, the copper-containing compound **7** was found to form a seemingly nonporous structure. As the iodine sorption experiment implies (backed by the structural determination of the iodine clathrate), sorption into this seemingly nonporous crystalline material should be feasible for gases such as H_2, CH_4, CO_2 and N_2.

A systematic study of the gas sorption parameters at relatively low pressure and room temperature was conducted. As Figure 50 shows, the gas selectivity follows the order $H_2 = O_2 < N_2 < CO < CH_4 < CO_2$ at an initial pressure of ~1350 mBar. This selectivity can be rationalised by taking into account the size and polarisability of the gas. CO_2 is the largest and most easily polarised of the gases. Methane is a large gas that can interact well with the organic constituents of the void. CO is more polarizable than N_2 and these two gases are comparable in size and therefore CO is absorbed better than N_2. H_2 is very small and not very easily polarised and is therefore not measurably absorbed at this pressure. Although the O_2 result cannot be explained, it is well-known that physical absorption of O_2 is often as difficult as that of H_2.

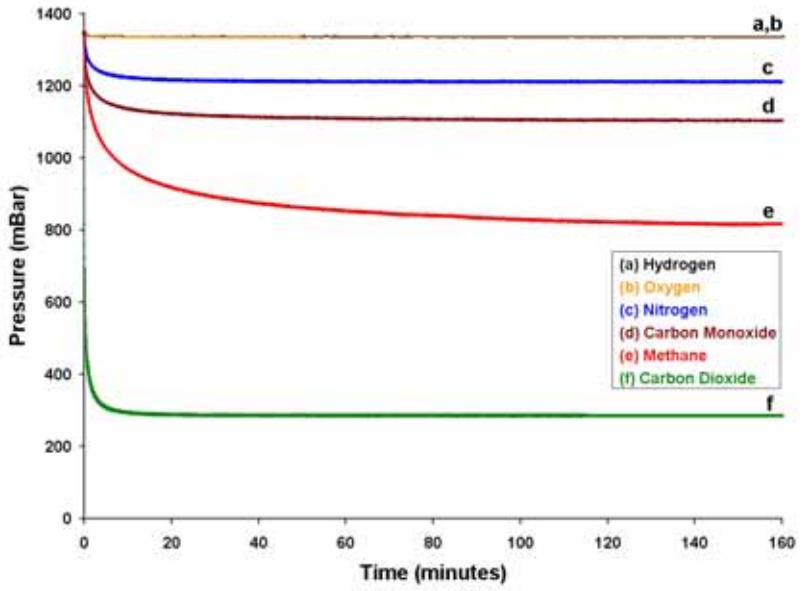

Figure 50. Gas sorption isotherms for H_2, O_2, N_2, CO, CH_4 and CO_2 (using a 1.101g sample of **7** placed in a chamber of volume 8.53 cm^3). The sample chamber was evacuated overnight between experiments in order to remove any residual gas.

The blue crystals undergo loss of methanol and water solvent guests without any discernible loss of monocrystallinity, thus allowing elucidation of the empty structure by single-crystal x-ray diffraction. The structural characteristics of the complex remain virtually identical and the cavity volume is approximately 109.6 Å (using a probe of radius 1.4 Å). As this structure has discrete pockets formed by the doughnut shaped molecules, the sorbed gas molecules are expected to be bound within these void spaces, presuming no structural changes take place. As the void is

relatively small it is reasonable to expect larger gas molecules such as CO_2 and acetylene to form 1:1 host:guest ratios at an occupancy of 100%. This was determined experimentally as shown in Figure 51.

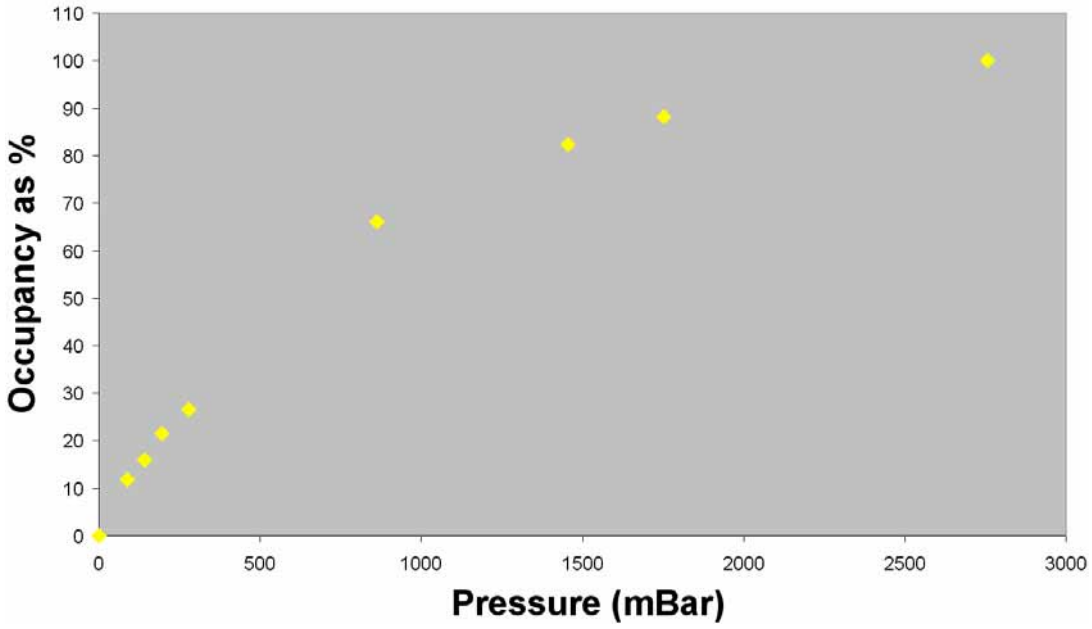

Figure 51. Occupancy as a function of pressure for the sorption of CO_2 by **7**.

The isosteric heat of sorption was determined as described for that of the *p-tert*-butylcalix[4]arene sublimed material, (Figure 52). The zero-coverage isosteric heat of sorption value (~25 kJ/mol) for this material is similar to that of activated carbons. The change in isosteric heat of sorption with degree of loading reveals once again that the sorption process is heterogenic in character and that there is a single sorption site.

An advantage of a small void space relates to the possible crystallographic disorder of the encapsulated guest gas molecules. In this regard, it was hoped that a structure of encapsulated CO_2 determined by single-crystal x-ray diffraction would aid in the determination of the gas sorption mechanism by unequivocally revealing where the gas molecules are bound within the structure.

The determination of the CO_2 containing structure could only be effected once a method of bathing the crystal in an atmosphere of pure gas was devised (Figure 53). Lindemann capillaries are used regularly in crystallography to maintain a constant atmosphere around a crystal. A crystal was glued to the end of a thin glass rod which

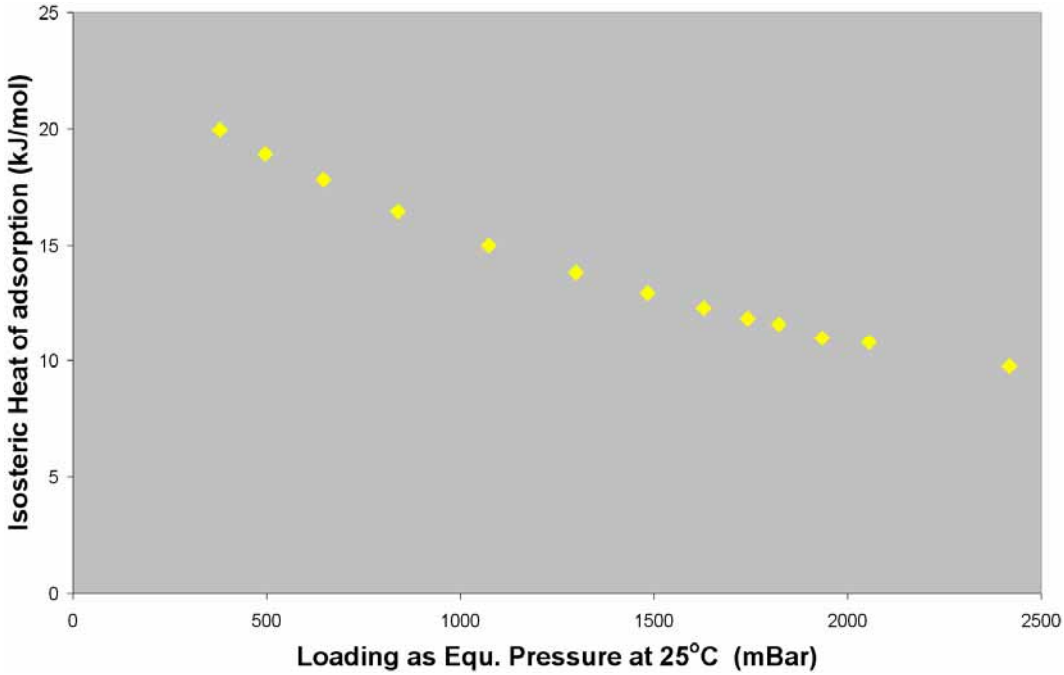

Figure 52. Isosteric heat of sorption of CO_2 by **7**.

was inserted into a Lindemann capillary. The capillary was attached by means of epoxy to a ¼ inch stainless steel pipe with an internal diameter only slightly larger than the external diameter of the capillary. This stainless steel tube was then connected to brass Swagelok components which, in turn, were connected to a Huber goniometer head to form the device shown in Figure 53. The device was then mounted vertically on the omega plate of the diffractometers in a manner that allowed precise positioning of the crystal in the x-ray beam. As the internal volume of the brass fittings and the steel tube is connected to the interior of the Lindemann capillary, the atmosphere of the entire internal volume can be controlled. The capability of withstanding high pressure was tested - rupture of the glass capillary did not occur, even at a pressure of 80 Bar of nitrogen gas. A vacuum leak test was also performed with satisfactory results. Single-crystal x-ray diffraction data can be collected with only minor changes to the data acquisition.

A suitably sized desolvated crystal was mounted in the abovementioned device and CO_2 was introduced at a pressure of 2.5 Bar. Data were collected and the structure was solved (compound **9**). A CO_2 gas molecule (disordered over two positions) was located within the cavity formed by the host complexes, thus confirming the void as the binding site of the gas (Figure 54). Interestingly, the guest-occupied void volume

(116.6 Å, 1.4 Å probe radius) is slightly larger relative to the empty void determined with the crystal under vacuum (109.6 Å, both structures were determined

Figure 53. Apparatus used for the determination of crystal structures under mild gas pressures.

at room temperature). Furthermore, the intramolecular Cu···Cu distance of 6.808 Å is longer compared to 6.598 Å of the vacuum structure. The disorder of the CO_2 molecule implies electrostatic interaction between the copper metal centres and the oxygen atoms of the CO_2.

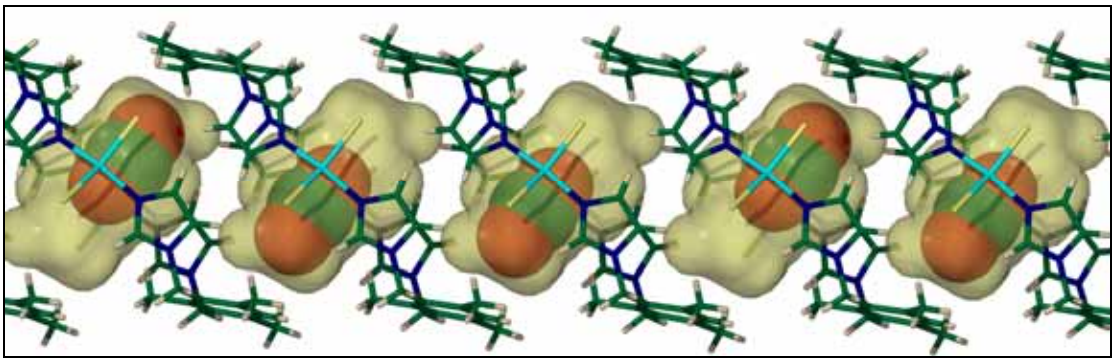

Figure 54. Structure of **9** visualised by mapping the void spaces (shown as semi–transparent yellow surfaces) within the copper metallocycles (shown in capped-stick representation). Disordered CO_2 guests are shown in spacefilling representation.

6. Summary and Conclusion

In its broadest terms, crystal engineering still encompasses the investigation of design strategies through serendipitous discoveries. The work presented here includes many results that originated as chance discoveries. Even so, the findings fully embody the ideals of discovery and design as elements of crystal engineering.

The successful synthesis of a variety of host compounds (in the context of their solid-state structures), including organic compounds and coordination compounds, provides an excellent basis for the preparation of a range of crystal forms. These materials were initially studied for their host:guest chemistry and, through the improved understanding of these phenomena some porous phases were produced.

Compound **1** acts as a solid-state host for a select series of guests. The formation of helical tubes, which are interconnected *via* hydroxyl-hydroxyl hydrogen bonds, confines the guests within one-dimensional channels. Small guests with trichloro and trimethylsilyl groups are aligned in a polar fashion within the host channels, resulting in the formation of crystals that are both chiral and polar. These crystals exhibit non-linear optical frequency doubling of laser light. As a direct result of trying to achieve an empty host structure, a stringently defined form of self-inclusion was discovered. By applying principles of crystal engineering to host compound **1** (*viz* thoughtful modification of the host), compound **2** was conceived. Compound **2** packs in a manner that is reminiscent of compound **1**, except for the replacement of some of the hydroxyl-hydroxyl hydrogen bonds with π-π interactions, and the formation of a quadruple helical arrangement instead of a triple helical arrangement. Compound **2** sublimes to yield what appears to be an empty structure that has flouted attempts to absorb gases.

Dianin's compound is arguably one of the most recognised archetypes of solid-state supramolecular chemistry. As part of our interest in its properties, the empty structure formed by sublimation under vacuum conditions represents an easily accessible material for the separation of hydrogen gas from *any* mixture of gases. This is due to the 100% selectivity of the pore defined by the hydrogen bonded hexamer of phenolic groups. New host:guest chemistry was also discovered when some liquid (i.e. at room temperature) organic compounds that contain amine functionality were crystallised with Dianin's compound. The initial result involved to the use of

morpholine as guest. The double deprotonation of the hydrogen bonded hexamer results in a lowering of symmetry from the usual *R*3 space group to *P*1. The lower symmetry facilitates the characterisation of the exact positions and numbers of the guests (virtually impossible in the *R*3 structures) and, consequently, the characterisation of interactions between guests within cavities as well as interactions between host and guest are possible. In the case of the morpholine clathrate, extensive hydrogen bonding occurs between the morpholinium cations and both the anionic and normally protonated phenolic groups. Furthermore, the two morpholinium guests within a cavity interact with one another *via* C–H···O hydrogen bonds. Use of other amines indicates that this is reproducible for amines, and represents a new paradigm in the host:guest chemistry of Dianin's compound. The improved understanding of host:guest and guest:guest interactions within the void space of Dianin's compound allowed the purposeful selection of allylamine as a potential guest. The successful inclusion of this guest resulted in the correct orientation of the double bonds so that they satisfy Schmidt's rules for photodimerisation.[15] Ethyldiamine is also a suitable guest for Dianin's compound but does not yield the *P*1 structural motif. Instead a type of supramolecular cocrystallisation occurs in that a structure is formed that contains both the deprotonated motif (inversion symmetry) as well as the normal Dianin's motif (3 symmetry). The overall structure can be refined in the space group *R*3, implying that there are three times as many deprotonated columns as there are "normal" columns.

p-tert-Butylcalix[4]arene sublimes under vacuum to yield a low-density phase capable of absorbing a large variety of gases and vapours. Characterisation of several temperature-dependent phase changes of this compound unequivocally identifies the phase that absorbs gases and proves that the sublimed compound is indeed the phase of interest in this regard.

Compound **3b**, formed by sublimation of 5,11,17,23-tetra-*tert*-butyl-25,26,27,28-tetramethoxy-2,8,14,20-tetrathiacalix[4]arene under reduced pressure represents a new member of the family of seemingly nonporous porous crystalline materials. This phase absorbs water into the small void space within the pincers of the calixarene. As there are no clearly definable pores within the structure, the mechanism if sorption is of great interest. Using the MSROLL software to locate the void spaces within the structure, a possible mechanism can be postulated. The larger void spaces

found between the calixarene columns tend towards connecting together when the *tert*-butyl groups are rotated relative to one another. Although these voids do not actually connect, as defined by the static atomic coordinates determined crystallographically, it is easily envisioned that the water molecules can "squeeze" between the small barriers between the larger voids and then find a pathway into the "clefts" of the calixarene, thereby finding a thermodynamically favourable location. This possible pathway was supported experimentally by elucidating the structure after sorption of iodine. The iodine guests are located within the larger voids and cause the methoxy groups to become disordered over two positions. It is once again easy to envision water molecules pushing their way past the flexible methoxy group to hydrogen bond to the oxygen atoms. These speculations still need to be investigated computationally.

The discrete coordination rings represent a new methodology to designing porous metallo-organic crystalline materials. In the case of compounds **4** and **5**, the cyclic complexes are cationic, resulting in the crystals being classified as salts. The successful removal of solvent guests results in a stable porous crystalline material that can be fully characterised using single-crystal x-ray diffraction. In the case of compound **7** and its host:guest structures, the neutral coordination cyclic host allows passage of molecules as large as iodine through the crystal lattice despite the lack of obvious pores. This compound represents the first coordination complex to be added to the new but growing family of seemingly nonporous porous crystalline materials.

Properties relating to the porosity of "empty" crystalline materials were investigated by measuring the sorption of gases by these compounds. Using apparatus built for this purpose several aspects of gas permeation were determined volumetrically. The determination of the isosteric heat of sorption of CO_2 into sublimed *p-tert*-butylcalix[4]arene shows that the material has discrete binding sites which corresponds well with the crystal structure. The binding sites are the void spaces created by a pair of calixarene molecules. Interestingly the binding energy is comparable to that of ion-exchanged zeolites where coordination of CO_2 to the naked metals occurs. This result indicates that supramolecular van der Waals binding of low boiling point compounds is a viable way of binding guests strongly, as has been demonstrated by the most simple member of the calixarene family, calix[4]arene.[45]

Compound **4** exhibits excellent capability of absorbing gases under mild conditions. This is presumed to be due to the crystal being a salt. The highly

electrostatic nature of the channel (the channel is positively charged owing to the presence of silver ions) may encourage induced dipole – induced dipole interactions involving the gas compounds. This is exemplified by the sorption of H_2 at 1 weight % (g/g) at ~70 Bar and room temperature. This value is relatively high compared to results of other studies despite fact that the silver-containing complex is heavy in comparison to the rather low molecular weight of H_2.

Compound **7** absorbs a variety of gases with a high degree of selectivity. Elucidation of the empty structure, as well as CO_2 included structure by single-crystal x-ray diffraction confirmed the binding site of the guest within the small pocket formed by the metallo-macrocycle. The preference by the CO_2 to bind through weak interactions to the "naked" copper sites provides experimental evidence for the important role that "naked" metal sites have in binding gas molecules. Interestingly, the determination of the isosteric heat of sorption of CO_2 resulted in a relatively low experimental binding energy. A possible explanation for this may be that, even though the binding of CO_2 in the void pocket is energetically favourable, the energy required to traverse from pocket to pocket may decrease the overall energy gain of sorption.

Overall success of studying the host:guest chemistry of the molecular host compound can be summarised as follows. New solid-state supramolecular paradigms were discovered. These include (1) deprotonation by the guest of the Dianin's host structure without serious change to the overall host framework; (2) self-inclusion; (3) polar/chiral crystals; (4) *subtle* thermal phase changes in TBC4; (5) seemingly nonporous porous diffusion of water in a hydrophobic host structure; and (6) use of discrete coordination cyclic compounds as hosts for gases.

Gas permeation studies of the apohosts of the above compounds were accomplished by designing apparatus for this specific purpose. This included the gas sorption apparatus and the single-crystal diffraction controlled gas atmosphere apparatus. Thermodynamic parameters for the sorption of CO_2 into two of the materials yielded results confirming that the unique void space within the crystal acts as a single binding site for the heterogeneous sorption of gas molecules. The gas sorption isotherms measured for the two coordination materials revealed how possessing "naked" metal sites can improve gas sorption binding energies. Dianin's compound reveals unprecedented selectivity, only absorbing hydrogen gas.

References

1. E. Fischer, *Ber. Dtsch. Chem. Ges.*, **1894**, ***27***, 2985.
2. A. Werner, *Z. Anorg. Chem.,* **1893**, *3***,** 267.
3. P. Ehrlich, *Studies on Immunity*, Wiley, NewYork, **1906**.
4. K. L. Wolf, F. Frahm & H. Harms, *Z. Phys. Chem. Abt*. ***B***, **1937**, *36*, 17.
5. C. Pedersen, *J. Am. Chem. Soc.*, 1967, **89**, 2495.
6. a) N. F. Curtis & D. A. House, *Chem. Ind. (London)*, **1961**, 1708; b) J. D. Curry & D. H. Busch, *J. Am. Chem. Soc.*, **1964**, *86*, 592; c) E. –G. Jäger, *Z. Chem.*, **1964**, *4*, 437.
7. D. Cram, *Angew. Chem. Int. Ed.*, **1988**, *27*, 1009.
8. J.-M. Lehn in *Comprehensive Supramolecular Chemistry*, ed. J. L. Atwood, J. E. D. Davies, D. D. MacNicol and F. Vögtle, Elsevier Science, Oxford, **1996**, Forward.
9. J.-M. Lehn, *Angew. Chem. Int. Ed.*, **1988**, *27*, 89.
10. J. W. Steed & J. L. Atwood, Supramolecular Chemistry, John Wiley & Sons, England, **2000**.
11. J.-M. Lehn, *Angew. Chem. Int. Ed.*, **1990**, *27*, 1304.
12. J. D. Dunitz, *Pure Appl. Chem.*, **1991**, *63*, 177.
13. G. R. Desiraju, *Crystal Engineering. The Design of Organic Solids*, Elsevier, Amsterdam, **1989**.
14. a) A. R. von Hippel, *Science*, **1962**, *138*, 91; b) R. Pepinsky, *Phys. Rev*., **1955**, *100*, 971.
15. (a) G. M. J. Schmidt, *Pure Appl. Chem*., **1971**, *27*, 647. (b) D. Rabinowich & G. M. J. Schmidt, *J. Chem. Soc (B)*, **1964**, 144.
16. D. Braga, F. Grepioni & G. Desiraju, *Chem. Rev.*, **1998**, *98*, 1375.
17. G. R. Desiraju, *Chem. Commun.*, **1997**, 1475.
18. B. Moulton & M. J. Zaworotko, *Chem. Rev.*, **2001**, *101*, 1629.
19. O. M. Yaghi, M. O'Keefe, N. W. Ockwig, H. K. Chae, M. Eddaoudi & J. Kim, *Nature*, **2003**, *423*, 705.
20. G. R. Desiraju & A. Gavezzotti, *J. Chem. Soc., Chem. Commun.*, **1989**, 621.
21. C. A. Hunters & J. K. M. Sanders, *J. Am. Chem. Soc.*, **1990**, *112*, 5525.
22. S. C. Nyburg & W. Wong-Ng, *Proc. R. Soc. London Ser. A*, **1979**, *367*, 29.
23. D. E. Williams & L. Y. Hsu, *Acta Crystallogr., Sect. A*, **1985**, *41*, 296.
24. G. R. Desiraju & R. Parthasarathy, *J. Am. Chem. Soc.*, **1989**, *111*, 8725.
25. N. Ramasubbu, R. Partasarathy & P. Murray-Rust, *J. Am. Chem. Soc.*, **1986**, *108*, 4308.
26. P. Metrangolo & G. Resnati, *Chem. Eur. J.*, **2001**, *7*,2511.
27. T. C. W. Mak & B. R. F. Bracke in *Comprehensive Supramolecular Chemistry*, ed. J. L. Atwood, J. E. D. Davies, D. D. MacNicol and F. Vögtle, Elsevier Science, Oxford, **1996**, vol. 6.
28. a) A. P. Dianin, *J. Russ. Phys. Chem. Soc.*, **1914**, *31*, 1310 (*Chem. Zentralbl*., **1915**, *1*, 1063); b) P. Finocchiaro & S. Failla in *Comprehensive Supramolecular Chemistry*, ed. J. L. Atwood, J. E. D. Davies, D. D. MacNicol and F. Vögtle, Elsevier Science, Oxford, **1996**, vol. 6.
29. a) Z. Asfari, V. Böhmer, J. Harrowfield & J. Vicens, Eds., in *Calixarenes 2001*, Kluver Academic Publishers, Dordrecht, **2001**; b) C. D. Gutsche, *Calixarenes Revisited* in *Monographs in Supramolecular Chemistry*, Royal Society of Chemistry, Cambridge, **1998**; c) R. Ungaro & M. Mandolini, Eds., in *Calixarenes in Action*, Imperial College Press, London, **2000**.
30. J. Szejtli & T. Osa in *Comprehensive Supramolecular Chemistry*, ed. J. L. Atwood, J. E. D. Davies, D. D. MacNicol and F. Vögtle, Elsevier Science, Oxford, **1996**, vol. 3.
31. G. Tsoucaris, in *Organic Solid State Chemistry*, ed. G. R. Desiraju, Elsevier, Amsterdam, **1987**, 207-270.
32. a) L. J. Barbour, G. W. Orr & J. L. Atwood, *Nature*, **1998**, *393*, 671. b) L. Infantes & S. Motherwell, *CrystEngComm*, **2002**, *4(75)*, 454. c) R. Ludwing, *Angew. Chem. Int. Ed.*, **2001**, *40*, 1808.
33. M. A. Viswamitra, R. Radhakrishnan, J. Bandekar & G. R. Desiraju, *J. Am. Chem. Soc.*, **1993**, *115*, 4868.
34. a) S. Kitagawa, R. Kitaura & S. –I. Noro, *Angew. Chem. Int. Ed.*, **2004**, *43*, 2334; b) S. Kitagawa & K. Uemera, *Chem. Soc. Rev.*, **2005**, *34*, 109; c) S. Kitagawa, S. –I. Noro & T. Nakamura, *Chem. Commun.,* **2006**, 701.
35. E. Weber, in *Encyclopedia of Supramolecular Chemistry*, ed. J. L. Atwood & J. W. Steed, Marcel Dekker, **2004**, 261.

36. a) H. Davy, *Philos. Trans. R. Soc. Lond.,* **1811**, *101*, 155; b) G. A. Jeffrey, in *Comprehensive Supramolecular Chemistry*, ed. J. L. Atwood, J. E. D. Davies, D. D. MacNicol and F. Vögtle, Elsevier Science, Oxford, **1996**, vol. 6.
37. L. B. Ebert, *Ann. Rev. of Mater. Sci.*, **1976**, *6*, 181.
38. *Cyclodextrins* in *Comprehensive Supramolecular Chemistry*, ed. J. L. Atwood, J. E. D. Davies, D. D. MacNicol and F. Vögtle, Elsevier Science, Oxford, **1996**, vol. 3.
39. R. Gerdil, in *Comprehensive Supramolecular Chemistry*, ed. J. L. Atwood, J. E. D. Davies, D. D. MacNicol and F. Vögtle, Elsevier Science, Oxford, **1996**, vol. 6.
40. a) D. D. MacNicol in *Inclusion Compounds*, ed. J. L. Atwood, J. E. D. Davies, D. D. MacNicol, Academic Press, London, 1984, vol. 2; b) S. –P. Kang, J. –H. Yoon & H. Lee, *Fluid Phase Equilibria*, **1997**, *137*, 265; c) S. A. Allison & R. M. Barrer, *Trans. Faraday Soc.*, **1968**, *64*, 549; d) S. A. Allison & R. M. Barrer, *Trans. Faraday Soc.*, **1968**, *64*, 557.
41. M. D. Hollongsworth & K. D. M. Harris in *Comprehensive Supramolecular Chemistry*, ed. J. L. Atwood, J. E. D. Davies, D. D. MacNicol and F. Vögtle, Elsevier Science, Oxford, **1996**, vol. 6.
42. G. R. Desiraju in *Comprehensive Supramolecular Chemistry*, ed. J. L. Atwood, J. E. D. Davies, D. D. MacNicol and F. Vögtle, Elsevier Science, Oxford, **1996**, vol. 6.
43. G. O. Lloyd, J. Alen, M. W. Bredenkamp, E. J. C. de Vries, C. Esterhuysen &. L. J. Barbour, *Angew. Chem. Int. Ed.*, **2006**, *45*, 5354..
44. M. Miyata & K. Sada in *Comprehensive Supramolecular Chemistry*, ed. J. L. Atwood, J. E. D. Davies, D. D. MacNicol and F. Vögtle, Elsevier Science, Oxford, **1996**, vol. 6.
45. J. L. Atwood, L. J. Barbour & A. Jerga, *Science*, **2002**, *296*, 2367.
46. J. Lipkowski in *Comprehensive Supramolecular Chemistry*, ed. J. L. Atwood, J. E. D. Davies, D. D. MacNicol and F. Vögtle, Elsevier Science, Oxford, **1996**, vol. 6.
47. R. Bishop in *Comprehensive Supramolecular Chemistry*, ed. J. L. Atwood, J. E. D. Davies, D. D. MacNicol and F. Vögtle, Elsevier Science, Oxford, **1996**, vol. 6.
48. a) G. R. Desiraju, *CrystEngComm*, **2005**, *5*, 466; b) J. D. Dunitz, *CrystEngComm*, **2005**, *5*, 506.
49. a) Ö. Almarsson & M. J. Zaworotko, *Chem. Commun.*, **2004**, 1889; b) M. C. Etter, *Acc. Chem. Res.*, **1990**, *23*, 120; c) D. Braga & F. Grepioni, *Chem. Commun.*, **2005**, 3635; d) C. B. Aakeröy & D. J. Salmon, *CrystEngComm*, **2005**, *7*, 439; e) J. Berstein, *Chem. Commun.*, **2005**, 5007.
50. a) S. R. Batten, *CrystEngComm*, **2001**, *3*, 67; b) S. R. Batten & R. Robson, *Angew. Chem. Int. Ed.*, **1998**, *37*, 1461.
51. a) P. J. Langley & J. Hulliger, *Chem. Soc. Rev.*, **1999**, *28*, 279; b) M. W. Hosseini, *Acc. Chem. Res.*, **2005**, *38*, 313.
52. a) M. R. Caira & L. R. Nassimbeni in *Comprehensive Supramolecular Chemistry*, ed. J. L. Atwood, J. E. D. Davies, D. D. MacNicol and F. Vögtle, Elsevier Science, Oxford, **1996**, vol. 6; b) L. R. Nassimbeni, *Acc. Chem. Res.*, **2003**, *36*, 631.
53. J. D. Dunitz, V. Schomaker & K. N. Trueblood, *J. Phys. Chem.*, **1988**, *92*, 856.
54. D. W. Breck in *Zeolite Molecular Sieves*, Wiley and Sons, New York, **1974**.
55. L. J. Barbour, *Chem. Commun.*, **2006**, 1163 and references therein.
56. J. L. Atwood, L. J. Barbour & A. Jerga, *Angew. Chem. Int. Ed.*, **2004**, *43*, 2948.
57. A. K. Cheetham, G. Férey & T. Loiseau, *Angew. Chem. Int. Ed.*, **1999**, *38*, 3268.
58. a) G. Férey, *Chem. Mater.*, **2001**, *13*, 3084; b) G. Férey, C. Mellot-Dzaznieks, C. Serre, F. Millange, J. Dutour, S. Surblé & I. Margiolaki, *Science*, **2005**, *309*, 2040.
59. a) A. J. Fletcher, K. M. Thomas & M. J. Rosseinsky, *J. Solid State Chem.*, **2005**, *178*, 2491; b) M. J. Rosseinsky, *Microporous and Mesoporous Mater.*, **2004**, *73*, 15; D. Bradshaw, J. B. Claridge, E. J. Cussen, T. J. Prior & M. J. Rosseinsky, *Acc. Chem. Res.*, **2005**, *38*, 273.
60. C. Janiak, *Dalton Trans.*, **2003**, 2781.
61. C. J. Kepert, *Chem. Commun.*, **2006**, 695.
62. a) D. M. Rudkevich & A. V. Leontiev, *Aust. J. Chem.*, **2004**, *57*, 713. b) D. M. Rudkevich & H. Xu, *Chem. Commun.*, **2005**, 2651.
63. a) T. Burchell & M. Rogers, SAE Technol. Pap. Ser., **2000**, 2000-01-2205; b) www.eere.ebergy.gov/hydrogenandfuelcells, **2006** c) *Basic Research Needs for the Hydrogen Economy*, Office of Basic Energy Sciences, US Department of Energy, **2004**; d) http://www.eere.energy.gov/afdc/altfuel/altfuels.html, **2006**.
64. J. L. C. Rowsell & O. M. Yaghi, *Angew. Chem. Int. Ed.*, **2005**, *44*, 4670.
65. a) X. B. Zhao, B. Xiao, A. J. Fletcjer, K. M. Thomas, D. Bradshaw & M. J. Rosseinsky, *Science*, **2004**, *306*, 1012; b) R. Kitaura, K. Seki, G. Akiyama & S. Kitagawa, *Angew. Chem.*

Int. Ed., **2003**, *42*, 428; c) D. N. Dybtsev, H. Chun & K. Kim, *Angew. Chem. Int. Ed.*, **2004**, *43*, 5033; d) T. K. Maji, G. Mostafa, R. Matsuda & S. Kitagawa, *J. Am. Chem. Soc.*, **2005**, *127*, 17152.

66. a) J.L. Atwood, L.J. Barbour and G.O. Lloyd, *Chem. Commun.,* **2004**, 922; b) P. K. Thallapally, G. O. Lloyd, T.B. Wirsig, M.W. Bredenkamp, J. L. Atwood and L. J. Barbour, *Chem. Commun.,* **2005**, 5272.
67. P. K. Thallapally, G. O. Lloyd, J. L. Atwood and L. J. Barbour, *Angew. Chem. Int. Ed.*, **2005**, ***44***, 3848.
68. a) G. O. Lloyd, M. W. Bredenkamp and L. J. Barbour, *Chem. Commun.*, **2005**, 4053; b) M. W. Bredenkamp and G.O. Lloyd, *Acta Crystallogr., Sect. E*, **2005**, *E61*, o1512.
69. a) F. Toda in *Inclusion Compounds*, ed. J. L. Atwood, J. E. D. Davies, D. D. MacNicol, Academic Press, London, 1984, vol. 4, 126–187; b) F. Toda in *Comprehensive Supramolecular Chemistry*, ed. J. L. Atwood, J. E. D. Davies, D. D. MacNicol and F. Vögtle, Elsevier Science, Oxford, 1996, vol. 6.
70. a) L. Dobrzańska, G. O. Lloyd, H. G. Raubenheimer and L. J. Barbour, *J. Am. Chem. Soc.*, **2005**, *127*, 13134; b) L. Dobrzańska, G. O. Lloyd, H. G. Raubenheimer and L. J. Barbour, *J. Am. Chem. Soc.*, **2006**, *128*, 698.
71. C. D. Gutsche and M Iqbal, *Org. Synth., Coll. Vol.*, **1993**, *8*, 75.
72. A. Arduini and A. Casnati, *Macrocyclic Synthesis, A Practical Approach (The practical approach in chemistry series)*, ed. D. Parker, Oxford, England, **1996**, Chapter 7.
73. N. Iki, C. Kabuto, T. Fukushima, H. Kumagai, H. Takeya, S. Miyanari, T. Miyashi & S. Miyano, *Tetrahedron*, **2000**, *56*, 1437.
74. M. L. Connolly, *Science,* **1983**, *221*, 709.
75. a) H. Cheng, G. P. Pez & A. C. Cooper, *J. Am. Chem. Soc.*, **2001**, *123*, 5845; b) H. Chen & D. S. Scholl, *J. Am. Chem. Soc.*, **2004**, *126*, 7778; c) R. Dagani, C. *Chem. & Eng. News*, **2002**, 25; d) C. Liu, Y. Y. Fan, M. Liu, H. T. Cong, H. M. Cheng & M. S. Dresselhaus, *Science*, **1999**, *286*, 1127; e) V. C. Menon & S. Komarneni, *J. Porous. Mater.*, **1998**, *5*, 43; f) M. G. Nijkamp, J. E. M. J. Raaymakers, A. J. van Dillen & K. P. de Jong, *Appl. Phys. A*, **2001**, *72*, 619; g) A. M. Seayad & D. M. Antonelli, *Adv. Mater.*, **2004**, *16*, 765; h)S.-I. Noro, S. Kitagawa, M. Kondo & K. Seki, *Angew. Chem. Int. Ed.*, **2000**, *39*, 2081; i) T. Düren, L. Sarkisov, O. M. Yaghi, & R. Q. Snurr, *Langmuir*, **2004**, *20*, 2683.
76. a) A. P. Côté, A. I. Benin, N. W. Ockwig, M. O'Keeffe, A. J. Matzger & O. M. Yaghi, *Science*, **2005**, *310*, 1166; b) P. Sozzani, S. Bracco, A. Comotti, L. Ferretti & R. Simonutti, *Angew. Chem. Int. Ed.*, **2005**, *44*, 1816.
77. a) T. Dewa, K. Endo & Y. Aoyama, *J. Am. Chem. Soc.*, **1998**, *120*, 8933; b) A. T. Ung, D. Gizachew, R. Bishop, M. L. Scudder, I. G. Dance & D. C. Craig, *J. Am. Chem. Soc.*, **1995**, *117*, 8745; c) B. T. Ibragimov, S. A. Talipov & T. F. Aripov, *J. Incl. Phenom.*, **1994**, *17*, 317; d) J. L. Scott, *J. Chem. Soc., Perkin Trans. 2*, **1995**, 485.
78. J. D. Wuest, *Chem. Commun*., **2005**, *47*, 5830.
79. a) P. K. Thallapally, T. B. Wirsig, L. J. Barbour & J. L. Atwood, *Chem. Commun.*, **2005**, 51; b) J. L. Atwood, L. J. Barbour, A. Jerga & B. L. Schottel, *Science*, **2002**, *298*, 1000.
80. D. A. Leigh, A. E. Moody and R. G. Pritchard, *Acta Crystallogr., Sect. C*, **1994**, *C50*, 129.
81. M. D. Hollingsworth and K. D. M. Harris in *Comprehensive Supramolecular Chemistry*, ed. J. L. Atwood, J. E. D. Davies, D. D. MacNicol and F. Vögtle, Elsevier Science, Oxford, **1996**, vol. 6.
82. The Aldrich Library of Infrared Spectra, Edition III, Charles J. Pouchert, Aldrich Chemical Company, pgs 52 & 561.
83. T. Hertzsch, F. Budde, E. Weber & J. Hulliger, *Angew. Chem. Int. Ed*., **2002**, *41*, 2281.
84. F. H. Herbstein and R. E. Marsh, *Acta Crystallogr., Sect. B*, **1977**, *33*, 2358
85. K. C. Pich, R. Bishop, D. C. Craig, I. G. Dance, A. D. Rae and M. L. Scudder, *Struct. Chem.*, **1993**, *4*, 41.
86. S. Aitipamula, G. R. Desiraju, M. Jaskólski, A. Nangia and R. Thaimattam, *CrystEngComm*, **2003**, *5(78)*, 447
87. a) M. Lii, F. Meng, D. Xu, D. Yuan & Q. Ren, *Prog. Cryst. Growth Charact.*, **2000**, *40*, 123. b) J. Zyss & J.-F. Nicoudt, *Current Opinion in Solid State & Materials Science*, **1996**, *1*, 533. c) K. T. Holman, A. M. Pivovar & M. D. Ward, *Science*, **2001**, *294*, 1907. d) R. Fu, H. Zhang, L. Wang,. S. Hu, Y. Li, Xihe Huang & X. Wu, *Eur. J. Inorg. Chem.*, **2005**, *16*, 3211. e) S. R. Marder, *Chem. Commun.,* **2006**, ***2***, 131.
88. a) F.R. Fronczek and M. S. Erickson, *J. Chem. Cryst.*, **1995**, *25*, 737. b) J. K. D. Surette, M.-A. MacDonald, M. J. Zaworotko, R. D. Singer, *J. Chem. Cryst.*, **1994**, *24*, 715

89. a) G. W. Coates, A. R. Dunn, L. M. Henling, D. A. Dougherty, R. H. Grubbs, *Angew. Chem. Int. Ed.*, **1997**, *36*, 248. b) M. Gdaniec, W. Jankowski, M. J. Milewsha and T. Polonski, *Angew. Chem. Int. Ed.*, **2003**, *42*, 3903.
90. E. Haedicke, K. Penzien and H. W. Schnell, *Angew. Chem. Int. Ed.*, **1971**, *10*, 940.
91. A. D. U. Hardy, D. D. MacNicol, J. J. McKendrick and D. R. Wilson, *J. Chem. Soc., Chem. Commun.,* **1977**, *166*, 292.
92. J. H. Gall, A. D. U. Hardy, J. J. McKendrick and D. D. MacNicol, *J. Chem. Soc., Perkin Trans. 2*, **1979**, 376.
93. D. D. MacNicol, H. H. Mills and F. B. Wilson, *J. Chem. Soc. D*, **1969**, 1332.
94. D. D. MacNicol, P. R. Mallinson, R. A. B. Keates and F. B. Wilson, *J. Incl. Phenom.,* **1987**, *5*, 373.
95. D. D. MacNicol and G. A. Downing in *Comprehensive Supramolecular Chemistry*, ed. J. L. Atwood, J. E. D. Davies, D. D. MacNicol and F. Vögtle, Elsevier Science, Oxford, **1996**, vol. 6.
96. M. J. Brienne and J. Jaques, *Tetrahedron Lett.*, **1975**, *28*, 2349.
97. J. W. Steed, *CrystEngComm*, **2003**, *5*, 169.
98. R. W. H. Small, *Acta Crystallogr., Sect. B*, **2003**, *59*, 141.
99. W. Abriel, A. DuBois, M. Zakrzewski and M. A. White, *Can. J. Chem.*, **1990**, *68*, 1352.
100. J. C. Flippen, J. Karle and I. L. Karle, *J. Am. Chem. Soc.,* **1970**, *92*, 3749.
101. G. D. Enright, C. I. Ratcliffe and J. A. Ripmeester, *Mol. Phys.,* **1999**, *97*, 1193.
102. W. Baker, A. J. Floyd, J. F. W. McOmie, G. Pope, A. S. Weaving and J. H. Wild, *J. Chem. Soc*, **1956**, 2010.
103. a) J. H. Loehlin, M. C. Etter, C. Gendreau & E. Cervasio, *Chem. Mater.*, **1994**, *6*, 1218; b) P. Rashidi-Ranjar, S. Taghvaei-Ganjali, S.-L. Wang, F.-L. Liao & A. Heydari, *J. Chem. Soc., Perkin Trans. 2*, **2001**, 1255; c) A. Gebert, A. Linden, G. Mloston, & H. Heimgartner, *Pol. J. Chem.*, **2003**, *77*, 157; d) R. A. Batey, D. B. MacKay & V. Santhakumar, *J. Am. Chem. Soc.*, **1999**, *121*, 5075; e) A. A. Espenbetov, Y. T. Struchkov, N. Y. Kuz'mina & G. S. Litvinenko, *Bull. Acad. Sci. Kazakhstan, Chem.*, **1982**, 59-5.
104. V. V. Gorbatchuk, A. G. Tsifarkin, I. S. Antipin, B. N. Solomonov, A. I. Konovalov, P. Lhotak & I. Stibor, *J. Phys. Chem. B*, **2002**, *106*, 5845.
105. E. B. Brouwer, K. A. Udachin, G. D. Enright, J. A. Ripmeester, K. J. Ooms and P. A. Halchuk, *Chem. Commun.*, **2001**, 565.
106. a) G. D. Andreetti, R. Ungaro, A. Pochini, *J . Chem. Soc., Chem. Commun.*, **1979**, 1005; b) L. J. Bauer & C. D. Gutsche, *J. Am. Chem. Soc.*, **1985**, *107***,** 6063; c) A. Arduini, R. Caciuffo, S. Geremia, C. Ferrero, F. Ugozzoli & F. Zontone, *Supramol. Chem.*, **1998**, *10*, 125; d) G. D. Enright, E. B. Brouwer, K. A. Udachin, C. I. Ratcliffe & J. A. Ripmeester, *Acta Crystallogr., Sect. B*, **2002**, *58*, 1032; e) E. B. Brouwer, G. D. Enright, C. I. Ratcliffe & J. A. Ripmeester, *Supramol. Chem.*, **1996**, *7*, 79.
107. J. L. Atwood, L. J. Barbour & A. Jerga, *Chem. Commun.*, **2002**, 2952.
108. E. B. Brouwer, G. D. Enright, K. A. Udachin, S. Lang, K. J. Ooms, P. A.Halchuk & J. A. Ripmeester, *Chem. Commun.*, 2003, **12**, 1416.
109. a) G. M. Preston, T. P. Carroll, W. B. Guggino, P. Agre, *Science*, **1992**, *256*, 385; b) P. Agre, M. Bonhivers, M. J. Borgnia, *J. Biol. Chem.*, **1998**, *273*, 14659; c) M. J. Borgnia, S. Nielsen, A. Engel, P. Agre, *Annu. Rev. Biochem.*, **1999**, *68*, 425; d) M. Yasui, T. H. Kwon, M. A. Knepper, S. Nielsen, P. Agre, *Proc. Natl. Acad. Sci. USA*, **1999**, *96*, 5808.
110. M. L. Zeidel, S. V. Ambudkar, B. L. Smith, P. Agre, *Biochemistry*, **1992**, *31*, 7436.
111. a) M. Ø. Jensen, E. Tajkhorshid, K. Schulten, *Biophys. J.,* **2003**, *85*, 2884; b) A. Yarnell, *Chem. Eng. News,* **2004**, *82*, 42.
112. a) C. J. T. Grotthuss, *Ann. Chim.*, **1806**, *LVIII*, 54; b) B. L de Groot, H. Grubmüller, *Science*, **2001**, ***294***, 2353; c) E. Tajkhorshid, P. Nollert, M. Ø. Jensen, L. J. W. Miercke, J. O'Connell, R. M. Stroud, K. Schulten, *Science*, **2002**, *296*, 525; d) B. L. de Groot, T. Frigato, V. Helms, H. Grubmüller, *J. Mol. Biol.,* **2003**, *333*, 279; e) A. Burykin, A. Warshel, *Biophys. J.*, **2003**, *85*, 3696; f) G. Hummer, J. C. Rasaiah, J. P. Noworyta, *Nature*, **2001**, *414*, 188; g) F. Zhu, K. Schultern, *Biophys. J.,* **2003**, *85*, 236; h) A. Berezhkovskii, G. Hummer, *Phys. Rev. Lett.,* **2002**, *89*, 64503/1.
113. a) J. Wang, Y. Zhu, J. Zhou, X.-H. Lu, *Phys. Chem. Chem. Phys.*, **2004**, *6*, 829; b) M. S. P. Sansom, P. C. Biggin, *Nature*, **2001**, *414*, 156; c) O. Beckstein, M. S. P. Sansom, *Proc. Natl. Acad. Sci. USA*, **2003**, *100*, 7063; d) H. Grubm_ller, *Proc. Natl. Acad. Sci. USA*, **2003**, *100*, 7421.

114. P. Lhoták, M. Himl, I. Stibor, J. Sýkora, H. Dvořáková, J. Lang & H. Petříčková, *Tetrahedron*, **2003**, *59*, 7581.
115. a) A. Kalra, S. Garde, G. Hummer, *Proc. Natl. Acad. Sci. USA*, **2003**, *100*, 10175; b) S. Joseph, R. J. Mashi, E. Jakobsson, N. R. Aluru, *Nano Lett.*, **2003**, *3*, 1399.
116. T. K. Maji, K. Uemura, H.-C. Chang, R. Matsuda, S. Kitagawa, *Angew. Chem. Int. Ed.*, **2004**, *43*, 3269.
117. A. Bondi, *J. Phys. Chem.*, **1964**, *68*, 441.
118. a) T. Uemura, R. Kitaura, Y. Ohta, M. Nagaoka & S. Kitagawa, *Angew. Chem. Int. Ed.*, **2006**, *45*, 4112; b) C. –D. Wu, A. Hu, L. Zhang & W. Lin, *J. Am. Chem. Soc.*, **2005**, *127*, 8940; c) J. S. Seo, D. Whang, H. Lee, S. I. Jun, J. Oh, Y. J. Jeon & K. Kim, *Nature*, **2000**, *404*, 982; d) M. Fujita, Y. J. Kwon, S. Washizu & K. Ogura, *J. Am. Chem. Soc.*, **1994**, *116*, 1151.
119. B. Chen, C. Liang, J. Yang, D. S. Contreras, Y. L. Clancy, E. B. Lobkovsky, O. M. Yaghi & S. Dai, *Angew. Chem. Int. Ed.*, **2006**, *45*, 1390.
120. a) M. Albrecht, M. Lutz, A. L. Spek & G. van Koten, *Nature*, **2000**, *406*, 970; b) O. Hallale, S. A. Bourne & K. R. Koch, *New J. Chem.*, **2005**, *29*, 1416; c) D. Maspoch, D. Ruiz-Molina & J. Veciana, *J. Mat. Chem.*, **2004**, *14*, 2713.
121. a) M. Tadokoro, S. Tasuzuka, M. Nakamura, T. Shinoda, T. Tatenuma, M. Mitsumi, Y. Ozawa, K. Toriumi, H. Yoshino, D. Shiomi, K. Sato, T. Takui, T. Mori & K. Murata, *Angew. Chem. Int. Ed.*, **2006**, *45*, 5144; b) D. Maspoch, D. Ruiz-Molina, K. Wurst, N. Domingo, M. Cavallini, F. Biscarini, J. Tejada, C. Rovira & J. Veciana, *Nature Mat.*, **2003**, *2*, 190.
122. C. Thompson, N. R. Champness, A. N. Khlobystov, C. J. Roberts, M. Schröder, S. J. B. Tendler & M. J. Wilkinson, *J. Microscopy*, **2004**, *214*, 261.
123. a) S. M. Kuznicki, V. A. Bell, S. Nair, H. W. Hillhouse, R. M. Jacubinas, C. M. Braunbarth, B. H. Toby & M. Tsapatsis, *Nature*, **2001**, *412*, 720; b) H. Lin, E. Van Wagner, B. D. Freeman, L. G. Toy & R. P. Gupta, *Science*, **2006**, *311*, 639.
124. a) S. –I. Noro, S. Kitagawa, M. Kondo & K. Seki, *Angew. Chem. Int. Ed.*, **2000**, *39*, 2081; b) R. Matsuda, R. Kitaura, S. Kitagawa, Y. Kubota, R. V. Belosludov, T. C. Kobayashi, H. Sakamoto, T. Chiba, M. Takata, Y. Kawazoe & Y. Mita, *Nature*, **2005**, *436*, 238.
125. H. Chun, D. N. Dybstev, H. Kim & K. Kim, *Chem. Eur. J.*, **2005**, *11*, 3521.
126. P. W. Atkins, *Physical Chemistry*, Oxford University Press, Oxford, **1999**.
127. P. K. Thallapally, T. B. Wirsig, L. J. Barbour & J. L. Atwood, *Chem. Commun.*, **2005**, 4420
128. a) S. Himeno, T. Komatsu & S. Fujita, *J. Chem. Eng. Data*, **2005**, *50*, 369; b) M. Bienfait, P. Zeppenfeld, N. Dupont-Pavlovsky, M. Muris, M. R. Johnson, T. Wilson, M. DePies & O. E. Vilches, *Physical Rev. B*, **2004**, *70*, 035410-1; c) Y. He & N. A. Seaton, *Langmuir*, **2006**, *22*, 1150; d) S. Takamizawa, E.-I. Nakata, T. Saito & H. Yokoyama, *Inorg. Chem. Commun.*, **2003**, *6*, 1326.
129. a) A.Khelifa, L. Benchehida & Z. Derriche, *J. Colloid & Interface Sci.*, **2004**, *278*, 9; b) D. Shen, M. Bülow, F. Siperstein, M. Engelhard & A. L. Myers, *Adsorption*, **2000**, *6*, 275.
130. M. Hyacinth, M. Chruszcz, K. S. Lee, M. Sabat, G. Gao & L. Pu, *Angew. Chem. Int. Ed.*, **2006**, *45*, 5358.
131. a) L. Pan, M. B. Sander, X. Huang, J. Li, M. Smith, E. Bittner, B. Bockrath & J. K. Johnson, *J. Am. Chem. Soc.*, **2004**, *126*, 1308; b) B. Kesanli, Y. Cui, M. R. Smith, E. W. Bittner, B. C. Bockrath, W. Lin, *Angew. Chem. Int. Ed.*, **2005**, *44*, 72.

Appendix A

Crystal Data

Compound 1_3·CCl_4 :- 2,7-dimethylocta-3,5-diyne-2,7-diol carbon tetrachloride solvate

Crystal data for **1·CCl_4**: $C_{31}H_{42}Cl_4O_6$, M = 652.45, colourless needles, 0.38 × 0.24 × 0.23 mm^3, trigonal, space group $R\bar{3}$ (No. 146), a = b = 22.479(7), c = 6.232(4) Å, V = 2727(2) Å^3, Z = 3, D_c = 1.192 g/cm^3, F_{000} = 1032, Bruker SMART Apex CCD diffractometer, MoKα radiation, λ = 0.71073 Å, T = 100(2)K, $2\theta_{max}$ = 55.6º, 2579 reflections collected, 1837 unique (R_{int} = 0.1326). Final *GooF* = 0.985, *R1* = 0.1167, *wR2* = 0.2738, *R* indices based on 1139 reflections with I >2sigma(I) (refinement on F^2), 129 parameters, 1 restraint. Lp and absorption corrections applied, μ = 0.362 mm^{-1}. Absolute structure parameter = 0.5(3) (Flack, H. D. *Acta Cryst*. **1983**, *A39*, 876-881).

Compound 1_3·C_6H_6 :- 2,7-dimethylocta-3,5-diyne-2,7-diol benzene solvate

Crystal data for **1·C_6H_6** : $C_{36}H_{48}O_6$, M = 576.74, colourless needle, 0.35 × 0.27 × 0.26 mm^3, trigonal, space group $R\bar{3}$ (No. 146), a = b = 22.422(9), c = 6.325(5) Å, V = 2754(3) Å^3, Z = 3, D_c = 1.043 g/cm^3, F_{000} = 936, Bruker SMART Apex CCD diffractometer, MoKα radiation, λ = 0.71073 Å, T = K, reflections collected, unique (R_{int} =). Final *GooF* = 1.149, *R1* = 0.0960, *wR2* = 0.3006, *R* indices based on reflections with I (refinement on F^2), 121 parameters, 1 restraint. Lp and absorption corrections applied, μ = 0.070 mm^{-1}. Absolute structure parameter = 6(4) (Flack, H. D. *Acta Cryst*. **1983**, *A39*, 876-881).

Compound 1_3·I_2 2,7-dimethylocta-3,5-diyne-2,7-diol iodine clathrate

Crystal data for **1·I_2**: $C_{30}H_{42}I_2O_6$, M = 752.44, red needle, 0.25 × 0.24 × 0.21 mm^3, trigonal, space group $R\bar{3}$ (No. 146), a = b = 22.2573(15), c = 6.2872(8) Å, V = 2697.3(4) Å^3, Z = 3, D_c = 1.390 g/cm^3, F_{000} = 1128, Bruker SMART Apex CCD diffractometer, MoKα radiation, λ = 0.71073 Å, T = 100(2)K, $2\theta_{max}$ = 56.5º, 4653 reflections collected, 2086 unique (R_{int} = 0.0910). Final *GooF* = 0.984, *R1* = 0.0782, *wR2* = 0.1948, *R* indices based on 1616 reflections with I >2sigma(I) (refinement on F^2), 130 parameters, 1 restraint. Lp and absorption corrections applied, μ = 1.782 mm^{-1}. Absolute structure parameter = 0.3(2) (Flack, H. D. *Acta Cryst*. **1983**, *A39*, 876-881).

Compound 1 self-inclusion:- **2,7-dimethylocta-3,5-diyne-2,7-diol**

Crystal data for **1·self-inclusion**: $C_{10}H_{14}O_2$, M = 166.21, colourless needle, 0.35 × 0.15 × 0.15 mm^3, trigonal, space group $R\bar{3}$ (No. 146), a = b = 22.0815(18), c = 6.3414(10) Å, V = 2677.8(5) Å^3, Z = 10.50, D_c = 1.082 g/cm^3, F_{000} = 945, Bruker SMART Apex CCD diffractometer, MoKα radiation, λ = 0.71073 Å, T = 100(2)K, $2\theta_{max}$ = 56.3º, 5112 reflections collected, 2522 unique (R_{int} = 0.0441). Final *GooF* = 1.015, *R1* = 0.0616, *wR2* = 0.1453, *R* indices based on 2134 reflections with I >2sigma(I) (refinement on F^2), 141 parameters, 8 restraints. Lp and absorption corrections applied, μ = 0.074 mm^{-1}. Absolute structure parameter = 0.41(6) (Flack, H. D. *Acta Cryst*. **1983**, *A39*, 876-881).

Compound 1_3·CCl_3Br_1 :- 2,7-dimethylocta-3,5-diyne-2,7-diol Trichlorobromomethane solvate

Crystal data for **1·CCl_3Br_1**: $C_{31}H_{36}Br_1Cl_3O_6$, M = 690.86, colourless needles, 0.38 × 0.21 × 0.20 mm^3, trigonal, space group $R3$ (No. 146), a = b = 22.559(3), c = 6.2526(18) Å, V = 2755.8(9) Å^3, Z = 3, D_c = 1.249 g/cm^3, F_{000} = 1068, Bruker SMART Apex CCD diffractometer, MoKα radiation, λ = 0.71073 Å, T = 100(2)K, $2\theta_{max}$ = 56.5º, 5459 reflections collected, 2694 unique (R_{int} = 0.0605). Final *GooF* = 0.894, *R1* = 0.1022, *wR2* = 0.2462, *R* indices based on 1246 reflections with I >2sigma(I) (refinement on F^2), 130 parameters, 1 restraint. Lp and absorption corrections applied, μ = 1.373 mm^{-1}. Absolute structure parameter = 0.47(6) (Flack, H. D. *Acta Cryst*. **1983**, *A39*, 876-881).

Compound 1_3·$C_2Cl_3N_1$:- 2,7-dimethylocta-3,5-diyne-2,7-diol Trichloroacetonitrile solvate

Crystal data for **1·$C_2Cl_3N_1$**: $C_{32}H_{42}Cl_3N_1O_6$, M = 214.34, colourless needles, 0.36 × 0.25× 0.24 mm^3, trigonal, space group $R3$ (No. 146), a = b = 22.273(2), c = 6.2972(13) Å, V = 2705.3(7) Å^3, Z = 3, D_c = 1.184 g/cm^3, F_{000} = 1020, Bruker SMART Apex CCD diffractometer, MoKα radiation, λ = 0.71073 Å, T = 100(2)K, $2\theta_{max}$ = 56.4º, 5001 reflections collected, 2589 unique (R_{int} = 0.0353). Final *GooF* = 1.009, *R1* = 0.0491, *wR2* = 0.1195, *R* indices based on 2426 reflections with I >2sigma(I) (refinement on F^2), 135 parameters, 1 restraint. Lp and absorption corrections applied, μ = 0.293 mm^{-1}. Absolute structure parameter = 0.55(8) (Flack, H. D. *Acta Cryst*. **1983**, *A39*, 876-881).

Compound 1_3·$C_3H_9Cl_1Si_1$:- 2,7-dimethylocta-3,5-diyne-2,7-diol Trimethylsillyl chloride solvate

Crystal data for **1·$C_3H_9Cl_1Si_1$**: $C_{33}H_{51}Cl_1O_6Si_1$, M = 202.42, colourless needles, 0.25 × 0.10 × 0.09 mm^3, trigonal, space group $R3$ (No. 146), a = b = 22.432(2), c = 6.2345(12) Å, V = 2716.9(6) Å^3, Z = 3, D_c = 1.113 g/cm^3, F_{000} = 984, Bruker SMART Apex CCD diffractometer, MoKα radiation, λ = 0.71073 Å, T = 100(2)K, $2\theta_{max}$ = 56.6º, 5203 reflections collected, 2282 unique (R_{int} = 0.0546). Final *GooF* = 1.006, *R1* = 0.0695, *wR2* = 0.1654, *R* indices based on 1909 reflections with I >2sigma(I) (refinement on F^2), 137 parameters, 3 restraints. Lp and absorption corrections applied, μ = 0.176 mm^{-1}. Absolute structure parameter = 0.7(2) (Flack, H. D. *Acta Cryst*. **1983**, *A39*, 876-881).

Compound 2 :- 2-methyl-6-phenylhexa-3,5-diyn-2-ol

Crystal data for **2**: $C_{13}H_{12}O$, M = 184.23, colourless needles, 0.34 × 0.18 × 0.16 mm^3, trigonal, space group $P3_2$ (No. 145), a = b = 13.607(5), c = 6.289(5) Å, V = 1008.4(9) Å^3, Z = 3, D_c = 0.910 g/cm^3, F_{000} = 294, Bruker SMART Apex CCD diffractometer, MoKα radiation, λ = 0.71073 Å, T = 173(2)K, $2\theta_{max}$ = 56.2º, 2618 reflections collected, 1977 unique (R_{int} = 0.1395). Final *GooF* = 0.870, *R1* = 0.1069, *wR2* = 0.2486, *R* indices based on 727 reflections with I >2sigma(I) (refinement on F^2), 127 parameters, 1 restraint. Lp and absorption corrections applied, μ = 0.056 mm^{-1}. Absolute structure parameter = -2(7) (Flack, H. D. *Acta Cryst*. **1983**, *A39*, 876-881).

***S*-Dianin's compound** :- **(*S*)-4-(4-Hydroxylphenyl)-2,2,4-trimethylchroman**

Crystal data for ***S*-Dianin's compound**: $C_{18}H_{20}O_2$, M = 268.34, Colourless Plates, 0.20 × 0.15 × 0.05 mm^3, orthorhombic, space group $P2_12_12_1$ (No. 19), a = 10.029(1), b = 10.476(1), c = 13.2088(13) Å, V

= 1387.8(2) Å^3, Z = 4, D_c = 1.284 g/cm^3, F_{000} = 576, Bruker SMART Apex CCD diffractometer, MoKα radiation, λ = 0.71073 Å, T = 100(2)K, $2\theta_{max}$ = 56.4º, 8768 reflections collected, 1885 unique (R_{int} = 0.0264). Final *GooF* = 1.058, *R1* = 0.0384, *wR2* = 0.0975, *R* indices based on 1758 reflections with I > 2sigma(I) (refinement on F^2), 185 parameters, 0 restraints. Lp and absorption corrections applied, μ = 0.082 mm^{-1}. Absolute structure parameter = -2.1(15) (Flack, H. D. *Acta Cryst*. **1983**, *A39*, 876-881).

Dianin's Compound·Morpholine clathrate

Crystal data for **Dianin's Compound Morpholine Clathrate**: $C_{58}H_{69}NO_7$, M = 892.14, Colourless Prismatic, 0.35 × 0.18 × 0.18 mm^3, triclinic, space group *P*-1 (No. 2), a = 11.0956(8), b = 16.0377(11), c = 26.6878(19) Å, α = 89.935(2), β = 89.931(1), γ = 77.387(1)°, V = 4634.4(6) Å^3, Z = 4, D_c = 1.279 g/cm^3, F_{000} = 1920, Bruker SMART Apex CCD diffractometer, MoKα radiation, λ = 0.71073 Å, T = 100(2)K, $2\theta_{max}$ = 56.7º, 29582 reflections collected, 20505 unique (R_{int} = 0.0382). Final *GooF* = 1.071, *R1* = 0.0849, *wR2* = 0.1624, *R* indices based on 14269 reflections with I >2sigma(I) (refinement on F^2), 1240 parameters, 0 restraints. Lp and absorption corrections applied, μ = 0.083 mm^{-1}.

Dianin's Compound·Propylamine clathrate

Crystal data for **Dianin's Compound Propylamine Clathrate**: $C_{114}H_{138}N_2O_{12}$, M = 1728.26, Colourless Prismatic, 0.29 × 0.16 × 0.16 mm^3, triclinic, space group *P*-1 (No. 2), a = 11.1485(14), b = 15.921(2), c = 26.958(3) Å, α = 89.811(2), β = 89.884(2), γ = 74.833(2)°, V = 4618.4(10) Å^3, Z = 2, D_c = 1.243 g/cm^3, F_{000} = 1864, Bruker SMART Apex CCD diffractometer, MoKα radiation, λ = 0.71073 Å, T = 100(2)K, $2\theta_{max}$ = 56.7º, 52941 reflections collected, 21172 unique (R_{int} = 0.0767). Final *GooF* = 1.006, *R1* = 0.0820, *wR2* = 0.2229, *R* indices based on 12852 reflections with I >2sigma(I) (refinement on F^2), 1155 parameters, 0 restraints. Lp and absorption corrections applied, μ = 0.079 mm^{-1}.

Dianin's Compound·Isopropylamine clathrate

Crystal data for **Dianin's Compound·Isopropylamine clathrate**: $C_{114}H_{138}N_2O_{12}$, M = 1728.26, colourless prism, 0.30 × 0.30 × 0.20 mm^3, triclinic, space group *P*-1 (No. 2), a = 11.0945(12), b = 15.8840(18), c = 26.757(3) Å, α = 89.966(2), β = 89.970(2), γ = 76.532(2)°, V = 4585.6(9) Å^3, Z = 2, D_c = 1.252 g/cm^3, F_{000} = 1864, Bruker SMART Apex CCD diffractometer, MoKα radiation, λ = 0.71073 Å, T = 173(2)K, $2\theta_{max}$ = 56.6º, 51877 reflections collected, 20968 unique (R_{int} = 0.0453). Final *GooF* = 1.184, *R1* = 0.1640, *wR2* = 0.3265, *R* indices based on 14559 reflections with I >2sigma(I) (refinement on F^2), 1155 parameters, 0 restraints. Lp and absorption corrections applied, μ = 0.080 mm^{-1}.

Dianin's Compound·sec-Butylamine clathrate

Crystal data for **Dianin's Compound·sec-Butylamine clathrate**: $C_{116}H_{142}N_2O_{12}$, M = 1756.32, colourless prismatic 0.35 × 0.20 × 0.20 mm^3, triclinic, space group P-1 (No. 2), a = 11.0996(9), b = 16.1469(14), c = 27.199(2) Å, α = 89.703(2), β = 89.660(2), γ = 75.384(2)°, V = 4716.8(7) Å^3, Z = 2, D_c = 1.237 g/cm^3, F_{000} = 1896, Bruker SMART Apex CCD diffractometer, MoKα radiation, λ = 0.71073 Å, T = 100(2)K, 2θ_{max} = 56.6º, 48176 reflections collected, 21573 unique (R_{int} = 0.0670). Final *GooF* = 0.904, *R1* = 0.0844, *wR2* = 0.1886, *R* indices based on 9643 reflections with I >2sigma(I) (refinement on F^2), 1171 parameters, 0 restraints. Lp and absorption corrections applied, μ = 0.079 mm^{-1}.

Dianin's compound Allylamine clathrate

Crystal data for **Dianin's compound Allylamine clathrate**: $C_{114}H_{134}N_2O_{12}$, M = 1608.02, colourless prisms, 0.28 × 0.26 × 0.22 mm^3, triclinic, space group P-1 (No. 2), a = 11.1355(10), b = 15.9695(15), c = 26.910(3) Å, α = 90.019(2), β = 90.029(2), γ = 103.452(2)°, V = 4654.1(8) Å^3, Z = 2, D_c = 1.147 g/cm^3, F_{000} = 1724, Bruker SMART Apex CCD diffractometer, MoKα radiation, λ = 0.71073 Å, T = 100(2)K, 2θ_{max} = 56.6º, 29442 reflections collected, 20500 unique (R_{int} = 0.0365). Final *GooF* = 1.257, *R1* = 0.1453, *wR2* = 0.3900, *R* indices based on 8969 reflections with I >2sigma(I) (refinement on F^2), 1081 parameters, 0 restraints. Lp and absorption corrections applied, μ = 0.073 mm^{-1}.

Dianin's compound Piperidine (triclinic) clathrate

Crystal data for **Dianin's compound Piperidine (triclinic) clathrate**: $C_{128}H_{142}N_2O_{12}$, M = 1900.55, colourless prism, 0.35 × 0.30 × 0.28 mm^3, triclinic, space group P-1 (No. 2), a = 11.2529(8), b = 16.0219(12), c = 26.969(2) Å, α = 90.001(1), β = 90.025(1), γ = 103.490(1)°, V = 4728.3(6) Å^3, Z = 2, D_c = 1.3347 g/cm^3, F_{000} = 2060, Bruker SMART Apex CCD diffractometer, MoKα radiation, λ = 0.71073 Å, T = 100(2)K, 2θ_{max} = 56.5º, 42260 reflections collected, 21387 unique (R_{int} = 0.0738). Final *GooF* = 1.392, *R1* = 0.1414, *wR2* = 0.3946, *R* indices based on 10851 reflections with I >2sigma(I) (refinement on F^2), 1168 parameters, 0 restraints. Lp and absorption corrections applied, μ = 0.087 mm^{-1}.

Dianin's compound Piperidine (trigonal) clathrate

Crystal data for **Dianin's compound Piperidine (Triganol) clathrate**: $C_{82}H_{102}N_2O_8$, M = 1243.72, colourless prism, 0.35 × 0.30 × 0.28 mm^3, trigonal, space group R-3 (No. 148), a = b = 53.968(3), c = 11.2569(11) Å, V = 28393(3) Å^3, Z = 18, D_c = 1.3091 g/cm^3, F_{000} = 11232, Bruker SMART Apex CCD diffractometer, MoKα radiation, λ = 0.71073 Å, T = 100(2)K, 2θ_{max} = 56.7º, 85060 reflections collected, 15173 unique (R_{int} = 0.0901). Final *GooF* = 1.564, *R1* = 0.1671, *wR2* = 0.4338, *R* indices based on 7799 reflections with I >2sigma(I) (refinement on F^2), 775 parameters, 0 restraints. Lp and absorption corrections applied, μ = 0.077 mm^{-1}.

Dianin's compound Ethyldiamine clathrate

Crystal data for **Dianin's compound Ethyldiamine clathrate**: $C_{76}H_{94}N_4O_8$, M = 1191.61, colourless prismatic, 0.30 × 0.30 × 0.20 mm^3, trigonal, space group R-3 (No. 148), a = b = 53.599(2), c = 11.0015(9) Å, V = 27371(3) Å^3, Z = 18, D_c = 1.3011 g/cm^3, F_{000} = 10944, Bruker SMART Apex CCD diffractometer, MoKα radiation, λ = 0.71073 Å, T = 100(2)K, $2\theta_{max}$ = 56.6º, 105940 reflections collected, 14685 unique (R_{int} = 0.0629). Final *GooF* = 1.019, *R1* = 0.0921, *wR2* = 0.2416, *R* indices based on 10298 reflections with I >2sigma(I) (refinement on F^2), 757 parameters, 0 restraints.

Dianin's compound Piperidine (monoclinic) clathrate

Crystal data for **Dianin's compound Piperidine (monoclinic) clathrate**: $C_{23}H_{31}NO_2$, M = 353.49, colourless prisms, 0.31 × 0.26 × 0.21 mm^3, monoclinic, space group $P2_1/c$ (No. 14), a = 15.4360(18), b = 12.9411(15), c = 10.3343(12) Å, β = 100.800(2)°, V = 2027.8(4) Å^3, Z = 4, D_c = 1.158 g/cm^3, F_{000} = 768, Bruker SMART Apex CCD diffractometer, MoKα radiation, λ = 0.71073 Å, T = 100(2)K, $2\theta_{max}$ = 56.5º, 12574 reflections collected, 4690 unique (R_{int} = 0.0356). Final *GooF* = 0.944, *R1* = 0.0479, *wR2* = 0.1196, *R* indices based on 3517 reflections with I >2sigma(I) (refinement on F^2), 239 parameters, 0 restraints. Lp and absorption corrections applied, μ = 0.073 mm^{-1}.

TBC4 25ºC

Crystal data for **TBC4 25ºC** : $C_{44}H_{56}O_4$, M = 648.89, colourless prism, 0.40 × 0.35 × 0.35 mm^3, monoclinic, space group $P2_1/n$ (No. 14), a = 12.581(2), b = 26.239(2), c = 12.718(2) Å, β = 90.34(2)°, V = 4198.2(10) Å^3, Z = 4, D_c = 1.027 g/cm^3, F_{000} = 1408, Bruker SMART Apex CCD diffractometer, CuKα radiation, λ = 1.54060 Å, T = 293(2)K, $2\theta_{max}$ = 119.9º, 12369 reflections collected, 5875 unique (R_{int} = 0.0315). Final *GooF* = 1.022, *R1* = 0.0545, *wR2* = 0.1345, *R* indices based on 3470 reflections with I >2sigma(I) (refinement on F^2), 586 parameters, 28 restraints. Lp and absorption corrections applied, μ = 0.496 mm^{-1}.

TBC4 130ºC

Crystal data for **TBC$_4$ 130ºC**: $C_{44}H_{56}O_4$, M = 648.89, colourless prism, 0.40 × 0.30 × 0.15 mm^3, monoclinic, space group $P2_1/n$ (No. 14), a = 12.804(3), b = 26.742(5), c = 12.799(3) Å, β = 90.13(3)°, V = 4382.5(15) Å^3, Z = 4, D_c = 0.983 g/cm^3, F_{000} = 1408, Bruker SMART Apex CCD diffractometer, MoKα radiation, λ = 0.71073 Å, T = 403(2)K, $2\theta_{max}$ = 44.0º, 7552 reflections collected, 5188 unique (R_{int} = 0.3464). Final *GooF* = 1.090, *R1* = 0.2373, *wR2* = 0.5396, *R* indices based on 845 reflections with I >2sigma(I) (refinement on F^2), 72 parameters, 0 restraints. Lp and absorption corrections applied, μ = 0.061 mm^{-1}.

Compound 3b

Crystal data for **3b**: C_{44} H_{56} O_4 S_4, M = 777.13, colourless prism, 0.30 × 0.30 × 0.10 mm^3, tetragonal, space group P42$_1$m (No. 113), a = b = 19.4937(16), c = 12.1024(13) Å, V = 4599.0(7) Å^3, Z = 4, D_c = 1.122 g/cm^3, F_{000} = 1664, Bruker SMART Apex CCD diffractometer, MoKα radiation, λ = 0.71073 Å,

T = 173(2)K, $2\theta_{max}$ = 54.2º, 16260 reflections collected, 5257 unique (R_{int} = 0.1006). Final *GooF* = 0.991, *R1* = 0.0684, *wR2* = 0.1553, *R* indices based on 2859 reflections with I >2sigma(I) (refinement on F^2), 260 parameters, 10 restraints. Lp and absorption corrections applied, μ = 0.243 mm^{-1}. Absolute structure parameter = 0.12(15) (Flack, H. D. *Acta Cryst*. **1983**, *A39*, 876-881).

Compound 3b·$H_2$0

Crystal data for **3b·H_2O**: C_{44} H_{56} O_5 S_4, M = 795.14, colourless prism, 0.30 × 0.30 × 0.10 mm^3, tetragonal, space group P42_1m (No. 113), a = b = 19.5161(16), c = 12.0956(14) Å, V = 4606.9(8) $Å^3$, Z = 4, D_c = 1.146 g/cm^3, F_{000} = 1704, Bruker SMART Apex CCD diffractometer, MoKα radiation, λ = 0.71073 Å, T = 173(2)K, $2\theta_{max}$ = 54.3º, 16327 reflections collected, 5277 unique (R_{int} = 0.0394). Final *GooF* = 1.030, *R1* = 0.0534, *wR2* = 0.1396, *R* indices based on 4388 reflections with I >2sigma(I) (refinement on F^2), 264 parameters, 0 restraints. Lp and absorption corrections applied, μ = 0.246 mm^{-1}. Absolute structure parameter = -0.02(10) (Flack, H. D. *Acta Cryst*. **1983**, *A39*, 876-881).

Compound 3b·$(I_2)_{1/2}$

Crystal data for **3b·$(I_2)_{1/2}$**: $C_{45}H_{59}I_{0.29}O_4S_4$, M = 829.28, red prism, 0.25 × 0.25 × 0.15 mm^3, tetragonal, space group P42_1m (No. 113), a = b = 19.638(17), c = 11.905(11) Å, V = 4591(7) $Å^3$, Z = 4, D_c = 1.200 g/cm^3, F_{000} = 1762, Bruker SMART Apex CCD diffractometer, MoKα radiation, λ = 0.71073 Å, T = 100(2)K, $2\theta_{max}$ = 53.9º, 39482 reflections collected, 5187 unique (R_{int} = 0.0546). Final *GooF* = 1.034, *R1* = 0.0470, *wR2* = 0.1200, *R* indices based on 4303 reflections with I >2sigma(I) (refinement on F^2), 298 parameters, 31 restraints. Lp and absorption corrections applied, μ = 0.442 mm^{-1}. Absolute structure parameter = 0.00(5) (Flack, H. D. *Acta Cryst*. **1983**, *A39*, 876-881).

Compound 3·I_2

Crystal data for **3·I_2** : C_{44} H_{56} O_4 S_4 I_2, M = 1030.93, red plates, 0.34 × 0.24 × 0.22 mm^3, orthorhombic, space group *Pnma* (No. 62), a = 23.1227(16), b = 13.6899(10), c = 15.1267(11) Å, V = 4788.3(6) $Å^3$, Z = 4, D_c = 1.211 g/cm^3, F_{000} = 1808, Bruker SMART Apex CCD diffractometer, MoKα radiation, λ = 0.71073 Å, T = 100(2)K, $2\theta_{max}$ = 56.6º, 29181 reflections collected, 5887 unique (R_{int} = 0.0373). Final *GooF* = 1.579, *R1* = 0.1526, *wR2* = 0.3947, *R* indices based on 3654 reflections with I >2sigma(I) (refinement on F^2), 267 parameters, 0 restraints. Lp and absorption corrections applied, μ = 0.876 mm^{-1}.

Compound 4 :- **$[Ag_2(IMID)_2](BF_4)_2·(CH_3CN)_2$**

Crystal data for **4** : $C_{36}H_{42}Ag_2B_2F_8N_{10}$, M = 1004.16, colourless prism, 0.25 × 0.20 × 0.15 mm^3, monoclinic, space group *C*2/*m* (No. 12), a = 14.911(1), b = 20.1383(14), c = 7.0209(5) Å, β = 90.293(1)°, V = 2108.2(3) $Å^3$, Z = 2, D_c = 1.582 g/cm^3, F_{000} = 1008, Bruker SMART Apex CCD diffractometer, MoKα radiation, λ = 0.71073 Å, T = 100(2)K, $2\theta_{max}$ = 56.4º, 6675 reflections collected, 2520 unique (R_{int} = 0.0203). Final *GooF* = 1.062, *R1* = 0.0257, *wR2* = 0.0625, *R* indices based on 2413

reflections with I >2sigma(I) (refinement on F^2), 139 parameters, 0 restraints. Lp and absorption corrections applied, $\mu = 1.004$ mm^{-1}.

Compound 5 :- $[Ag_2(IMID)_2](BF_4)_2$

Crystal data for **5**: $C_{32}H_{36}Ag_2B_2F_8N_8$, M = 922.05, colourless prism, 0.25 × 0.20 × 0.10 mm^3, monoclinic, space group $C2/m$ (No. 12), a = 14.8307(10), b = 20.5641(13), c = 7.0449(5) Å, β = 90.118(1)°, V = 2148.5(3) Å^3, Z = 2, D_c = 1.425 g/cm^3, F_{000} = 920, Bruker SMART Apex CCD diffractometer, MoKα radiation, λ = 0.71073 Å, T = 100(2)K, $2\theta_{max}$ = 56.5º, 6760 reflections collected, 2555 unique (R_{int} = 0.0199). Final *GooF* = 1.071, *R1* = 0.0267, *wR2* = 0.0639, *R* indices based on 2430 reflections with I >2sigma(I) (refinement on F^2), 120 parameters, 0 restraints. Lp and absorption corrections applied, $\mu = 0.977$ mm^{-1}.

Compound 6 :- $[Cu_2(BITMB)_2(Cl)_4]\cdot CH_3OH\cdot H_2O$

Crystal data for **6**: $C_{35}H_{43}Cl_4Cu_2N_8O_2$, M = 876.65, Green-blue prisms, 0.20 × 0.10 × 0.10 mm^3, monoclinic, space group $P2_1/c$ (No. 14), a = 8.4349(11), b = 10.7308(14), c = 22.018(3) Å, β = 99.379(2)°, V = 1966.2(4) Å^3, Z = 2, D_c = 1.481 g/cm^3, F_{000} = 902, Bruker SMART Apex CCD diffractometer, MoKα radiation, λ = 0.71073 Å, T = 100(2)K, $2\theta_{max}$ = 56.5º, 11696 reflections collected, 4549 unique (R_{int} = 0.0399). Final *GooF* = 1.059, *R1* = 0.0574, *wR2* = 0.1359, *R* indices based on 3638 reflections with I >2sigma(I) (refinement on F^2), 234 parameters, 0 restraints. Lp and absorption corrections applied, $\mu = 1.396$ mm^{-1}.

Compound 7 :- $[Cu_2(BITMB)_2(Cl)_4]$

Crystal data for **7**: $C_{34}H_{40}Cl_4Cu_2N_8$, M = 829.62, Green-blue prisms, 0.20 × 0.10 × 0.10 mm^3, monoclinic, space group $P2_1/c$ (No. 14), a = 8.362(6), b = 10.550(8), c = 22.438(16) Å, β = 99.093(14)°, V = 1954(3) Å^3, Z = 2, D_c = 1.410 g/cm^3, F_{000} = 852, Bruker SMART Apex CCD diffractometer, MoKα radiation, λ = 0.71073 Å, T = 293(2)K, $2\theta_{max}$ = 57.2º, 11765 reflections collected, 4587 unique (R_{int} = 0.1231). Final *GooF* = 0.789, *R1* = 0.0640, *wR2* = 0.1180, *R* indices based on 1850 reflections with I >2sigma(I) (refinement on F^2), 217 parameters, 0 restraints. Lp and absorption corrections applied, $\mu = 1.396$ mm^{-1}.

Compound 8 :- $[Cu_2(BITMB)_2(Cl)_4]\cdot I_2$

Crystal data for **8**: $C_{34}H_{40}Cl_4Cu_2I_2N_8$, M = 1083.42, Brown prisms, 0.20 × 0.15 × 0.10 mm^3, monoclinic, space group $P2_1/c$ (No. 14), a = 8.3975(18), b = 10.861(2), c = 21.890(5) Å, β = 98.340(4)°, V = 1975.5(7) Å^3, Z = 2, D_c = 1.821 g/cm^3, F_{000} = 1064, Bruker SMART Apex CCD diffractometer, MoKα radiation, λ = 0.71073 Å, T = 100(2)K, $2\theta_{max}$ = 56.5º, 12192 reflections collected, 4593 unique (R_{int} = 0.0721). Final *GooF* = 1.026, *R1* = 0.0670, *wR2* = 0.1360, *R* indices based on 2998 reflections with I >2sigma(I) (refinement on F^2), 235 parameters, 0 restraints. Lp and absorption corrections applied, $\mu = 2.947$ mm^{-1}.

Compound 9 :- $[Cu_2(BITMB)_2(Cl)_4]\cdot CO_2$

Crystal data for **9**: $C_{35}H_{40}Cl_4Cu_2N_8O_2$, M = 873.66, green-blue prisms, 0.26 × 0.24 × 0.18 mm^3, monoclinic, space group $P2_1/c$ (No. 14), a = 8.387(2), b = 10.646(4), c = 22.529(6) Å, β = 99.103(8)°, V = 1986.4(10) $Å^3$, Z = 2, D_c = 1.461 g/cm^3, F_{000} = 896, Bruker SMART Apex CCD diffractometer, MoKα radiation, λ = 0.71073 Å, T = 298(2)K, $2\theta_{max}$ = 56.0º, 3450 reflections collected, 2648 unique (R_{int} = 0.1082). Final *GooF* = 0.738, *R1* = 0.0511, *wR2* = 0.0723, *R* indices based on 1013 reflections with I >2sigma(I) (refinement on F^2), 223 parameters, 3 restraints. Lp and absorption corrections applied, μ = 1.382 mm^{-1}.

Appendix B

Infrared spectra

Sublimed **1**

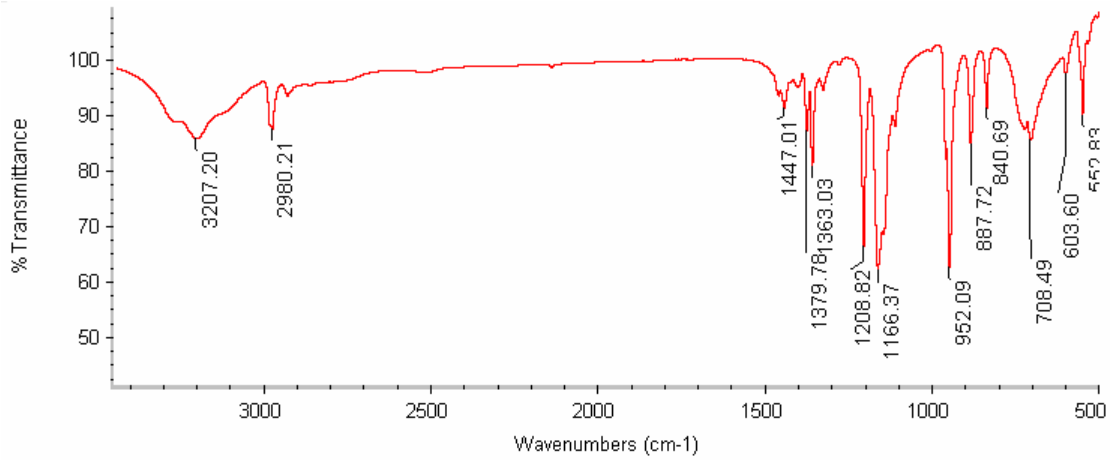

1$_3$·Benzene

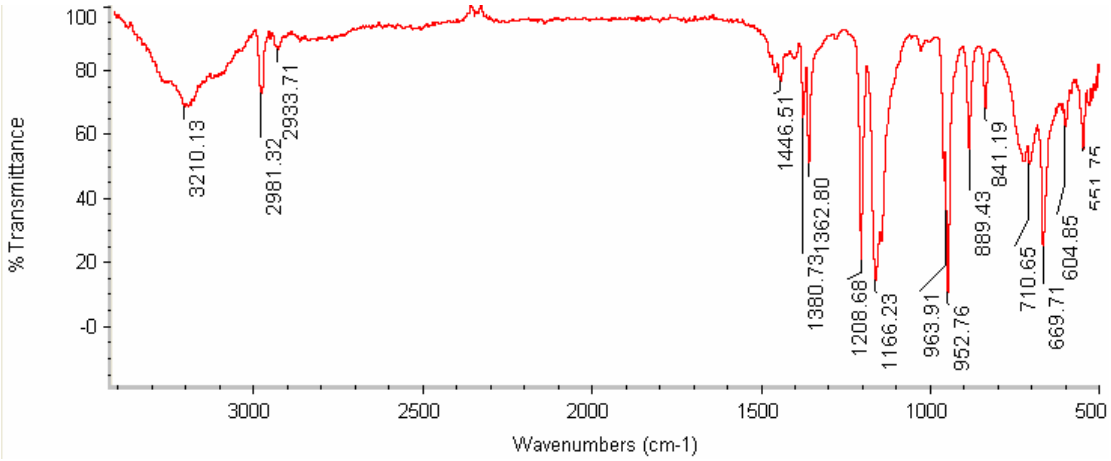

1₃·CCl_4

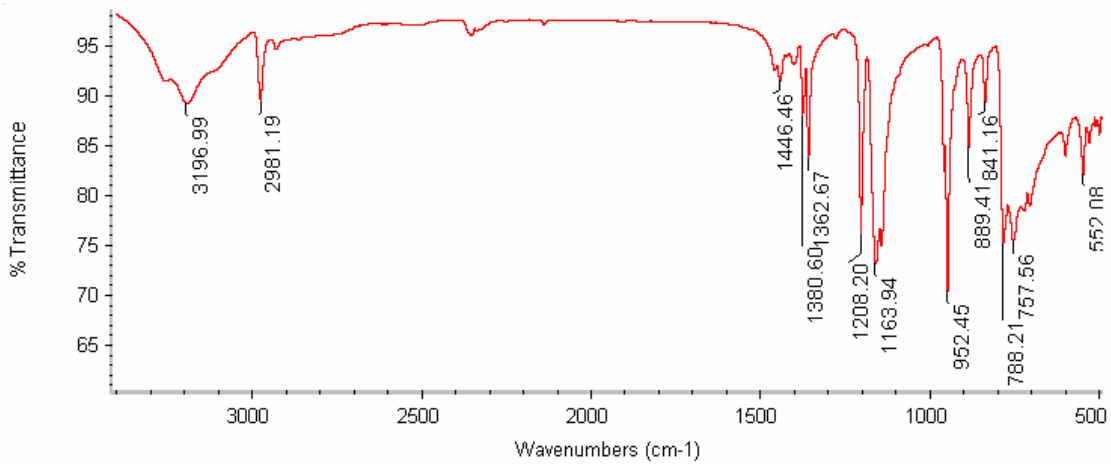

1₃·CCl_3Br

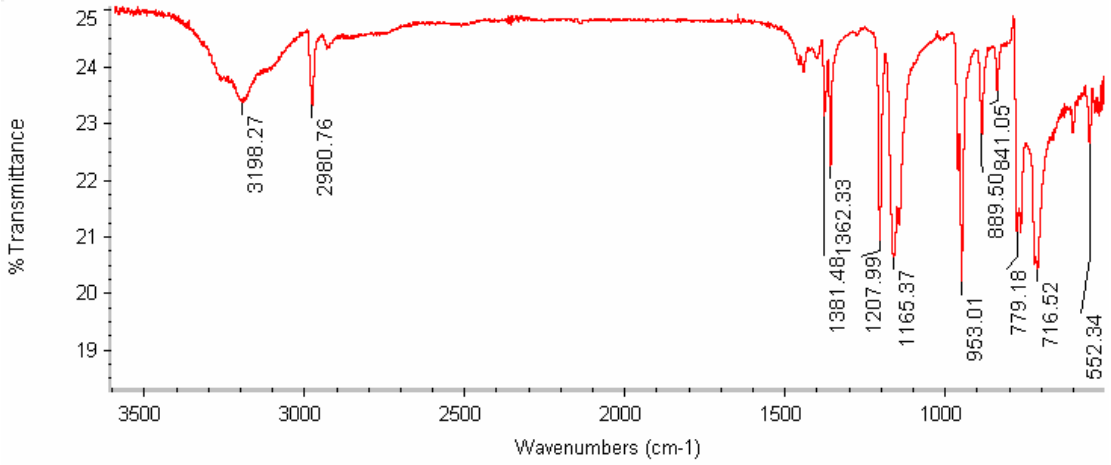

1₃·$Si(CH_3)_3Cl$

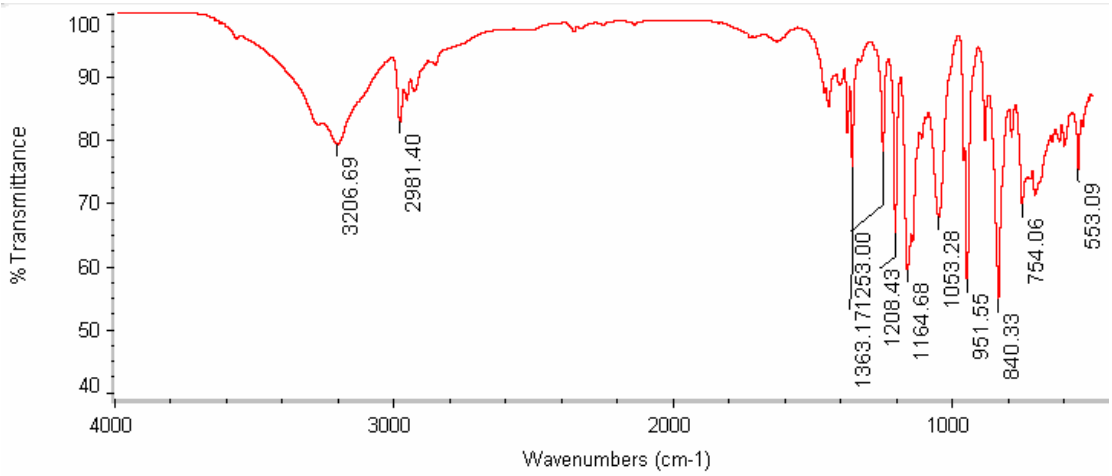

Overlay of 3b (blue) and 3c (red).